UNIVERSITÀ DEGLI STUDI DI PADOVA

Dipartimento di Fisica e Astronomia "Galileo Galilei"

Master Degree in Physics

Final Dissertation

Test of Statistical Isotropy of the Universe using Gravitational Waves

Thesis supervisor

Prof. Nicola Bartolo

Thesis co-supervisor

Dr. Angelo Ricciardone

Candidate

Giacomo Galloni

Academic Year 2019/2020

To my mother, Rita, and to my little brother, Tommaso.

ACKNOWLEDGEMENTS

First and foremost I would like to thank my supervisors, Nicola Bartolo and Angelo Ricciardone, which were able to convey to me their profound passion for Cosmology, galvanizing me to pursue this physics' field and supporting me through this Thesis. Alongside them, I want to thank also Sabino Matarrese; the three of them have helped me to delineate my next-future career as a scientist and were able to encourage me in times of trial.

Secondly, I want to thank my family: Rita, Alessandro, Alessia and Tommaso. You have always been a solid rock in my life, even if I can be a tough family member to deal with. In particular, I dedicated this work to my mother, because of the incredible wholehearted love she gave all of us through our lives and the strength she had demonstrated in these last few years. Also, I dedicated this to my little brother, Tommaso. I know that the "huge" age-gap between us has created some friction, from time to time, but I hope that this Thesis can be an inspiration for him to put all himself in achieving his dreams and a milestone of the love I feel for him.

I want to thank all my friends, starting from "i cuccioli". You have been a lighthouse, which, even in the most dramatic storms, could lead me to some moments of carelessness and actual happiness.
Then, I want to thank my housemates, all six of them (Giamma included), because thank to you I could have the most amazing experience of "house-sharing" one could possibly hope to have at University.
A special credit also goes to "i bombers", which have accompany me in this journey, since the bachelor's degree. Unfortunately, in few months we will be scattered throughout the world following our careers, but I will be always up for one of our reunions.

Last but not least, I want to thank my beloved better half, Alessandra. There would be so much to say here, from our over seven years together, that I could literally write the Thesis about you. Such as, how you can cheer me up only by crashing into my house while I am writing this and finishing this Thesis, with all the distress that this implies; or how you have been able to love me in spite of all my countless defects.
The only thing that is really worth saying is that you are the love of my life and I am looking forward to discover what life has in store for us.

ABSTRACT

In the last years the Cosmology community is showing a lot of interest on an eventual departure from isotropy of our Universe, spurred by the presence of some "anomalies" in the Cosmic Microwave Background (CMB) measurements. This would represent a radical revision in Cosmology, since statistical isotropy is one of the pillars underlying the standard cosmological model. One of these anomalies is the so called "power asymmetry", which seems to escape the "unknown-systematics paradigm", showing a relatively high level of significance. Such power asymmetry was first measured by the Wilkinson Microwave Anisotropy Probe (WMAP) satellite and then also by the Planck satellite, both of which have showed an excess of power in a preferred hemisphere [1–3]. This can be a sign of a violation of statistical isotropy on large scales, that might have a cosmological origin, suggesting the presence of new physics.

In the literature, people have tried to describe such an anomaly as an effect of a local break of isotropy (in our local observable Universe) due to a (dipole) modulation of the scalar gravitational potentials present in the Boltzmann equation for the CMB photons (see e.g. [4–9] for alternative proposal solutions involving non-Gaussianity), which substantially involves the presence of long-wavelength modes acting on scales larger than the Hubble volume (e.g. during an early epoch of inflation). These fields generate a local break of statistical isotropy through their gradient and act on the CMB [10], e.g. though the Sachs-Wolfe (SW) effect, leaving as a relic the asymmetry we observe, without flawing the hypothesis on an underlying global isotropy of the Universe, since the modulation gets averaged over many Hubble volumes (see, e.g. [10]).

On the other hand, in the next future we expect to observe two other background signals in the Gravitational Wave (GW) sector. The first one is the so-called Astrophysical Gravitational Wave Background (AGWB), which comes from the overwhelming quantity of astrophysical sources that our interferometers will be able to detect, to the point that it will be impossible to distinguish them [11, 12]. On the other side of the coin, we know that a "smoking-gun" of inflationary models is a Cosmological Gravitational Wave Background (CGWB) propagating from every direction in the sky as a direct consequence of the quantum fluctuation of the metric enhanced by inflation (see e.g. [13–17] for possible cosmological sources).

Besides their average contribution to the energy density of the Universe, these two backgrounds are also characterized by anisotropies (as the CMB [18]), which are produced by their propagation through a perturbed Universe (and also at the time of the generation of the GW backgrounds) [19]. In spite of what happens for the CMB, where essentially anisotropies date back up to the Last Scattering Surface (LSS) [20–22], in the case of the CGWB they

could provide us with crucial insights on the Early Universe, since the latter is transparent to GWs below the Planck energy [23, 24].

In this master's Thesis, we study the effect of a (dipole) modulation of the gravitational potential (as predicted by the models trying to explain the CMB anomalies) on the CGWB anisotropies, following the approach introduced in [25, 26], of which this Thesis represents a first expansion.
In particular, exploiting the statistical features of GWs, it is possible to define a distribution function for the CGWB, which will evolve accordingly to the Boltzmann equation in a flat Friedmann-Lemâitre-Robertson-Walker (FLRW) Universe perturbed at first order in scalar and tensor perturbations. The evolution will then depend of the gravitational potentials, i.e. the scalar first-order perturbations of the metric, which act like a source term of GWs in the equations, together with a contribution coming from the initial conditions and a tensor sourced term.
The aforementioned primordial modulations can be plugged in the scalar sourced part, changing the evolution of the distribution function and its statistical properties, encoded at the end of the day in the angular power spectrum of the GW energy density.
[25, 26] show that the CGWB behaves analogously to the CMB, e.g. the gravitational potentials generate the SW effect, thus we can include modulations in the CGWB framework in a straight-forward way. Then, the angular power spectrum of GWs energy density is studied, with particular attention on the anisotropies stemmed from the newly introduced modulation.

Summarizing some of the results found in this Thesis, as expected, the CGWB is affected by both the SW effect and the Integrated Sachs-Wolfe (ISW) one. For the CMB (with the modulations on the gravitational potentials, thus [10]) the ISW is neglected, simplifying greatly the calculation. In this Thesis, dedicated to the CGWB, both effects are accounted for, including the primordial modulation of the gravitational potentials, extending the work done in [25, 26].
Furthermore, we proved that analogously to the CMB, the CGWB acquires non-trivial couplings between multipoles due to the presence of the modulation of the gravitational potentials. In other words, the correlation between multipoles is not anymore diagonal in ℓ (thus $\propto \delta_{\ell\ell'}$), but a coupling between modes with ℓ to $\ell \pm 1$ and $\ell \pm 2$ is introduced. This is the first signature of a departure from local isotropy that one can try to observe in the foreseeable future with future GW detectors, such as Laser Interferometer Space Antenna (LISA) [27–31], DECi-hertz Interferometer Gravitational wave Observatory (DECIGO) [32], Einstein Telescope (ET) [33, 34] and Cosmic Explorer (CE) [35].
In addition, we found that the presence of the modulation produces original modifications of the ISW contributions to the angular power spectrum of the CGWB, suppressing them in a more prominent way to what is expected following the standard procedure, without any modulation. This represent a second signature of an eventual violation of local isotropy encoded in the

CGWB.

One of the future developments stemming from this Thesis is the production of sky-maps of the CGWB. Indeed, following [10], which develops simulation tools for predicting the CMB temperature and polarization maps from models equipped with the aforementioned modulations, one can obtain such maps. In this sense, both softwares as Cosmic Linear Anisotropy Solving System (CLASS) [36] and Hierarchical Equal Area isoLatitude Pixelation of a sphere (HEALPix) [37] can be very useful, since the former allows to compute the angular power spectrum, whereas the latter produces sky-maps once given the angular power spectrum contributions of different multipoles (see [38–41] for some insights on sky-maps of the GW backgrounds and the angular resolution of GW Astronomy).

CONTENTS

LIST OF TABLES

LISTINGS

ACRONYMS

AGWB Astrophysical Gravitational Wave Background

ALP Associate Legendre Polynomial

BAO Barionic Acoustic Oscillation

BH Black Hole

CE Cosmic Explorer

CGWB Cosmological Gravitational Wave Background

CL Confidence Level

CLASS Cosmic Linear Anisotropy Solving System

CMB Cosmic Microwave Background

COBE COsmic Background Explorer

DECIGO DECi-hertz Interferometer Gravitational wave Observatory

DOF Degree Of Freedom

EM Electro-Magnetic

EOM Equation Of Motion

ET Einstein Telescope

FLRW Friedmann-Lemâitre-Robertson-Walker

GR General Relativity

GUT Grand Unified Theory

GW Gravitational Wave

HEALPix Hierarchical Equal Area isoLatitude Pixelation of a sphere

H-Z Harrison-Zel'dovich

ISW Integrated Sachs-Wolfe

K-G Klein-Gordon

LHS Left Hand Side

LIGO Laser Interferometer Gravitational-Wave Observatory

LISA Laser Interferometer Space Antenna

LP Legendre Polynomial

LSS Last Scattering Surface

RHS Right Hand Side

RS Rees-Sciama

SBF Spherical Bessel Function

SGWB Stochastic Gravitational Wave Background

SH Spherical Harmonic

SW Sachs-Wolfe

TT Transverse-Traceless

WMAP Wilkinson Microwave Anisotropy Probe

Part I

THEORETICAL BACKGROUND

In this part of the Thesis, we will describe what are the basics of Cosmology, what brought people to introduce an inflationary stage of the Universe and what consequences this period leaves behind in the following evolution. In particular, we will focus on a gravitational background signal arising from quantum fluctuations of the metric tensor in very early times. While doing this, we will define the convention and the notation, which will be carried on for the rest of the work.

1 BASICS OF COSMOLOGY

In this chapter we will review some basic notions which must be very well understood for a better comprehension of the following arguments. The key aspects will be the Einstein's field equations and the FLRW metric.
We will skip the unnecessary details through this chapter, since we can assume with pretty high confidence that all these concepts are already clear to the reader.
The main references for this chapter are [18, 42–44], thus if you want more details on the subjects we are treating here, you can surely find them there.

1.1 EINSTEIN'S EQUATIONS AND FLRW METRIC

The famous Einstein's equations read [42]

$$G_{\mu\nu} \equiv R_{\mu\nu} - \frac{1}{2} R g_{\mu\nu} = 8\pi G T_{\mu\nu} \tag{1}$$

where: $R^{\lambda}{}_{\sigma\mu\nu} \equiv \partial_\mu \Gamma^\lambda_{\sigma\nu} - \partial_\nu \Gamma^\lambda_{\sigma\mu} + \Gamma^\lambda_{\mu\rho}\Gamma^\rho_{\nu\sigma} - \Gamma^\lambda_{\nu\rho}\Gamma^\rho_{\mu\sigma}$ is the Riemann tensor;
$R_{\mu\nu}$ = Ricci tensor, defined as the contraction of the first and third indexes of the Riemann one;
R = is the Ricci Scalar, defined as the full contraption of the Ricci tensor;
$\Gamma^\mu_{\nu\lambda} \equiv \frac{1}{2} g^{\mu\rho}\left(\frac{\partial g_{\rho\nu}}{\partial x^\lambda} + \frac{\partial g_{\rho\lambda}}{\partial x^\nu} - \frac{\partial g_{\nu\lambda}}{\partial x^\rho}\right)$ are the Christoffel symbols;
$g_{\mu\nu}$ = metric tensor;
G = gravitational constant;
$T_{\mu\nu}$ = stress-energy tensor.

Eq.1 can be derived from the variation w.r.t. the metric of the total action $S_{TOT} = S_{HE} + S_m$ [45, 46], where

$$S_{HE} \equiv \int d^4x \sqrt{-g} \frac{R}{16\pi G} \tag{2}$$

is the Hilbert-Einstein action that accounts for gravity, in which g is the determinant of the metric tensor, while

$$S_m = \int d^4x \sqrt{-g} \mathscr{L}_m \tag{3}$$

is the action associated to all the other particles (scalar fields, fermions, gauge bosons, ...), where $\mathscr{L}_m$ indicates their Lagrangian density. In particular, from the variation $\frac{\delta S_{HE}}{\delta g^{\mu\nu}}$ it derives the geometric Left Hand Side (LHS)

of Eq.1 while the stress-energy tensor $T_{\mu\nu}$ on the Right Hand Side (RHS) is defined as [46]

$$T_{\mu\nu} \equiv -\frac{2}{\sqrt{-g}}\frac{\delta S_m}{\delta g^{\mu\nu}} \,. \tag{4}$$

This tensor can be computed in two possible ways:

- focusing on its global properties and treat it as a perfect fluid; this lead to the very well known form (true for a generic reference frame) [42]

$$T_{\mu\nu} = u_\mu u_\nu(\rho + P) + P g_{\mu\nu} \text{ [1]}, \tag{5}$$

  where: ρ = energy density;
  P = isotropic pressure;
  u_μ = 4-velocity of the fluid in its reference frame.

- studying every single field and write a contribution for each of them. However this road requires a very detailed theory.

There are other two important relations that must be taken into account every time that Einstein's equations enter in the game; these are the Bianchi identity $\nabla_\mu G^{\mu\nu} = 0$ and the continuity equation $\nabla_\mu T^{\mu\nu} = 0$ (∇ here indicates the covariant derivative), which indeed are consequence of one another, given the Einstein's equations.
It is also important to remember that Eq.1 can be either used to find metrics that satisfy some symmetries or, using some specific spacetime and constraints, to find some system. If we proceed in first way, looking for a metric that describes an expanding Universe with curvature κ and which is symmetric under rotation and spatial translation (isotropic and homogeneous)[2], we find the FLRW metric [43]

$$ds^2 = -c^2dt^2 + a^2(t)\left[\frac{dr^2}{1-\kappa r^2} + r^2 d\Omega^2\right], \tag{6}$$

1 Actually a fluid can be characterized also by some form of anisotropies, as viscosity or thermal conductivity; these effects can be taken into account adding to the previous $T_{\mu\nu}$ an appropriate tensor $\Pi_{\mu\nu}$. Since here we only want to summarize briefly some fundamental tool and concept, from now on we will use a perfect fluid, unless differently stated.

2 We do not ask for the time translation invariance because we want a Universe able to change throughout time.

where: t = cosmic time, whereas the time coordinate of an observer co-moving with the cosmic fluid;
r = radial coordinate;
$a(t)$ = scale factor, which spans the expansion of the Universe;
$d\Omega^2 = d\theta^2 + \sin^2\theta d\phi^2$ is the infinitesimal solid angle;
κ = curvature, which can be either positive (closed Universe), null (flat Universe) or negative (open Universe)[3].

Usually, one parametrizes κ as

$$\kappa = \begin{cases} -1 & \text{open} \\ 0 & \text{flat} \\ +1 & \text{close} \end{cases} . \tag{7}$$

It is important to underline that the set (r, θ, ϕ) is made of comoving co-

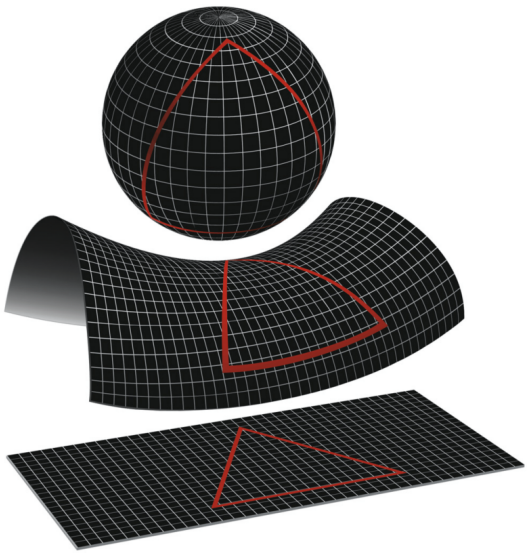

Figure 1: Different geometries encoded in the FLRW metric
[http://wmap.gsfc.nasa.gov/media/990006/990006_2048.jpg]

ordinates, i.e. they do not depend on the evolution and remain constant, so that, once they are multiplied by the scale factor, the physical coordinates

3 One can show that these three cases represent respectively the geometry of a sphere, a plane and an hyperboloid. It is intuitive that in all of these the "landscape" around a specific point is completely isotropic and it is the same in every point one chooses, hence they indeed are isotropic and homogeneous.

are recovered[4]. From the symmetry properties of Eq.6, it can be found the very easy form for the stress-energy tensor [18]

$$T_{\mu\nu} = \mathrm{diag}[\rho(t), P(t), P(t), P(t)], \tag{9}$$

where $\rho(t)$ and $P(t)$ are respectively the energy density and the isotropic pressure of the fluid, which do not depend on $\vec{x}$[5] because of isotropy and homogeneity.

1.2 FRIEDMANN EQUATIONS

The dynamics of the expanding Universe can be explicitly seen by unfolding the Einstein's equations

$$R_{\mu\nu} - \frac{1}{2} g_{\mu\nu} R = 8\pi G T_{\mu\nu} - \Lambda g_{\mu\nu} \,, \tag{10}$$

where, w.r.t. Eq.1, we have added for the sake of completeness Λ, the cosmological constant. Microscopically speaking, Λ can be interpreted as the energy of the quantum vacuum state of the system, the vacuum energy density contributed by *any* particle species[6]. We have already seen what are the main actors appearing in Eq.10 while discussing Eq.1, thus, one can find the Friedmann equations by writing explicitly the $_{00}$ and $_{ij}$ components of the Einstein's equations and by exploiting the conservation laws $\nabla_\mu T^{\mu\nu} = 0$ (in this specific case the ∇ refers to the covariant derivative). Hence, one can find

$$H^2 + \frac{\kappa}{a^2} = \frac{8\pi G}{3}\rho + \frac{\Lambda}{3} \,, \tag{11}$$

$$\frac{\ddot{a}}{a} = -\frac{4\pi G}{3}(\rho + 3P) + \frac{\Lambda}{3} \,, \tag{12}$$

$$\dot{\rho} + 3H(\rho + P) = 0 \,, \tag{13}$$

where: $\cdot$ = derivative w.r.t. cosmic time t;
$H \equiv$ $\frac{\dot{a}}{a}$ is the Hubble rate.

These equation are indeed dependent from one another through the Bianchi identities so that only two of them are independent (from now on we will neglect the contribution of the cosmological constant, since it is very small at early times) [42].

4 Considering the comoving coordinates, one can show that the coordinate separation between two points remain constant in time. Then the spatial splices of the metric in the parenthesis gets rescaled by the scale factor, in such a way that for any distance λ, it holds

$$\lambda_{\mathrm{physical}}(t) = a(t) \cdot \lambda_{\mathrm{comoving}} \,. \tag{8}$$

5 In this Thesis, 3-vectors will be indicated with a $\rightarrow$, whereas the same quantity without this symbol will indicate its modulus.

6 Also the contribute of continuous particle creation and annihilation.

To close the system, one needs an extra relation linking $P(t)$ and $\rho(t)$, named equation of state $P(\rho)$. The simplest choice is

$$P = \omega\rho \quad \text{with} \quad \omega = \text{constant} \,, \tag{14}$$

where ω depend on the energy content considered

$$\omega = \begin{cases} 0 & \text{dust or pressureless matter} \\ \frac{1}{3} & \text{radiation} \\ -1 & \Lambda \end{cases} . \tag{15}$$

Solving this system of equations, one finds the explicit expression of the scale factor $a(t)$, which in FLRW has the usual solution with a singularity back in time

$$a(t) = a_* \left(\frac{t}{t^*}\right)^{\frac{2}{3(\omega+1)}} \,, \tag{16}$$

where $_*$ indicates a reference scale[7].
For what regards ρ:

$$\rho = \rho_* \left(\frac{a}{a_*}\right)^{-3(1+\omega)} \quad \Rightarrow \quad \rho \propto \begin{cases} a^{-3} & \omega = 0 \\ a^{-4} & \omega = \frac{1}{3} \\ \text{constant} & \omega = -1 \end{cases} . \tag{17}$$

These dependency can be intuitively derived if one thinks at how energy gets diluted with the expansion of the Universe: in the case of pressureless matter (e.g. we can think of a bunch of protons), the energy density will scale as volume^{-1}, so a^{-3}, since the number of particles in that volume will not change; for radiation, the energy gets an extra a^{-1} factor because the wave length of radiation will also be diluted by expansion; finally Λ is by definition a constant, so even if the Universe expands, its value will not change.
All these relations and definitions can be written in function of conformal time η exploiting the transformation $dt = a(\eta)d\eta$ in order to obtain a metric in which $a(\eta)$ factorizes in front of all terms[8].

7 From this relation one can appreciate the fact that only ratios of scale factors are physical, assuming a spatially flat Universe. In fact, the coordinate can always be rescaled by a constant without any physical consequence.
Whereas in the case of $\kappa \neq 0$ the normalization of $a(t)$ becomes physical, since in the Friedmann equations, specifically in Eq.11, the term $\propto \kappa$ cannot be rescaled freely.

8 For any generic function of cosmic time $f(t)$ hold

$$\dot{f}(t) = \frac{f'(\eta)}{a(\eta)} \,, \qquad \ddot{f}(t) = \frac{f''(\eta)}{a^2(\eta)} - \mathcal{H}\frac{f'(\eta)}{a^2(\eta)} \,,$$

where the prime refers to the derivative w.r.t. conformal time. The Hubble rate in cosmic time H is then named $\mathcal{H} \equiv \frac{a'}{a}$ in conformal one.

1.3 COSMOLOGICAL HORIZON

One could ask: what is the maximum distance from which we have received a light signal within the whole life of the Universe t? This quantity is called the cosmological horizon and represent the radius of the region of causal connection centered on us

$$d_H(t) \equiv a(t) \int_0^t \frac{c dt'}{a(t')} \,. \tag{18}$$

It is related to its comoving counterpart

$$l \equiv \int_0^t \frac{c dt'}{a(t')} \,, \tag{19}$$

called comoving distance[9]. This horizon is similar to the event horizon of a Black Hole (BH), but it is a past horizon, instead of a future one. Also, if $d_H(t)$ exists finite, it is called particle horizon. In particular in a FLRW Universe, $d_H(t)$ is finite if $\omega > -1/3$, in fact [47]

$$d_H(t) = \frac{3(1+\omega)ct}{1+3\omega} \simeq ct \simeq \frac{1}{H(t)} \,, \tag{20}$$

and

$$d_H(t) = \begin{cases} 3ct & \omega = 0 \\ 2ct & \omega = 1/3 \\ \infty & \omega = -1/3 \end{cases} \,. \tag{21}$$

Furthermore, exploiting the Friedman equations, one can find that $d_H(t)$ is finite iff $\ddot{a}(t) < 0$, so iff the Universe acceleration is negative.

1.4 HUBBLE RADIUS

The Hubble radius is defined as [18]

$$R_C(t) \equiv \frac{c}{H(t)} = c\tau_H \,, \tag{22}$$

where τ_H is Hubble time defined as the inverse of the Hubble rate $H(t)$, representing the characteristic time of expansion[10].

9 This quantity also represents the physical interpretation of conformal time, given that $d\eta = dt/a$.

10 One can show that for every τ_H passing by, the scale factor doubles.

Making explicit, the expression of H, we can find the relation between R_C and d_H

$$R_C(t) = \frac{3}{2}(1+\omega)ct = \frac{1+3\omega}{2} d_H(t) \,, \tag{23}$$

which in standard FLRW means $R_C(t) \sim d_H(t)$. However, they have a significant physical difference: if d_H accounts for the causal connection over the whole history of the Universe, R_C accounts only for the connection over one Hubble time.
Also R_C has its comoving counterpart called comoving Hubble radius r_H, defined as

$$r_H(t) \equiv \frac{R_C(t)}{a(t)} = \frac{1}{\dot{a}(t)} \,, \tag{24}$$

which is related to the comoving particle horizon through

$$\frac{d_H(t)}{a(t)} = \int_0^t \frac{c dt'}{a(t')} = \int_0^a \frac{c da'}{a'\dot{a}'} = \int_0^a \frac{c da'}{a'} r_H(t) \,. \tag{25}$$

In conclusion, calling t_0 the age of the Universe today, we can say that the largest distance one can experimentally inspect is $d_H(t_0) = 2R_C(t_0) \approx 6000 h^{-1}$ Mpc $\approx 10^4$ Mpc.

2

SHORTCOMINGS OF HOT BIG-BANG MODEL

Even though the Hot Big-Bang Model has successfully described a broad range of phenomena characterizing our Universe, such as the abundance of light elements, the large-scale structures and Hubble's law, it is flawed by the existence of the so-called "shortcomings". They are not intrinsic problems of the model, but still, they are inconsistencies in the form of strangely precise requirements on the initial conditions, in order to obtain what we observe today.
In this chapter we will present these issues and we will present their solution by adding an extra ingredient to our recipe of the Universe: a period of accelerated expansion in early times, "inflation", which instead will be treated in Ch.3.
The aspects we are going to treat in this chapter can be further explored in many different references, such as [18, 42–44].

2.1 HORIZON PROBLEM

The first inconsistency that we want to discuss is known as *Horizon problem*. In order to fully understand it, let us firstly observe that in a FLRW Universe the comoving Hubble radius is always growing; indeed, recalling that in FLRW

$$r_H = \frac{1}{\dot{a}(t)}, \tag{26}$$

it is easy to see that its time derivative

$$\dot{r_H} = -\frac{\ddot{a}(t)}{\dot{a}(t)^2} \tag{27}$$

is positive when we consider radiation, or pressureless matter, whereas becomes negative when considering for example the cosmological constant. In other words, for equation of states for the cosmic fluid with $\omega > -1/3$ the comoving Hubble radius always increases.
This means that, sooner or later, all the scales λ will enter in the horizon and the region of causal connection around the observe become bigger and bigger. This is illustrated in Fig.2. At first sight one does not notice any problem: as time flows the Hubble radius grows and larger scales can cross it, starting to communicate with the rest of the causal connected region. However, the issue stems from an "experimental" point of view looking at the CMB. Indeed, we know that a crucial prediction of the hot Big-Bang model is a left-over thermal radiation generated when radiation and matter decoupled. When the temperature of the Universe was $T > 0.3\,\text{eV}$, photons and electrons were tightly coupled through Compton and Thompson scattering, which

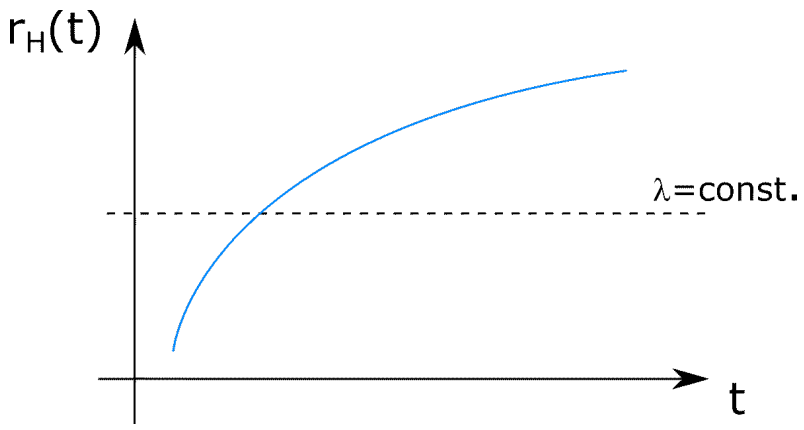

Figure 2: Comoving Hubble radius evolution in a Big-Bang model.

assured that these two species remained at the same temperature with short free mean paths. However, when the temperature dropped below that threshold, electrons and protons start to create neutral hydrogen.
In this newly generate neutral environment photons were not able anymore to scatter, basically free-streaming from that moment on. The resulting radiation is called CMB and is nearly isotropic, having the same temperature in every direction in the sky and showing a nearly perfect black-body distribution peaked in the microwave region.
Actually, this is not completely true, we will briefly explore the CMB anisotropies in Ch.5, but for the purpose of this section is it sufficient to state that we can observe regions that share the same statistical properties (in particular the same temperature T, up to very tiny fluctuations), without having been in causal connection ever before, since they are separated by distances that are much larger than the largest distance traveled by light in all the history of the Universe. This is a clear inconsistency with our theoretical expectations.
In such a framework, one has to assume that the initial condition from which the Universe born was already isotropic and homogeneous in order to explain consistently what we observe[11]. However, even doing so hides some further difficulties given that one would have to deal with the fact that indeed small anisotropies are present on the CMB and it is not trivial to obtain the right amount of them in such a context.

11 This explanation is not satisfactory for us, firstly because is a zero-measure condition, which have basically zero probability to have occurred, also, as physicists we would like to have an actual explanation of how things ended up this way from the most general set of initial conditions.

2.2 FLATNESS PROBLEM

Another issue which arises in the Hot Big Bang model is related to the importance of the curvature term and it is known as *Flatness problem*. The easiest way to see it is to analyze the first Friedmann equation

$$H^2 = \frac{8}{3}\pi G\rho - \frac{\kappa}{a^2}. \tag{28}$$

In the standard FLRW Universe, during the radiation and the matter domination epoch, the energy density scales, respectively, as a^{-4} and a^{-3}. Now, the probability of having $\kappa = 0$ is almost null: indeed κ could take, in principle, whatever finite value so that the probability that it is exactly 0 is infinitesimally small. We immediately realize that as long as $\kappa \neq 0$, there will be a moment such that the curvature term κ/a^2 overcomes the other one, since it decreases slower than ρ with the expansion of the Universe.
Also, introducing the density parameter $\Omega(t) \equiv \rho(t)/\rho_c(t)$, where $\rho_c(t) \equiv 3H^2(t)M_p^2$ is the total energy density for a flat Universe, this contribution given by curvature is fated to increase more and more as time goes by; Fig.3 summarizes this concepts.
First of all, Fig.3 shows that independently on the value of the curvature, at

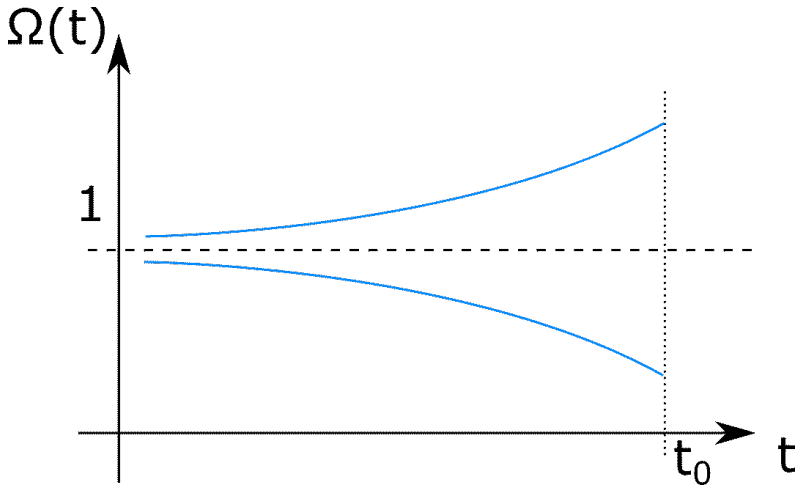

Figure 3: Density parameter behavior in a hot Big-bang model context.

very early times Ω is approximately 1. Indeed, going back with time translates into a decrease of the scale factor, which implies that the curvature term becomes negligible so that (as happens in $\kappa = 0$ case) the density parameter becomes 1.
The scenario changes as time starts to flow, depending on the value of κ. Indeed, in this case [42]

$$\Omega(t) - 1 = \frac{\kappa}{a^2(t)H^2(t)} = \kappa r_H^2(t) \equiv \Omega_\kappa(t) \tag{29}$$

and, besides of the sign κ, the total parameter density Ω departs from the initial value.
Here there is the problem: today, thanks to our cosmological observations as Planck, we know that $|\Omega(t_0) - 1| = 0.0007 \pm 0.0037$ at 95% CL [48], which is still a very tiny value, compatible with zero; However, since we know that κ is different from zero[12], how can be possible that still today the energy contribution of the curvature term is so small?
A possible answer is that the initial value of Ω was so close to 1 that even nowadays a not sufficient amount of time has passed in order to see its effects. Nevertheless, if we want to remain in the "comfortable zone" of the standard hot Big Bang model, accepting the previous explanation would result in the so called *fine tuning problem*.
Indeed, one can show that in order to account for the nowadays observations, the difference between the density parameter and 1, at the Planck epoch t_P which corresponds to a temperature $T_P \approx 10^{19} GeV$, has to be

$$\left[\Omega^{-1}(t_P) - 1\right] \simeq \left(\Omega_0^{-1} - 1\right) \left(\frac{T_0}{T_P}\right)^2 10^3 \approx 10^{-60}. \tag{30}$$

The problem is clear: if we want to explain the smallness of Ω_κ today we have to *fine tune* (i.e. put by hand with an high precision) the initial value of Ω to 1 up the 60^{th} decimal place. This seems to be quite unnatural, in particular if we consider that such a tiny interval of acceptable initial values substantially has a "null measure" w.r.t. the whole possible ones [13].

2.3 UNWANTED RELICS

Another problem related to the hot Big-Bang model is the presence of "unwanted relics" [44] produced in the early Universe as a consequence of the spontaneous symmetry breaking (SSB) of some Grand Unified Theory (GUT) at $T_{GUT} \sim 10^{14} \div 10^{16}$ GeV. An example are domain walls, i. e. topological objects (non-perturbative solutions), which can arise after the SSB in a given theory. Generally speaking, these relics are massive and very stable, since they are characterized by a small annihilation cross section; it is, indeed, this last property that makes them *unwanted*, because their density parameter has the form $\Omega_\chi \sim 1/\sigma_\chi \sim 10^{14} \gg 1$. In this context this problem is *unavoidable*, becoming a very serious flaw of the theory.

12 We can say to know this because the probability of it being exactly zero is itself null.
13 We stress again that this last sentences are not properly "true". Indeed from a pragmatic point of view, one could argue that the Universe had that exact initial condition and then evolved following the Big-Bang model until now, stopping there to question himself. However, physicists do not usually like such an explanation, finding it unsatisfactory. We want then to find some mechanism that pushes the Universe to such a conclusion, without imposing any particular initial condition.
From a Bayesian point of view this is equivalent to impose the less restricting prior distribution as possible, in order to avoid to bias the conclusions drawn at the end.

2.4 INFLATION AS A SOLUTION TO THESE SHORTCOMINGS

A solution that solves the aforementioned problems as a natural consequence of it very characteristics is a phase of accelerated expansion in early times, named *inflation*.

2.4.1 *Horizon Problem Solution*

Inflation has the net effect of pushing to $-\infty$ the initial singularity [44]. This allows photons to be at some point in causal connection with all the others. From the point of view of the Hubble radius, inflation made it to decrease causing scales λ to exit it. Then, once this period ended and r_H began to grow again, all the λs started to re-enter in the horizon, this time having been causally connected with the rest when they were inside the horizon the first time, before inflation. Then if we suppose that the largest scale that we can probe experimentally today, i.e. the CMB one, was under the horizon when inflation took place, there are no problems with causality since it was already causal connected before inflation.
At this point, one could argue: how much did the Universe have to expand to solve the problem?
Introducing the useful quantity

$$N \equiv \int_{t_i}^{t_f} H(t)dt = \ln\left(\frac{a_f}{a_i}\right), \tag{31}$$

which is called *number of e-folds*[14], and applying an exponential on both sides, Eq.31 reads also as

$$\frac{a_f}{a_i} = e^N. \tag{32}$$

We can see that N immediately tell us how much bigger was the Universe at the end of inflation w.r.t. its beginning.
One can show that solving the horizon problem results in asking at least $N \approx 60 \div 70$ [42], which approximately corresponds to an expansion of a factor 10^{26}, from atomic scales to the size of the solar system.

2.4.2 *Flatness Problem Solution*

The solution can be argued taking Eq.29 and observing that, if we consider inflation, making the Universe to expand exponentially makes Ω_κ to reach a so small value that even today it is still negligible. This means that even if at the beginning of this epoch the value of the total parameter density was very different from 1, as a consequence of the tremendous expansion, at the end of the this phase it was pushed incredibly near to it. This solution would

14 Here with the subscripts "i" and "f" we are referring, respectively, to the start and the end of inflation.

explain, then, the reason why even if the value of the curvature is different from zero, nowadays the measurements are consistent with a flat Universe, without imposing any initial condition. The condition $r_H(t_i) \geqslant r_H(t_0)$ that

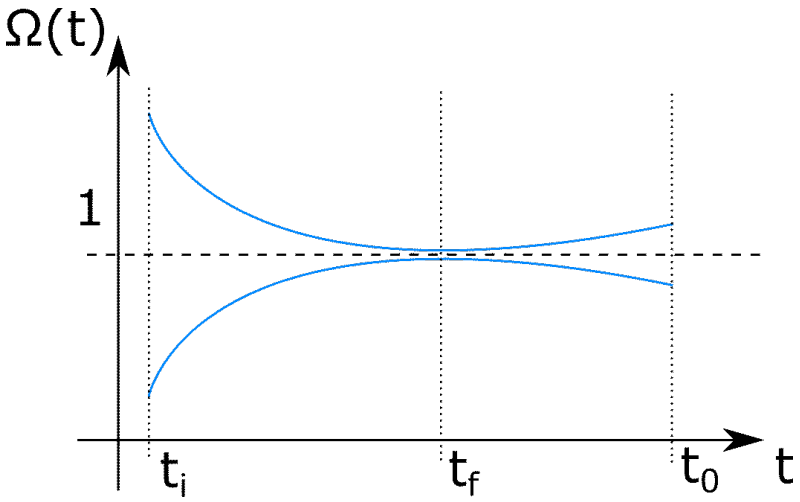

Figure 4: In this plot the expansion of the Universe occurring nowadays is neglected for the sake of simplicity. In any way it would only mean that the value of $\Omega(t)$ is getting pushed toward 1 even more, as happened during inflation.

was needed to solve the *horizon problem* now translates into

$$\frac{\Omega^{-1}(t_i) - 1}{\Omega^{-1}(t_0) - 1} \geqslant 1 \tag{33}$$

and one can show that it solves also this problem with a required number of e-folds of again $60 \div 70$ [42].
Intuitively speaking this solution can be visualized if one thinks to an inflating balloon: if it is very small even an ant onto its surface could see the curvature, however inflating the balloon to the sides of e.g. the Earth, the curvature would get severely diluted and our ant would think to live on a flat-earth.

2.4.3 *Unwanted Relics*

We briefly mention that inflation solves naturally the unwanted relics problem. Indeed, an inflationary scenario would give rise to an epoch of expansion, with $a(t) \propto e^{Ht}$, strongly suppressing the number density of these relics, being $n_x \propto a^{-3Ht}$. In this way one ends up having ≈ 1 of these objects in all the observable Universe, without concerns of its contribution to the overall energy density [44].

3

INFLATION

In Ch.2 we introduced inflation as a solution to the shortcomings of the hot Big-Bang model. Now, we will discuss in more details the standard inflationary model of the Universe. Specifically, we will consider the most simple example of a single-field model with a real scalar inflaton.
We have seen in Ch.1, that in order to have accelerated expansion it is required to have

$$\ddot{a} > 0 \iff P < -\frac{1}{3}\rho\,, \tag{34}$$

which are attained by a simple simple scalar field. Also, we will see how this will produce one of the so-called "smoking gun" of inflationary models, i.e. a CGWB, which is the main actor in this Thesis.
In the same way as Ch.2, the information contained in this chapter can be found in many references, such as [18, 42–44].

3.1 WHY A SCALAR FIELD?

Recalling the case of the cosmological constant, we can write the Einstein's equations as

$$R_{\mu\nu} - \frac{1}{2}g_{\mu\nu}R = 8\pi G T_{\mu\nu} - \Lambda g_{\mu\nu}\,. \tag{35}$$

Here, Λ is associated to a stress-energy tensor, which can be written in the form of a perfect fluid once we define $P_\Lambda = -\rho_\Lambda = -\frac{\Lambda}{8\pi G}$ ($\omega_\Lambda = -1$) as [44]

$$T^{\Lambda}_{\mu\nu} \equiv (P_\Lambda + \rho_\Lambda)u_\mu u_\nu + P_\Lambda g_{\mu\nu} = P_\Lambda g_{\mu\nu}\,. \tag{36}$$

As we already mentioned, Λ can be interpreted as the energy of the quantum vacuum state of the system.
Furthermore, from Eq.11, it is possible to see that in a Universe where Λ dominates the scale factor will be $a(t) \propto e^{Ht}$, meaning that it expand exponentially. This is very similar to what we want to achieve with our scalar field, however, being Λ a constant, the expansion would never end.
Thus, we can then generate an effective Λ by assuming to have a scalar field in its ground state. In fact, the field φ, will have the lagrangian density equal to [42]

$$\mathscr{L} = \frac{1}{2}g^{\mu\nu}\partial_\mu\varphi\,\partial_\nu\varphi - V(\varphi), \tag{37}$$

where $V(\varphi)$ is the potential and to which we can associate a stress-energy tensor [42]

$$T^{\varphi}_{\mu\nu} = \partial_\mu\varphi\,\partial_\nu\varphi + g_{\mu\nu}\mathscr{L}. \tag{38}$$

In the ground state $\langle\varphi\rangle =$ constant, in time and space, thus we end up with having a stress-energy tensor, contributing to the total energy of the vacuum state, of the form

$$T_{\mu\nu} = -V(\langle\varphi\rangle)g_{\mu\nu}\ , \tag{39}$$

where we have neglected the kinetic term being in the vacuum state.
Even if it is apparently simple to generate such an effective vacuum energy, as aforementioned this calculation hides a flaw: inflation must end at some point. There must be some dynamics regulating such a process, so the simplest acceptable system will give [15]

$$\varphi(\vec{x},t) \quad\rightarrow\quad \langle 0|\varphi|0\rangle = f(t) \neq \text{constant}\ . \tag{40}$$

3.1.1 *Model with a Real Scalar Field*

The full action is

$$\begin{aligned} S^{TOT} =& S_{HE} + S_\varphi + S_m = \\ =& \frac{1}{16\pi G}\int d^4x\sqrt{-g}(R + \mathscr{L}_\varphi[\varphi,\partial_\mu\varphi] + \mathscr{L}_{\text{fields}})\ , \end{aligned} \tag{41}$$

where S_{HE} is the Hilbert-Einstein action, S_φ is the inflaton scalar field action and S_m is the action of the "rest-of-the-world" made of fermions, gauge fields, other scalars, etc. In the following, we will neglect S_m because, in general, they are subdominant at early times, since by definition the inflaton drives inflation dominating the energy density.
The generic lagrangian of a real scalar field has the form shown by Eq.37, where the potential can have different forms depending on the model and usually is taken to be minimally coupled (for the sake of simplicity), for example a simple quadratic potential is $V(\varphi) = \frac{1}{2}m^2_\varphi\varphi^2$, where m_φ is the mass of the particle associated to φ.

15 Giving away simplicity one can consider a wide variety of cases, which however must respect the underlying symmetries of the considered system. What if, e.g., we consider the case of a vector gauge field A^μ? This is not a viable choice in the standard scenario, since taking a $\langle 0|\,A^\mu\,|0\rangle \neq 0$ violates rotational invariance (isotropy), bringing to observational consequences. Other choices can be a spinor field ψ, but $\langle 0|\,\psi\,|0\rangle \neq 0$ gives the same problem. A way to solve it is to consider scalar condensates $\langle 0|\bar{\psi}\psi|0\rangle$, from which to build the model.

3.2 EVOLUTION OF φ

To characterize the evolution of a scalar field in an expanding Universe, we can associate to φ its stress-energy momentum $T_{\mu\nu}$, thus reminding Eq.4 we can write

$$T_{\mu\nu} \equiv \frac{-2}{\sqrt{-g}}\frac{\delta S}{\delta g^{\mu\nu}} = \frac{-2}{\sqrt{-g}}\left[-\frac{\partial(\sqrt{-g}\mathscr{L})}{\partial g^{\mu\nu}} + \partial_\alpha \frac{\partial(\sqrt{-g}\mathscr{L})}{\partial \partial_\alpha g^{\mu\nu}} + \dots\right] , \quad (42)$$

where higher order derivatives terms can arise in case $\mathscr{L}$ depends on higher derivatives of the metric. Plugging Eq.37, one obtains

$$\begin{aligned} T^{\varphi}_{\mu\nu} &= -2\frac{\partial \mathscr{L}_\varphi}{\partial g^{\mu\nu}} + g^{\mu\nu}\mathscr{L}_\varphi \\ &= \partial_\mu\varphi\,\partial_\nu\varphi + g_{\mu\nu}\left[-\frac{1}{2}g^{\alpha\beta}\varphi_{;\alpha}\,\varphi_{;\beta} - V(\varphi)\right] . \end{aligned} \quad (43)$$

Then, we can express φ as the sum of the classical background value and the field fluctuations as

$$\begin{aligned} \varphi \equiv \varphi(\vec{x},t) &= \langle 0|\,\varphi(\vec{x},t)\,|0\rangle + \delta\varphi(\vec{x},t) \\ &= \varphi_0(t) + \delta\varphi(\vec{x},t) \end{aligned} \quad (44)$$

This approach is useful in order to do perturbation theory, thus if

$$\langle \delta\varphi^2(\vec{x},t)\rangle \ll \varphi_0^2(t) \quad (45)$$

we can perform expansions in orders of the fluctuations.
Furthermore, the fact that $\langle\delta\varphi\rangle = 0$ means that Eq.45 is indeed the variance of the fluctuation of φ.

3.2.1 *Classical Dynamics*

The background value $\varphi_0(t)$ is an homogeneous and isotropic scalar field in FLRW, so we can associate an stress-energy tensor such as [42]

$$\begin{aligned} T^0_{\ 0} &= -\left[\frac{1}{2}\dot{\varphi}_0^2(t) + V(\varphi_0)\right] = -\rho_\varphi(t) , \\ T^i_{\ j} &= \left[\frac{1}{2}\dot{\varphi}_0^2(t) - V(\varphi_0)\right]\delta^i_{\ j} = \delta^i_{\ j}P_\varphi(t) , \end{aligned} \quad (46)$$

where $\rho_\varphi(t)$ is the energy density and $P_\varphi(t)$ the isotropic pressure[16]. The fact that $T_{\mu\nu}$ is diagonal and the spatial part is the same in every direction is a consequence of isotropy and homogeneity, resulting in a tensor typical of perfect fluids.
Also, from the first relation, we can intuitively think of φ as a classical degree

16 In the following we will refer to background field with φ and fluctuations with δφ, without writing every time φ_0.

of freedom. Recalling that for inflation it is required a negative isotropic pressure $P_\varphi < 0$, we can see that taking $V(\varphi) \gg \frac{1}{2}\dot{\varphi}^2$ brings to $P_\varphi \approx -V(\varphi) \approx -\rho_\varphi$, which gives rise to a quasi-de-Sitter phase.
This can be achieved simply considering a sufficiently flat potential. Suppose that initially we have the unsuitable (for inflation) condition $\frac{1}{2}\dot{\varphi}^2 \gg V(\varphi)$; therefore, from Eq.46 $\omega_\varphi = \frac{P_\varphi}{\rho_\varphi} = 1$ and knowing the energy density scaling with the scale factor, we obtain $\rho_\varphi \sim \rho_{KIN} \propto a^{-3(1+\omega_\varphi)} = a^{-6}$. Due to this strong dependency and a sufficiently flat potential configuration, the latter will come to dominate, washing completely away the kinetic energy. This is called *slow-roll* regime, during which one realizes inflation: $V(\varphi) \simeq$ constant provides accelerated expansion driven by the vacuum energy density of φ, which mimics an effective Λ.
Most importantly, this solution is an attractor because, whatever are the initial conditions of kinetic energy and potential, at some point this regime will make the potential to act as a cosmological constant, allowing also some dynamics to it, enabling to exit inflation. As aforementioned this attractive behavior is crucial to avoid fine tuning issues and other artifacts.

3.2.2 *Equation of Motion*

The equation of motion for the scalar field φ comes from the variational principle[17] [43]

$$\frac{\delta S}{\delta \varphi} = 0 \rightarrow \Box\varphi = \frac{\partial V}{\partial \varphi}\,, \tag{47}$$

where the D'Alambertian operator $\Box$ in a curved spacetime gives

$$\varphi^{;\mu}{}_{;\mu} = \frac{1}{\sqrt{-g}}(g^{\mu\nu}\sqrt{-g}\,\varphi_{;\mu})_{;\nu}\,. \tag{48}$$

In a spatially flat ($\kappa = 0$) FLRW spacetime $\sqrt{-g} = a^3(t)$, therefore

$$\Box\varphi = -\ddot{\varphi} - 3H\dot{\varphi} + \frac{\nabla^2\varphi}{a^2}\,. \tag{49}$$

The resulting equation is the Klein-Gordon (K-G) equation for a quantum scalar field in FLRW [18]

$$\ddot{\varphi} + 3H\dot{\varphi} - \frac{\nabla^2\varphi}{a^2} = -\frac{\partial V}{\partial \varphi}\,. \tag{50}$$

Through $3H\dot{\varphi}$ the field "feels" a friction due to the expansion of the Universe, which will play a crucial role in the following paragraphs.

17 The plus sign in front of the derivative of the potential come from the metric signature $(-,+,+,+)$.

18 Having considered $\kappa \neq 0$ would have only changed the explicit expression of ∇^2, but the equation would have appeared in the same form.

Focusing on the background field $\varphi_0(t) \equiv \varphi(t)$ as in Eq.44, we can study the background dynamics

$$\begin{cases} \ddot{\varphi} + 3H\dot{\varphi} = -\frac{\partial V}{\partial \varphi} \\ H^2 = \frac{8\pi G}{3}\left(\frac{1}{2}\dot{\varphi}^2 + V(\varphi)\right) = \frac{8\pi G}{3}\rho_\varphi \end{cases} \quad [19]. \tag{51}$$

Let us now introduce two conditions required to realize inflation for a sufficiently long amount of time while solving the Big-Bang shortcomings.
We have already presented the *first slow-roll condition*

$$V(\varphi) \gg \dot{\varphi}^2 \, , \tag{53}$$

which brings the potential to dominate over the kinetic energy during inflation. This is realized if the potential is sufficiently flat w.r.t. φ. Furthermore, we expect that also its derivatives w.r.t. φ depend weakly on φ[20].
Then, we can introduce a *second slow-roll condition*

$$\ddot{\varphi} \ll 3H\dot{\varphi} \, , \tag{54}$$

which brings to

$$\dot{\varphi} \sim -\frac{V'}{3H} \, . \tag{55}$$

This means that Eq.51 are expressed as functions of $a(t)$ and $\varphi(t)$ once the model, i.e. the potential $V(\varphi)$, is specified.

3.2.3 *Slow-roll Parameters*

Now we need a way to quantify the slow-roll regime dynamics in order to give predictions of specific models and to compare it with others and with observations. In particular, we will make use of the so-called *slow-roll parameters* ε and η.
Firstly, from an intuitive point of view one can check how much H changes during inflation in order to define ε. In fact, in the cosmological constant

19 In full generality we would have to account also for other contributions to the Hubble rate as

$$H^2 = \frac{8\pi G}{3}(\rho_\varphi + \rho_r + \rho_m) - \frac{k}{a^2} \, , \tag{52}$$

however $\rho_m \propto a^{-3}$, $\rho_r \propto a^{-4}$, $\rho_k \propto a^{-2}$ and $\rho_\varphi \simeq V(\varphi) \simeq$ constant, so the latter will come to dominate resulting in $a \simeq e^{Ht}$. This strong dependency of the other energy densities will wash them away very proficiently, so we can safely neglect them.

20 Here, we will indicate the derivative w.r.t. φ as $' \equiv \frac{\partial}{\partial \varphi}$. Be aware of the ambiguity with the derivative on conformal time, which however can be easily solved looking at the contects.

case H is a constant, thus we can expect that adding some dynamics to the system would make H to change. Thus we define [42]

$$\varepsilon \equiv -\frac{\dot{H}}{H^2} \,. \tag{56}$$

Using the Friedmann equations and the attractor solution, one can show that the first slow-roll parameter can be expressed as

$$\varepsilon \simeq \frac{3}{2}\frac{\dot{\varphi}^2}{V(\varphi)} \simeq \frac{1}{16\pi G}\left(\frac{V'}{V}\right)^2 \,. \tag{57}$$

Therefore, we can interpret ε as the ratio between the kinetic energy and the potential. Hence assuming $V(\varphi) \gg \dot{\varphi}^2$, one obtains

$$\varepsilon \ll 1 \,. \tag{58}$$

Furthermore, if $\varepsilon \ll 1$, V' is small and the potential is flat. In this sense ε quantifies the flatness of the potential.

Exploiting now the second slow-roll condition $\ddot{\varphi} \ll 3H\dot{\varphi}$, we can define the second slow-roll parameter as [42]

$$\eta \equiv -\frac{\ddot{\varphi}}{H\dot{\varphi}} \ll 1 \,. \tag{59}$$

Again, one can show that

$$\eta \simeq \frac{V''}{3H^2} - \frac{\dot{H}}{H^2}\frac{V'}{3H\dot{\varphi}} \simeq \eta_V - \varepsilon \,, \tag{60}$$

where $\frac{V'}{3H\dot{\varphi}} \simeq -1$ and $\eta_V \equiv \frac{V''}{3H^2} \simeq \frac{1}{8\pi G}\frac{V''}{V}$ since during slow-roll H^2 is dominated by the potential. Thus again, having $\eta \ll 1$, means to have a flat potential.
Indeed ε alone can be sufficient to realize inflation when $\varepsilon < 1$, however having also $\eta \ll 1$ will assure that inflation lasts for long enough.
ε and η_V are merely the first two parameters of a whole hierarchy of higher order ones, but generally one considers only these two. Also, at first order, they can be considered as constants.
It is also interesting to notice that in the simple case of a single-field scalar inflation ε is always positive, given that $\dot{H} < 0$.

3.3 QUANTUM FLUCTUATIONS OF THE INFLATON FIELD

How is it possible to generate cosmological perturbations $\frac{\delta\rho}{\rho}$ on large cosmological scales, $\lambda \gg H^{-1}$, from the fluctuations $\delta\varphi$ of the inflaton field? Let us start from the Equation Of Motion (EOM) for the inflaton

$$\ddot{\varphi} + 3H\dot{\varphi} - \frac{\nabla^2\varphi}{a^2} = -\frac{\partial V}{\partial\varphi} \,. \tag{61}$$

Looking for the background evolution one obtains Eq.44; however including the perturbations and focusing on the linear level, one obtains the following relations [43]

$$\begin{cases} \ddot{\delta\varphi} + 3H\dot{\delta\varphi} - \frac{\nabla^2\delta\varphi}{a^2} = -V''\delta\varphi \\ (\dot{\varphi_0})^{\cdot\cdot} + 3H(\dot{\varphi_0})^{\cdot} = -V''\dot{\varphi_0} \end{cases} . \tag{62}$$

Indeed on large-scales where $\lambda_{phys} \gg H^{-1} \iff k \ll aH$, $\dot{\varphi_0}$ and $\delta\varphi$ evolve following the same identical equation. Looking at the Wronskian, one can indeed notice that they are related; specifically [42]

$$\delta\varphi(\vec{x}, t) = -\delta t(\vec{x})\dot{\varphi}_0(t) \,. \tag{63}$$

In other words, the perturbation can be thought as a slight time shift of the evolution of φ_0. Quantitatively, the scalar field is related to its background evolution as [42]

$$\varphi(\vec{x}, t) = \varphi_0(t - \delta t(\vec{x})) \,. \tag{64}$$

Thus, on large scales φ will assume the same value φ_0 everywhere, making every point in the Universe experience the same history, but at slightly different times.

3.3.1 *Approximated Solutions*

Eq.62 can be solved easily in Fourier space, where

$$\delta\varphi(\vec{x}, t) = \frac{1}{(2\pi)^3}\int d^3k e^{i\vec{k}\cdot\vec{x}}\delta\varphi(k, t) \,, \tag{65}$$

with $\delta\varphi(k,t) = \delta\varphi^*(k,t)$, since $\delta\varphi(\vec{x},t)$ is real[21], and where different modes as $\delta\varphi(k,t)$ and $\delta\varphi(k',t)$ evolve independently (only at linear level). The EOM reads, for a given Fourier component,

$$\delta\ddot{\varphi}_k + 3H\delta\dot{\varphi}_k + \frac{k^2\delta\varphi_k}{a^2} = -V''\delta\varphi_k \,. \tag{66}$$

We must now quantize the field, considering a field rescaled as $\delta\varphi \equiv \frac{\delta\widehat{\varphi}}{a(t)}$, hence [43]

$$\delta\widehat{\varphi}(\eta,\vec{x}) = \frac{1}{(2\pi)^3}\int d^3k \left[u_k(\eta)\widehat{a}_k e^{-i\vec{k}\cdot\vec{x}} + u_k^*(\eta)\widehat{a}_k^\dagger e^{i\vec{k}\cdot\vec{x}}\right] \,, \tag{67}$$

where $\widehat{a}, \widehat{a}^\dagger$ are the annihilation and creation operators, $a_k|0\rangle = 0\ \forall\ k$ and η is the conformal time. Here $|0\rangle$ is the free vacuum state, because linearizing we are not considering any interaction, exception made for the quadratic term giving mass to the field.
The normalization condition for $u_k(\eta)$ is [22] $u_k^*(\eta)u_k'(\eta) - u_k(\eta)u_k^{*\prime}(\eta) = -i$, which ensures the canonical quantization conditions for $\widehat{a}, \widehat{a}^\dagger$ operators [43]:

$$[\widehat{a}_k, \widehat{a}_{k'}] = 0\,; \qquad \left[\widehat{a}_k, \widehat{a}_{k'}^\dagger\right] = \hbar\,\delta^3(k-k') \,. \tag{68}$$

In a flat spacetime

$$u_k(\eta) = \frac{e^{-i\omega_k\eta}}{\sqrt{2\omega_k}} \quad \text{with} \quad \omega_k = \sqrt{k^2+m^2} \,, \tag{69}$$

but in a curved spacetime u_k is not necessarily a plane wave; there is indeed an ambiguity in the definition of the vacuum state. At early times and small scales $k \gg aH$, we have $\omega_k \sim k$ and we require to be able to reproduce a flat spacetime metric, due to the equivalence principle, thus we can assume

$$u_k(\eta) \approx \frac{e^{-ik\eta}}{\sqrt{2k}} \,. \tag{70}$$

These requirements are called the *Bunch-Davis vacuum choice*. Let us obtain the K-G equation in Fourier space starting by Eq.61. Passing to conformal time it gets recast to

$$\varphi'' + 2\frac{a'}{a}\varphi' - \nabla^2\varphi = -a^2\frac{\partial V}{\partial\varphi} \,, \tag{71}$$

21 We use 3d Fourier transform because it is not invariant under time translation, and we use plane waves to transform because spatially flat FLRW is assumed, for $\kappa \neq 0$ we have to use solutions of Helmholtz equation: $\nabla^2 Q_k + k^2 Q_k = 0$.

22 Here we use $' = \frac{\partial}{\partial\eta}$.

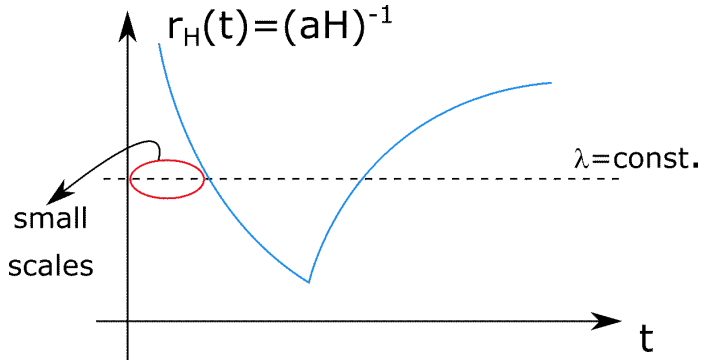

Figure 5: Hubble comoving radius with small scales highlighted.

thus looking at the perturbation one obtains

$$\delta\varphi'' + 2\frac{a'}{a}\delta\varphi' - \nabla^2\delta\varphi = -a^2\frac{\partial^2 V}{\partial\varphi^2}\delta\varphi \,. \tag{72}$$

Applying then $\delta\varphi = \frac{\delta\widehat{\varphi}}{a(\eta)}$, we get

$$\delta\widehat{\varphi}'' - \frac{a''}{a}\delta\widehat{\varphi} - \nabla^2\delta\widehat{\varphi} = -a^2\frac{\partial^2 V}{\partial\varphi^2}\delta\widehat{\varphi} \,. \tag{73}$$

At this point, going to Fourier space and using $|\delta\widehat{\varphi}_k| = |u_k|$, we can finally write [43]

$$u_k''(\eta) + \left[k^2 - \frac{a''}{a} + \frac{\partial^2 V}{\partial\varphi^2}a^2\right] u_k(\eta) = 0 \,. \tag{74}$$

This equation describes an harmonic oscillator with a frequency changing in time, due to the expansion of the Universe.

Considering a massless scalar field, $m_\varphi^2 = V''(\varphi) = 0$ in pure de-Sitter ($H = \text{constant}$), the equation is

$$u_k''(\eta) + \left[k^2 - \frac{a''}{a}\right] u_k(\eta) = 0 \,. \tag{75}$$

Before studying more in depth the solutions to this equation, let us firstly clarify the role of conformal time. We know that it is related to the cosmic time through $a\,d\eta = dt$, thus in this case we can write

$$d\eta \propto \frac{dt}{e^{Ht}} \quad\longrightarrow\quad \eta \propto -\frac{1}{H}e^{-Ht} = -\frac{1}{aH} < 0 \,, \tag{76}$$

hence during inflation η belongs to $]-\infty\ ,\ 0[$. So, we can relate

$$\frac{a''}{a} = \frac{2}{\eta^2} = 2a^2H^2 = \frac{2}{r_H^2}\ . \tag{77}$$

Let us now solve the EOM of u_k in two different regimes:

1. **Sub-horizon**: we have $\lambda_{\text{phys}} \ll H^{-1} \longleftrightarrow k \gg aH \to \frac{a''}{a}$, thus the EOM reduces to

$$u_k'' + k^2 u_k = 0 \longrightarrow u_k(\eta) = \frac{1}{\sqrt{2k}} e^{-ik\eta}\ , \tag{78}$$

whereas an oscillating solution. For what regards the field

$$\delta\varphi_k = \frac{u_k}{a} = \frac{1}{a}\frac{1}{\sqrt{2k}} e^{-ik\eta}\ , \tag{79}$$

from which we can notice that it has a decreasing amplitude $|\delta\varphi| = \frac{1}{a\sqrt{2k}}$, which depends on the inverse of a, so during inflation it decreases extremely fast.

2. **Super-horizon**: we have $\lambda_{\text{phys}} \gg H^{-1} \longleftrightarrow k \ll aH \to \frac{a''}{a}$, thus the EOM reduces to

$$u_k'' - \frac{a''}{a} u_k = 0\ . \tag{80}$$

This kind of equations are solved by [43]

$$u_k(\eta) = B(k)a(\eta) + A(k)a^{-2}(\eta)\ , \tag{81}$$

where A, B are integration constant in η which depends on k. In terms of the field we get

$$\delta\varphi_k = B(k) + A(k)a^{-3}(\eta) \simeq B(k) = \text{constant}\ , \tag{82}$$

where we have neglected the decaying term which gets washed away by inflation. Such a frozen solution makes sense intuitively if one argue that microphysics cannot play any role in such large scales phenomena. We can find the amplitude in this regime making a matching between the two regimes at horizon crossing, since from that moment on it will get constant. At horizon-crossing $k = aH$, thus

$$u_k^{sup} = |B(k)|a = \frac{1}{\sqrt{2k}}\Big|_{k=aH} = u_k^{sub}\ , \tag{83}$$

therefore

$$|\delta\varphi_k| = |B(k)| = \frac{1}{a\sqrt{2k}}\Big|_{k=aH} = \frac{H}{\sqrt{2k^3}}\ . \tag{84}$$

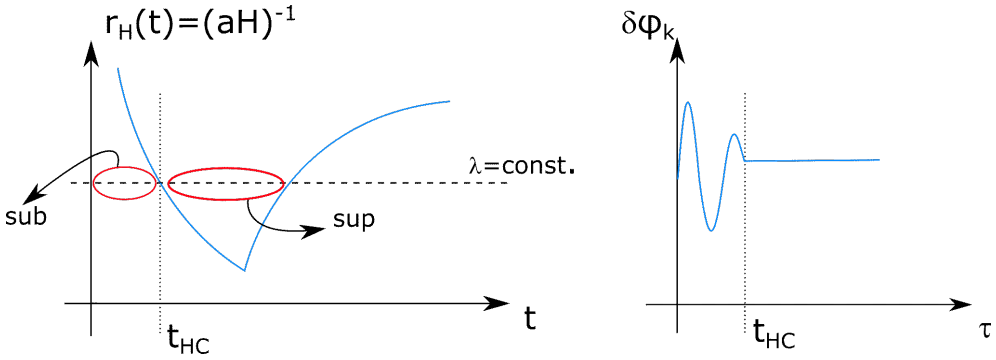

Figure 6: Panel (a): Hubble comoving radius with both small and large scales highlighted. Panel (b): Passage from a zero average perturbation to a classical one.

In general averaging on sub-horizon scales one gets $\langle\delta\varphi\rangle_t = 0$ if t is a macroscopic time interval. However, we are considering an expanding background in which $\lambda_{phys} \propto a \propto e^{Ht}$. This means that fluctuations do not remain on the vacuum state, but fluctuations get frozen and $\langle\delta\varphi\rangle \neq 0$. In other words, we are generating classical perturbations of φ, so in some sense we have realized a state characterized by a net number of particles.
Finally, one can show that the exact solution of massless scalar field in pure de-Sitter is [18]

$$u_k(\eta) = \frac{e^{ik\eta}}{\sqrt{2k}}\left(1 - \frac{i}{k\eta}\right) \qquad \forall\, k \quad \text{and} \quad \forall\eta\,, \tag{85}$$

which gives the aforementioned solutions in the two asymptots.

3.3.2 *Exact Solutions in Quasi de-Sitter Spacetime*

Let us now consider a massless scalar field in quasi de-Sitter, reminding that the slow-roll parameter is $\varepsilon \equiv -\frac{\dot{H}}{H^2} \ll 1$. By definition of conformal time, as we have done before, we can write [43]

$$\eta \simeq -\frac{1}{aH(1-\varepsilon)}\,, \qquad \frac{a''}{a} = \frac{2}{\eta^2}\left[1 + \frac{3}{2}\varepsilon\right]\,, \tag{86}$$

at lowest order in ε. The EOM can be rewritten in terms of the slow-roll parameter as

$$u_k''(\eta) + \left[k^2 - \frac{\nu^2 - \frac{1}{4}}{\eta^2}\right] u_k(\eta) = 0, \tag{87}$$

where $\nu = \frac{9}{4} + 3\varepsilon$. In this form, it is equivalent to the Bessel equation [49]

$$z^2 y''(z) + z y'(z) + (z^2 - \nu^2) y(z) = 0\,, \tag{88}$$

whose solutions are known to be of the form [43]

$$u_k(\eta) = \sqrt{-\eta}\left[c_1(k)H_\nu^{(1)}(-k\eta) + c_2(k)H_\nu^{(2)}(-k\eta)\right] \text{ [23]}, \tag{89}$$

- On sub-horizon scales we require $u_k(\eta) \sim \frac{e^{-ik\eta}}{\sqrt{2k}}$ for $\left(\frac{k}{aH}\right) \to \infty$, so introducing $x = -k\eta$ and given that

$$H_\nu^{(1)}(x) \simeq \sqrt{\frac{2}{\pi x}} e^{i\left(x-\frac{\pi}{2}\nu-\frac{\pi}{4}\right)} \xrightarrow{x\gg 1} \frac{e^{ix}}{\sqrt{x}}\sqrt{\frac{2}{\pi}}\,, \tag{90}$$

  we must impose $c_2(k) = 0$ and $c_1(k) = \frac{\sqrt{\pi}}{2}\exp\left\{i\left(\nu+\frac{1}{2}\right)\frac{\pi}{2}\right\}$, resulting in [43]

$$u_k(\eta) = \sqrt{-\eta}\frac{\sqrt{\pi}}{2}\exp\left\{i\left(\nu+\frac{1}{2}\right)\frac{\pi}{2}\right\}\frac{e^{-ik\eta}}{\sqrt{-k\eta}}\,. \tag{91}$$

- On super-horizon scales ($k \ll aH$), we have instead

$$H_\nu^{(1)}(x) \simeq \sqrt{\frac{2}{\pi}} e^{-\frac{\pi}{2}} 2^{\nu-\frac{3}{2}} \left(\frac{\Gamma(\nu)}{\Gamma(\frac{3}{2})}\right) x^{-\nu} \xrightarrow{x\ll 1} x^{-\nu} \text{ [24]}, \tag{92}$$

  where $\nu^2 = \frac{9}{4} + 3\varepsilon \to \nu \simeq \frac{3}{2} + \varepsilon$, therefore $\nu - \frac{3}{2} = \varepsilon$. Thus [43]

$$u_k(\eta) \simeq \frac{1}{\sqrt{2k}} e^{i(\nu-\frac{1}{2})\frac{\pi}{2}} 2^{\nu-\frac{3}{2}} \left(\frac{\Gamma(\nu)}{\Gamma(\frac{3}{2})}\right) (-k\eta)^{\frac{1}{2}-\nu}\,. \tag{94}$$

  The solution for the perturbation is, using $\frac{1}{a} \propto -\eta$ at lowest order in the slow roll parameters

$$|\delta\varphi_k| = \frac{|u_k|}{a} = 2^{\nu-\frac{3}{2}} \left(\frac{\Gamma(\nu)}{\Gamma(\frac{3}{2})}\right) \frac{H}{\sqrt{2k^3}} \left(\frac{k}{aH}\right)^{\frac{3}{2}-\nu}\,, \tag{95}$$

  which can be approximated by

$$|\delta\varphi_k| \simeq \frac{H}{\sqrt{2k^3}} \left(\frac{k}{aH}\right)^{\frac{3}{2}-\nu}\,, \tag{96}$$

23 $H_\nu^{(i)}(-k\eta)$ are the Hankel functions of i^{th} species and order ν [49]. Also, it holds $H_\nu^{(2)}(-k\eta) = H_\nu^{(1)*}(-k\eta)$. Instead, the c_i are integration constants.

24 Here, $\Gamma(x)$ is the Euler-Gamma function [49], defined as

$$\Gamma(z) \equiv \int_0^\infty x^{z-1}e^{-x}\,dx \quad \text{for} \quad \mathrm{Re}\,(z) > 0\,. \tag{93}$$

where one can notice that the de-Sitter solution is recovered with $\varepsilon = 0 \iff \nu = \frac{3}{2}$.
Being *quasi* de-Sitter switches on a scale dependency on $k^{-\varepsilon}$, which is a unique prediction of inflationary models

The form of this solution is maintained even if we consider more general frameworks. In particular in the most general case, one considers a massive inflaton and substitutes to the perturbations $\delta\varphi$ the so-called Sasaki-Mukhanov variable [42]

$$Q_\varphi \equiv \delta\varphi + \frac{\dot{\varphi}}{H}\widehat{\phi} \,, \tag{97}$$

where $\widehat{\phi}$ is related to the scalar perturbations of the spatial part of the metric δg_{ij},

$$g_{ij} = a^2(\eta)\left[(1-2\phi)\delta_{ij} + \chi_{ij}\right] \,. \tag{98}$$

One can show that even in this case the following holds [43]

$$\widehat{Q}_\varphi''(\eta) + \left[k^2 - \frac{\nu^2 - \frac{1}{4}}{\eta^2}\right]\widehat{Q}_\varphi(\eta) = 0 \,, \tag{99}$$

with $\nu^2 = \frac{9}{4} + 9\varepsilon - 3\eta_\nu$, thus at first order $\frac{3}{2} - \nu \simeq \eta_\nu - 3\varepsilon$. The amplitude will be

$$|Q_\varphi| \simeq \frac{H}{\sqrt{2k^3}}\left(\frac{k}{aH}\right)^{\frac{3}{2}-\nu} \,, \tag{100}$$

which is the most general solution we can consider.

3.3.3 *Gravitational Waves from Inflation*

As aforementioned the perturbations of the inflaton will induce perturbations of the metric. These disturbances constitute a stochastic background of GWs which are represented by tensor perturbations of the metric.
A stochastic background of waves is a continuous set of waves, fully characterized only by their global statistical properties. Indeed, they consist of a signal coming from every direction in the sky and having a whole spectrum in the frequency domain, whereas, e.g. a single couple of merging neutron stars produces GW which come from a specific direction in the sky and are peaked at a specific frequency at coalescence[25].

25 Indeed, if we consider a large enough quantity of merging astrophysical objects, one can obtain the astrophysical analogue of the cosmic GW background, i.e. an AGWB. The only requirement is to have a sufficiently high amount of objects (called the confusion limit) in order not to be able to distinguish one from the other in our detectors.

The perturbed spatially flat FLRW metric is, neglecting scalar and vector perturbations[26],

$$ds^2 = -dt^2 + a^2(t)\left[\delta_{ij} + h_{ij}\right] dx_i dx_j \,, \tag{101}$$

with h_{ij} such that

$$h_{ij} = h_{ji} \quad , \quad h^i{}_i = 0 \quad , \quad h^i{}_{j|i} = 0 \text{ [27]}. \tag{102}$$

The gauge bringing to these relations is called Transverse-Traceless (TT) gauge.

At linear level, the EOM for h_{ij} reads [42]

$$\ddot{h}_{ij} + 3H\dot{h}_{ij} - \frac{\nabla^2 h_{ij}}{a^2} = \Pi^{TT}_{ij} \,, \tag{103}$$

where Π^{TT}_{ij} is a tensor with the same properties as Eq.102, which is a source term coming from possible anisotropic stress of the matter source. It is related to the last term of the stress-energy tensor of a perfect fluid $T_{\mu\nu} = (\rho + P)u_\mu u_\nu + P g_{\mu\nu} + \pi_{\mu\nu}$, called anisotropic stress tensor, which for example can get a contribution by the quadrupole momentum of two merging objects. At first order, it is vanishing for single field inflation, therefore during inflation holds

$$\ddot{h}_{ij} + 3H\dot{h}_{ij} - \frac{\nabla^2 h_{ij}}{a^2} = 0 \,, \tag{104}$$

which is the same equation we solved for the quantum vacuum fluctuation of a massless scalar field. Here we are looking to the quantum fluctuations of the metric itself, since there is no source term. Cosmological GWs are the result of intrinsic quantum fluctuations of the metric, and, if we will be able to detect them, we will have found a "smoking gun" of inflation. Also, they would be the first ever detected evidence of quantum gravity.

Eq.104 describes the evolution of a tensor object, with 2 independent Degree Of Freedom (DOF)[28], corresponding to the two possible polarizations of GWs $\lambda = (+, \times)$. We can decompose such object in Fourier space as [42]

$$h_{ij}(\vec{x}, \eta) = \sum_{+\times} \int \frac{d^3k}{(2\pi)^3} e^{i\vec{k}\vec{x}} h_\lambda(\vec{k}, \eta) \varepsilon^\lambda_{ij}(\vec{k}) \,, \tag{105}$$

26 At linear level scalar, vector and tensor perturbations are decoupled, meaning that their evolution do not depend on one another. For this reason considering only the tensor ones is not a physical simplification, but only a way to obtain easier calculi.

28 h_{ij} is a 3×3 object, symmetric condition reduces the 9 initial DOF into 6, while "traceless" and "transverse" conditions consist in other 4 constraints. Therefore h_{ij} has 2 DOF

where $\varepsilon^{\lambda}_{ij}(\vec{k})$ are the polarization tensors, which satisfy $\forall\lambda$

$$\varepsilon_{ij} = \varepsilon_{ji} \quad , \quad \varepsilon^{i}{}_{i} = 0 \quad , \quad k^{i}\varepsilon_{ij}(\vec{k}) = 0, \tag{106}$$

and the normalization conditions

$$\varepsilon^{\lambda}_{ij}(\vec{k})\varepsilon^{*ij}_{\lambda'}(\vec{k}) = \delta_{\lambda\lambda'} \quad , \quad \left(\varepsilon^{\lambda}_{ij}(\vec{k})\right)^{*} = \varepsilon^{\lambda}_{ij}(-\vec{k}) \, . \tag{107}$$

Suppose to have a plane monochromatic gravitational wave propagating in the $\hat{z}$ direction, in Fourier space we obtain

$$\varepsilon^{+}_{ij} = \begin{pmatrix} 1 & 0 \\ 0 & -1 \end{pmatrix} \quad , \quad \varepsilon^{\times}_{ij} = \begin{pmatrix} 0 & 1 \\ 1 & 0 \end{pmatrix} \quad , \tag{108}$$

$$h_{ij}(\vec{k},\eta) = h_{+}(\vec{k},\eta)\varepsilon^{+}_{ij}(\vec{k}) + h_{\times}(\vec{k},\eta)\varepsilon^{\times}_{ij}(\vec{k}) \, . \tag{109}$$

The EOM in Fourier becomes

$$\ddot{h}_{\lambda} + 3H\dot{h}_{\lambda} + k^{2}\frac{h_{\lambda}}{a^{2}} = 0 \, , \tag{110}$$

which is the same for each polarization state and it is again analog to the equation of motion of a minimally coupled scalar field ($h_{+,\times} \leftrightarrow \sqrt{32\pi G}\phi_{+,\times}$). On super horizon scales, $k \ll aH$, the solution is $h_{+,\times}$ =constant plus a decaying mode. The amplitude is, due to canonical normalization [42]:

$$|h_{+,\times}| = \sqrt{32\pi G}|\phi_{+,\times}| = \sqrt{32\pi G}\frac{H}{\sqrt{2k^{3}}}\left(\frac{k}{aH}\right)^{-\varepsilon} . \tag{111}$$

On sub horizon scales, $k \gg aH$, $h_{+,\times} = \frac{e^{-ik\eta}}{a(\eta)}$.

3.3.4 *Correlation Functions and Power Spectrum*

In order to compare theoretical predictions with observations, we must introduce what are the observable quantities related to these fluctuations. Quantum fluctuations are not deterministic, but can described by a quantum random field $\delta\varphi(\vec{x},t)$ which describes the amplitude of these fluctuations in each point of spacetime. These fluctuations however are correlated through different points. In fact, even if the ensemble average is zero by definition (it is in fact the vacuum expectation value), one can compute the two point correlation function

$$\xi \equiv \langle \delta(\vec{x}+\vec{r},t)\,\delta(\vec{x},t)\rangle \, . \tag{112}$$

If we take the two point correlation function of the Fourier transform of a generic stochastic field

$$\delta(\vec{x},t) = \frac{1}{(2\pi)^3}\int d^3k e^{i\vec{k}\cdot\vec{x}}\delta_k(t)\,, \tag{113}$$

the result is

$$\langle\delta(\vec{k},t)\,\delta(\vec{k}',t)\rangle = (2\pi)^3 P(k)\delta^3(\vec{k}+\vec{k}')\ ^{29}\,, \tag{114}$$

which in a homogeneous and isotropic Universe is a function of $|\vec{r}|$ [30] and where P is the *power spectrum*. It depends only on the modulus of $\vec{k}$ due to isotropy, the presence of the delta function comes due to homogeneity.
Furthermore, the power spectrum P is the Fourier transform of ξ, namely using Eq.114

$$\xi(\vec{r}) = \frac{1}{(2\pi)^3}\int d^3k' e^{i\vec{k}'\vec{r}} P(k_1)\,. \tag{116}$$

The variance results

$$\langle\delta^2(\vec{x},t)\rangle = \xi(0) = \frac{1}{2\pi^2}\int_0^\infty \frac{dk}{k}k^3P(k) = \int_0^\infty \frac{dk}{k}\Delta(k)\,, \tag{117}$$

where we defined the *adimensional power spectrum* as $\Delta(k) \equiv \frac{k^3}{2\pi^2}P(k)$, which is the contribution to the variance per logarithmic integral. It is mostly used in Cosmology, more than $P(k)$, for inflationary physics.
For the inflaton field quantum fluctuations $|\delta\varphi_k| = \frac{|u_k|}{a}$ [43],

$$\langle\delta\varphi_{\vec{k}_1},\delta\varphi^*_{\vec{k}_2}\rangle = (2\pi)^3|\delta\varphi_{\vec{k}_1}|^2\delta^3(\vec{k}_1-\vec{k}_2)\,, \tag{118}$$

therefore [42]

$$P(k) = |\delta\varphi_k|^2 = \frac{|u_k|^2}{a^2} \qquad \rightarrow \qquad \Delta(k) = \frac{k^3}{2\pi^2}\frac{|u_k|^2}{a^2}\,. \tag{119}$$

On super horizon scales, $\delta\varphi_k = \frac{H}{\sqrt{2k^3}}\left(\frac{k}{aH}\right)^{\frac{3}{2}-\nu}$

$$P_\varphi(k) = \frac{H^2}{2k^3}\left(\frac{k}{aH}\right)^{3-2\nu} \qquad \Delta_\varphi(k) = \left(\frac{H}{2\pi}\right)^2\left(\frac{k}{aH}\right)^{3-2\nu}\,, \tag{120}$$

29 An equivalent definition of power spectrum is

$$\langle\delta(\vec{k},t)\,\delta^*(\vec{k}',t)\rangle = (2\pi)^3 P(|\vec{k}|)\delta^3(\vec{k}-\vec{k}') \tag{115}$$

since $\delta(\vec{x},t)$ is real we have $\delta^*(\vec{k},t) = \delta(-\vec{k},t)$.
In addition, the notation in Fourier space reads $\delta(\vec{k},t) = \delta_{\vec{k}}(t)$.

30 It is very similar to a propagator, but it regards only the spatial part.

where in the most general case $3-2\nu = 2\eta_V - 6\varepsilon$ [44]. We can then define the *spectral index* $n(k)$ as [42]

$$n(k) - 1 \equiv \frac{d\ln\Delta(k)}{d\ln k}\,, \tag{121}$$

which describes the shape of the power spectrum.

1. $n = 1 \leftrightarrow$ Harrison-Zel'dovich (H-Z) spectrum: it means that the amplitude of $\delta\varphi$ does not depend on the cosmological scale.

2. $n =$ constant $\leftrightarrow \Delta(k)$ can be written w.r.t. a "pivot scale" k_0 as

$$\Delta(k) = \Delta(k_0)\left(\frac{k}{k_0}\right)^{n-1}. \tag{122}$$

n and $\Delta(k_0)$ are indeed the two main observables one can constrain observing the CMB.

3.3.5 *Super-horizon Perturbations*

Firstly, let us introduce a couple of definitions. ζ is called *curvature perturbation on uniform energy density hypersurfaces*:

i) ζ is a gauge invariant quantity defined as[31] [42]

$$\zeta \equiv -\widehat{\phi} - H\frac{\delta\rho}{\dot{\rho}}\,, \tag{123}$$

where $\delta\rho$ is the scalar perturbation of the energy density.
In the $\widehat{\phi} = 0$ gauge, therefore, we have

$$\zeta = -H\frac{\delta\rho}{\dot{\rho}}. \tag{124}$$

ii) This is a very general definition, since in the case of inflation the density is the density of the scalar field, but it also applies during all the evolution of the Universe:

$$\zeta \to \frac{\delta\rho_\varphi}{\dot{\rho}_\varphi},\quad \frac{\delta\rho_m}{\dot{\rho}_m},\quad \frac{\delta\rho_\gamma}{\dot{\rho}_\gamma},\quad \frac{\delta\rho_\Lambda}{\dot{\rho}_\Lambda}. \tag{125}$$

iii) On super horizon scales it is constant in time (in single field models of inflation)

$$\zeta\Big|_{t_H^{(1)}(k)} = \zeta\Big|_{t_H^{(2)}(k)}\,. \tag{126}$$

31 $\widehat{\phi}$ is related to the spatial perturbations of the metric $\delta g_{\mu\nu}$.

These properties give us the possibility to compare the amplitude of primordial inflaton perturbations with known quantities, as CMB temperature fluctuations.

Let us now suppose to look at two different scales λ, λ', where the latter re-enters during matter dominated epoch and the former during radiation domination. Let us then call $t_H^{(1)}(k)$ the time at which λ crosses out the horizon and $t_H^{(2)}(k)$ the time in which it re-enters. The same will apply to $\lambda' \to k'$. Thanks to Eq.126, we can compare density perturbation at the time of inflation with respect to radiation epoch

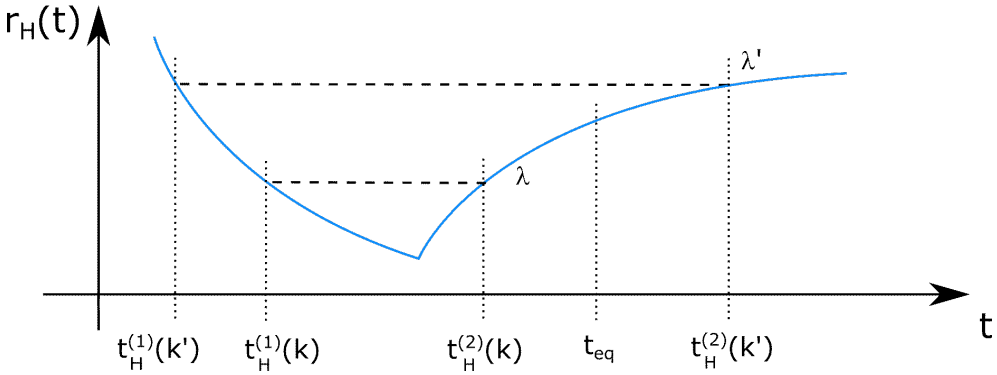

Figure 7: Comparison between different epochs using ζ conservation

$$\begin{aligned} \zeta\Big|_{t_H^{(1)}(k)} &= \zeta\Big|_{t_H^{(2)}(k)} \\ -H\,\frac{\delta\varphi}{\dot{\varphi}}\Big|_{t_H^{(1)}(k)} &= \frac{1}{4}\,\frac{\delta\rho_\gamma}{\rho_\gamma}\Big|_{t_H^{(2)}(k)} \end{aligned}, \tag{127}$$

since during radiation domination the density is given by $\rho = \rho_\gamma \propto T^4 \to \frac{\delta\rho}{\rho} = 4\frac{\delta T}{T}$ and $\dot{\rho}_\gamma \simeq -4H\rho_\gamma$. In other words, there is a direct link between temperature fluctuation and primordial inflaton fluctuations

$$\zeta_\varphi \simeq \frac{\delta T}{T} \simeq 10^{-5}. \tag{128}$$

3.4 PRIMORDIAL DENSITY PERTURBATION

We have just seen that the adimensional power spectrum for primordial energy perturbations is related to the inflaton power spectrum (see Eq.127), thus

$$\Delta_{\frac{\delta\rho}{\rho}}(k) = \frac{H^2}{\dot{\varphi}^2}\Delta_{\delta\varphi}(k)\Big|_{t_H^{(1)}(k)} = \left(\frac{H^2}{2\pi\dot{\varphi}}\right)^2\left(\frac{k}{aH}\right)^{3-2\nu} = \\ = \left(\frac{H^2}{2\pi\dot{\varphi}}\right)^2\Bigg|_{t_H^{(1)}(k)} . \tag{129}$$

We can now compute the scalar spectral index of primordial density perturbations, which is one of the most important prediction of inflationary models, defined as [42]

$$n_s - 1 \equiv \frac{d\ln\Delta_{\frac{\delta\rho}{\rho}}(k)}{d\ln k} = 3 - 2\nu = 2\eta_\nu - 6\varepsilon\ . \tag{130}$$

Inflationary models predict a power spectrum of density perturbations to have a spectral index which deviates from one by $\mathcal{O}(\varepsilon,\eta)$. Indeed, we have found a power spectrum very close to H-Z [48]

$$n_s = 0.9671 \pm 0.0038 \quad \text{at} \quad 68\%\text{CL}\ , \tag{131}$$

but not exactly $n_s = 1$. The measured value is compatible with $n_s < 1$ at 8σ, which is a very robust statement.
Furthermore, a power spectrum classification is given in terms of its spectral index.

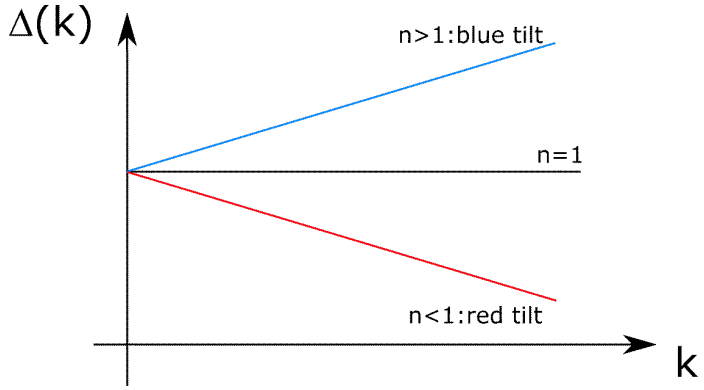

Figure 8: Spectral index classification. In a more general context, the distinction between blue/red tilted and scale-invariant spectra is made w.r.t. 0, where, respectively $n > 0$, $n < 0$ and $n = 0$. In this case, we use 1 as the watershed because we refer to the particular notation used for the spectrum in Eq.129. Notice, e.g., that for the tensor spectrum the former distinction is indeed valid (Eq.134).

3.5 STOCHASTIC BACKGROUND OF GWS

Let us analyze the power spectrum for a single polarization state of tensor perturbations of the metric, which corresponds to gravitational waves; remembering Eq.111 it is given by

$$\begin{aligned}\Delta_T^{+,\times}(k) =& 32\pi G\frac{k^3}{2\pi^2}|h_{+,\times}|^2 = 32\pi G\left(\frac{H}{2\pi}\right)^2\left(\frac{k}{aH}\right)^{-2\varepsilon}\\ =& \frac{8}{\pi}\left(\frac{H}{M_P}\right)^2\Big|_{t_H^{(1)}(k)}\,,\end{aligned} \tag{132}$$

where $t_H^{(1)}(k)$ is the time of horizon exit, in which the scale of gravitational waves gets fixed, and k is the GW one $k = \frac{2\pi}{\lambda_{GW}}$ [32]. The total power spectrum is the sum of the two polarizations

$$\Delta_T(k) = \frac{16}{\pi}\left(\frac{H}{M_P}\right)^2\Big|_{t_H^{(1)}(k)} = \frac{16}{\pi}\left(\frac{H}{M_P}\right)^2\left(\frac{k}{aH}\right)^{-2\varepsilon}\,. \tag{133}$$

Therefore the spectral index of inflationary GWs is defined as

$$n_T \equiv \frac{d\ln\Delta_T(k)}{d\ln k} = -2\varepsilon\,. \tag{134}$$

As aforementioned, in the simplest models one has $\varepsilon > 0$ so n_T is always red tilted, thus on smaller and smaller scales the amplitude decreases. This fact will play a key role in assessing the feasibility of a detection of such a background with future GW detectors (see e.g. [29]).
In addition, we can define the *tensor-to-scalar perturbation ratio* as [42]

$$r \equiv \frac{\Delta_T}{\Delta_{\frac{\delta\rho}{\rho}}} = \frac{\Delta_T}{\Delta_\zeta}\,. \tag{135}$$

One can notice that since Δ_T at horizon crossing depends only on H^2, measuring it would indeed provide us information of the energy scale of inflation because $V \simeq E_{INF}^4$. The present upper bound is $r_{0.002} < 0.06$ (95% CL) from CMB anisotropies [48][33], which results in $E_{INF} \approx 10^{15}\div10^{16}$, recalling GUTs.

We can also rewrite it as function of the slow-roll parameters. In fact reminding $\varepsilon = -\frac{\dot H}{H^2} = 4\pi G\frac{\dot\varphi^2}{H^2}$, we can express Δ_ζ as

$$\Delta_\zeta = \frac{H^4}{4\pi\dot\varphi^2}\Big|_{t_H} = \frac{H^2}{4\pi^2}\frac{4\pi G}{\varepsilon}\Big|_{t_H} = \frac{H^2}{\pi M_P^2\varepsilon}\,, \tag{136}$$

32 Also tensor perturbations remain constant on super horizon scales.
33 The subscript 0.002 indicates that a pivot scale of $0.002\,\mathrm{Mpc}^{-1}$ has been considered.

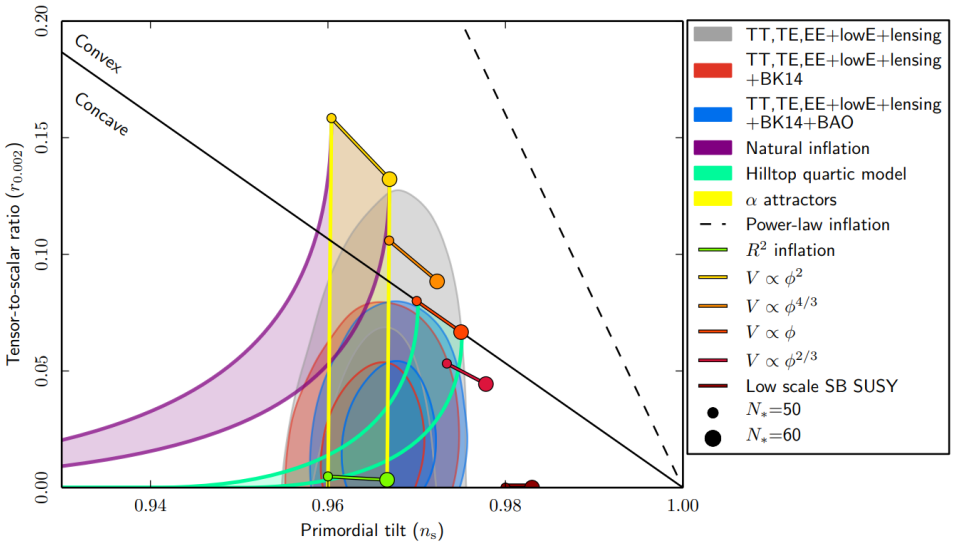

Figure 9: Marginalized joint 68% and 95% CL regions for n_S and r at $k = 0.002\ \mathrm{Mpc}^{-1}$. Note that the marginalized joint 68% and 95% CL regions assume $\frac{dn_S}{d\ln k} = 0$ (no index running) [50].

with which

$$r = \frac{\Delta_T}{\Delta_\zeta} = \frac{\frac{16H^2}{\pi M_P^2}}{\frac{H^2}{\pi M_P^2 \varepsilon}} = 16\varepsilon\ . \tag{137}$$

Also, since we know the spectral index of tensor modes, $n_T = -2\varepsilon$ we have the so-called *consistency relation of inflation* [42]

$$r = -8n_T\ , \tag{138}$$

which is a relation between two observable quantities. All inflationary models must obey this relation; observing it is a clear proof of inflation, given that there are no other scenarios in the early Universe providing this same prediction. This is not an easy task at all, it requires a full measurement of the CGWB in its amplitude and spectral index, but it would be so crucial to the Cosmology community that this is also referred to as *"holy grail of inflation"*.

4

COSMOLOGICAL GRAVITATIONAL WAVE BACKGROUND

At this point, we have seen the whole path bringing to one of the most important predictions of inflationary models, the CGWB, thus we can start focusing specifically onto it and on its characterization following a Boltzmann approach. This will be completely analogous to what is typically done for CMB photons.
In this case instead, we will study the evolution of the distribution function of gravitons in a FLRW Universe equipped with scalar and tensor perturbations. Specifically, we will focus on the description of the first order term of the distribution function through the final angular power spectrum.
The main reference for this chapter will be [25, 26], where the reader can find the complete treatment of the CGWB via the Boltzmann approach, here instead we will only report the equations and concepts useful to our purpose.

4.1 BOLTZMANN EQUATIONS

Firstly, exploiting the statistical nature of primordial GWs, we can define a distribution function for gravitons as $f = f(x^\mu, p^\mu)$, which in general depends on their position x^μ and momentum along their trajectory $p^\mu(x)$, parametrized by an affine parameter λ. This function will evolve according to the well-known Boltzmann equation[18, 51, 52]

$$\mathscr{L}[f(x^\mu, p^\mu)] = \mathscr{C}[f(x^\mu, p^\mu)] + \mathscr{I}[f(x^\mu, p^\mu)] \,, \tag{139}$$

where:

- $\mathscr{L}$ is the Liouville operator providing the evolution of the distribution function. Indeed, in General Relativity (GR), it can be written as

$$\mathscr{L} \equiv \frac{d}{d\lambda} = p^\alpha \frac{\partial}{\partial x^\alpha} - \Gamma^\alpha{}_{\beta\gamma} p^\beta p^\gamma \frac{\partial}{\partial p^\alpha} \,, \tag{140}$$

  where $\Gamma^\alpha_{\beta\gamma}$ are the Christoffel symbols associated to the considered metric.

- $\mathscr{C}$ is the collision operator accounting for GW scatterings. For a generic process involving a particle σ which interacts with other $\alpha = a, b, \ldots$ particles to produce $\beta = 1, 2, \ldots$ particles can be written as [44]

$$\begin{aligned}\mathscr{C}[f_\sigma] = -\int \prod_{\alpha=a,b,\ldots} \prod_{\beta=1,2,\ldots} d\Pi_\alpha d\Pi_\beta (2\pi)^4 \\ \times \delta^{(4)}(p_\sigma + p_a + p_b + \ldots - p_1 - p_2 - \ldots) \\ \times \Big[|\mathcal{M}|_{\sigma+a+b+\ldots\to 1+2+\ldots} f_\sigma f_a f_b \ldots (1 \pm f_1)(1 \pm f_2)\ldots \\ - |\mathcal{M}|^2_{1+2+\ldots\to\sigma+a+b+\ldots} f_1 f_2 \ldots (1 \pm f_\sigma)(1 \pm f_1)(1 \pm f_2)\ldots \Big] ,\end{aligned} \tag{141}$$

where: $d\Pi_\alpha \equiv g_\alpha \frac{d^3 p_\alpha}{(2\pi)^3 2E_\alpha}$;
g_α = intrinsic DOF of the species;
E_α = energy of the species;
$\delta^{(4)} \to$ assures the conservation of momentum through the process;
$|\mathcal{M}|$ = amplitudes of the processes involved;
f_α = distribution functions;
$(1 \pm f_\alpha) \to$ accounts for the nature of the particles, either bosonic $(+)$ or fermionic $(-)$.

- $\mathscr{I}$ is the emission operator [53]. This operator can in principle contain the contributions coming from a number of possible sources of GWs. E.g. from an astrophysical point of view, we know that merging binary systems emit GWs, thus they would appear in terms of their changing quadrupole momenta (see e.g. [54, 55]).
  From a cosmological point of view, instead, we know that many production mechanisms of GWs can come into play (see e.g. phase transitions [56] or enhanced density perturbations leading to primordial BHs [57–59], which occur at energies well below the Planck scale). However, in our case we are considering solely inflation as a production mechanism (see e.g. [60, 61]).

In our treatment we will disregard both the collision term, given that graviton scatterings affects the distribution function at higher levels w.r.t. what we are considering in this Thesis (see [62] for a discussion on collisional effects involving gravitons), and the source terms coming from astrophysical sources, since we are only interested in the GW background of cosmological origin. The GW emission coming from inflation is treated as an initial condition on the distribution, thus the Boltzmann equation are recast to

$$\frac{df}{d\lambda} = 0 = \frac{d\lambda}{d\eta}\frac{df}{d\lambda} = \frac{df}{d\eta} = \frac{\partial f}{\partial \eta} + \frac{\partial f}{\partial x^i}\frac{dx^i}{d\eta} + \frac{\partial f}{\partial q}\frac{dq}{d\eta} + \frac{\partial f}{\partial n^i}\frac{dn^i}{d\eta} = 0 , \tag{142}$$

where: η = conformal time;
$\hat{n}$ = GW direction of motion;
$q = a|\vec{p}|$ is the comoving momentum modulus.

4.1.1 *EOM in a Perturbed Universe*

In order to proceed further we need to explore how gravitons travel in a perturbed Universe. This will provide us the necessary tool to make explicit the above expression for the evolution of the distribution function.
We know that the metric of a flat and unperturbed FLRW Universe is

$$ds^2 = a^2(\eta)\left[-d\eta^2 + \delta_{ij}dx^i dx^j\right] . \tag{143}$$

In full generality the perturbed FLRW metric can be decomposed in [14]

$$g_{00} = -a^2(\eta)\left(1 + 2\sum_{r=1}^{+\infty}\frac{1}{r!}\Phi^{(r)}\right) , \tag{144}$$

$$g_{i0} = g_{0i} = a^2(\eta)\sum_{r=1}^{+\infty}\frac{1}{r!}\omega_i^{(r)} , \tag{145}$$

$$g_{ij} = a^2(\eta)\left\{\left[1 - 2\left(\sum_{r=1}^{+\infty}\frac{1}{r!}\Psi^{(r)}\right)\right]\delta_{ij} + \sum_{r=1}^{+\infty}\frac{1}{r!}\chi_{ij}^{(r)}\right\} , \tag{146}$$

where: (r) = order of the perturbation ;
Φ, Ψ = scalar perturbations called "gravitational potentials" ;
ω_i = vector perturbations;
χ_{ij} = TT tensor perturbations, for which $\chi_i^{i(r)} = 0 = \partial^i\chi_{ij}$.

It is easy to notice that sending all the perturbations to zero one recovers the background metric.
Considering only first order perturbations, we can recast the metric to

$$ds^2 = a^2(\eta)\left[-(1+2\Phi)d\eta^2 + 2\omega_i d\eta dx^i + \left[(1-2\Psi)\,\delta_{ij} + \chi_{ij}\right]dx^i dx^j\right] . \tag{147}$$

Now, exploiting the Helmholtz's theorem one can always decompose a N-vector to identify the nature of the DOF embedded in it [42]. Hence, $\omega_i = \omega_i^{\perp} + \partial_i\omega^{\parallel}$, where $\omega^{\parallel}$ is an irrotational, or curl-free, scalar component (also called potential flow); on the other hand, $\omega_i^{\perp}$ is a divergence-free, or solenoidal, vector with $\partial^i\omega_i^{\perp} = 0$ (also called vorticity), which is perpendicular to $\hat{k}$ in

Fourier space. Decomposing in a similar way a tensor, one can distinguish scalar, vector and tensor DOF resulting in[34]:

$$\chi_{ij} = D_{ij}\chi^{\parallel} + \partial_i\chi_j^{\perp} + \partial_j\chi_i^{\perp} + \chi_{ij}^{T} \,, \tag{148}$$

where $D_{ij} = \left(\partial_i\partial_j - \frac{1}{3}\delta_{ij}\nabla^2\right)$ is the trace-free operator, $\chi^{\parallel}$ is a scalar function and $\chi_i^{\perp}$ is a solenoidal vector field.
At this point we have identified all the DOF, so we can choose a gauge in which to perform our calculations. In this case we use the Poisson's gauge, translating into $\omega^{\parallel} = \chi^{\parallel} = \chi_i^{\perp} = 0$. In addition, we neglect the remaining vectorial perturbations given that they are rapidly diluted by the accelerated expansion [42]. This results in having

$$ds^2 = a^2(\eta)\left[-(1+2\Phi)d\eta^2 + \left[(1-2\Psi)\,\delta_{ij} + \chi_{ij}\right]dx^i dx^j\right] \,, \tag{149}$$

where $\chi_{ij} = \chi_{ij}^{T}$ for the sake of notation.
Mimicking the procedure typical of CMB (see e.g.[51]), in this metric the Christoffel symbols take the form

$$\begin{aligned}
\Gamma^0_{00} &= \mathcal{H} + \phi' \,, \\
\Gamma^0_{0i} &= \partial_i\phi \,, \\
\Gamma^i_{00} &= \partial^i\phi \,, \\
\Gamma^i_{0j} &= \delta^i_j\left[\mathcal{H} - \psi'\right] + \frac{1}{2}\chi'^i_j \,, \\
\Gamma^0_{ij} &= \mathcal{H}\delta_{ij} + \frac{1}{2}\chi'_{ij} - \psi'\delta_{ij} + \mathcal{H}\chi_{ij} - 2\mathcal{H}\delta_{ij}\phi - 2\mathcal{H}\delta_{ij}\psi \,, \\
\Gamma^i_{jk} &= -\frac{1}{2}\partial^i\chi_{jk} + \delta_{jk}\partial^i\psi + \frac{1}{2}\partial_j\chi^i_k - \delta^i_k\partial_j\psi + \frac{1}{2}\partial_k\chi^i_j - \delta^i_j\partial_k\psi \,,
\end{aligned} \tag{150}$$

where: $' \;=\;$ derivative w.r.t. conformal time;
$\partial_i \equiv \frac{\partial}{\partial x^i}$ are the spatial derivatives;
$\mathcal{H} \equiv \frac{a'}{a}$ is the conformal Hubble parameter.

At this point, we need to look into the explicit expression of the gravitons momenta. Indeed, remembering Eq.140, we need an expression for $p^\alpha \equiv \frac{dx^\alpha}{d\lambda}$.

The first thing we can do is to exploit some basic property of momenta in GR; indeed, calling p the modulus of the spatial momentum $\vec{p}$ and $\hat{n}$ its versor, we know that both the following expressions will hold

$$g_{ij}p^i p^j = p^2 \quad \text{and} \quad p^\mu p^\nu g_{\mu\nu} = -m^2 \,. \tag{151}$$

34 These properties hold: $\chi^T_{ij} = \chi^T_{ji}$, $\partial^i\chi^T_{ij} = 0$ and $\chi^{j\ T}_{\ i} = 0$.

Asking now that the spatial momentum takes the form [51] $p^i = G(p, n^i, a, \Phi, \Psi, \chi)n^i$, where G can be in principle a function of all the perturbations, the modulus of the momentum and the scale factor, we can find its expression exploiting the first relation of Eq.151 [35] Indeed, plugging this parametrization of p^i into it, we can write[36]

$$p^i = \frac{p}{a}e^{\Psi}\left(1 - \frac{1}{2}\chi_{jk}n^j n^k\right)n^i \,. \tag{152}$$

Looking instead at the second relation in Eq.151 and assuming the graviton to be massless, we can write

$$p_\mu p^\mu = g_{00}\left(p^0\right)^2 + g_{ij}p^i p^j = -m^2 = 0 \,. \tag{153}$$

This allows us to find the explicit expression for p^0:

$$\begin{aligned} g_{00}\left(p^0\right)^2 + g_{ij}p^i p^j = -a^2 e^{2\Phi}\left(p^0\right)^2 + p^2 = 0 \\ \left(p^0\right)^2 = \frac{p^2}{a^2}e^{-2\Phi} \Rightarrow p^0 = \frac{p}{a}e^{-\Phi} \,. \end{aligned} \tag{154}$$

Then, we can then define the comoving momentum as $q^\mu \equiv p^\mu/a$, which is useful to write in an alternative way p^0 and p^i as [51]

$$p^0 = \frac{q}{a^2}e^{-\Phi} \quad , \quad p^i = \frac{q}{a^2}e^{\Psi}\left(1 - \frac{1}{2}\chi_{jk}n^j n^k\right)n^i \tag{155}$$

At this point we have all the tools to reconstruct the full expression of Eq.142.

- Let us start from $\frac{dx^i}{d\eta}$. In order to use what we have just obtained for the momenta, we can recast it to [51]

$$\frac{dx^i}{d\eta} = \frac{p^i}{p^0} = \frac{\frac{q}{a^2}e^{\Psi}(1 - \frac{1}{2}\chi_{jk}n^j n^k)n^i}{\frac{q}{a^2}e^{-\Phi}} = e^{\Phi+\Psi}\left(1 - \frac{1}{2}\chi_{jk}n^j n^k\right)n^i \,. \tag{156}$$

  This term is multiplied by $\frac{\partial f}{\partial x^i}$, thus on the dependency of the distribution function on the position. However, due to our homogeneity assumption of the background spacetime, this term already provides a first order contribution, hence we must keep only the term at zeroth order of the above expression of $\frac{dx^i}{d\eta}$, i.e.

$$e^{\Phi+\Psi}\left(1 - \frac{1}{2}\chi_{jk}n^j n^k\right)n^i \simeq \left(1 - \frac{1}{2}\chi_{jk}n^j n^k\right)n^i \simeq n^i \,. \tag{157}$$

35 The procedure used to extract the expression of the momentum, together with the explicit expression of the Boltzmann equation we are about to treat, is very similar to what is usually done for CMB photons. E.g. see [18, 51].

36 Here only first order contributions are kept into the equation.

Summarizing

$$\frac{\partial f}{\partial x^i}\frac{dx^i}{d\eta} \simeq \frac{\partial f}{\partial x^i} n^i \,. \tag{158}$$

This term, together with $\frac{\partial f}{\partial \eta}$, encodes the free-streaming behavior of gravitons, i.e. the propagation of perturbations on all scales [18] [37].

- The next term to evaluate is the one $\propto \frac{dq}{d\eta}$. To obtain its expression, it is useful to consider the following equation [51]

$$\frac{dp^0}{d\lambda} + \Gamma^0_{\alpha\beta} p^\alpha p^\beta = 0 = \frac{dp^0}{d\lambda}\frac{d\lambda}{d\eta} + \frac{\Gamma^0_{\alpha\beta} p^\alpha p^\beta}{\frac{d\eta}{d\lambda}} = \frac{dp^0}{d\eta} + \frac{\Gamma^0_{\alpha\beta} p^\alpha p^\beta}{p^0} \,. \tag{159}$$

In fact, with some algebra and dropping higher order contributions, one can find

$$\frac{dp^0}{d\eta} \simeq \frac{dq}{d\eta}\frac{1-\Phi}{a} - \frac{q}{a^2}\left[2\mathcal{H}(1-\Phi) + \frac{d\Phi}{d\eta} + n^i \frac{d\Phi}{dx^i}\right] \tag{160}$$

$$\frac{\Gamma^0_{\alpha\beta} p^\alpha p^\beta}{p^0} \simeq \frac{q}{a^2}\left[2\mathcal{H}(1-\Phi) + \frac{d\Phi}{d\eta} - \frac{d\Psi}{d\eta} + \frac{1}{2}\frac{d\chi_{jk}}{d\eta} n^j n^k + 2\frac{d\Phi}{dx^i} n^i\right] , \tag{161}$$

which contains the term we are interested in, i.e. $\frac{dq}{d\eta}$. Summing the two equations as in Eq.159,

$$\frac{dq}{d\eta} \simeq q\left[\frac{d\Psi}{d\eta} - \frac{d\Phi}{dx^i} n^i - \frac{1}{2}\frac{d\chi_{jk}}{d\eta} n^j n^k\right] . \tag{162}$$

This contribution accounts for the red-shifting of gravitons during the evolution of the Universe. We will se that this includes the SW, ISW and Rees-Sciama (RS) effects.

- The last term $\propto \frac{\partial f}{\partial n^i}$ do not need to be computed. In fact, $\frac{\partial f}{\partial n^i}$ is already at least of order one and $\frac{dn^i}{d\eta}$ account for the gravitational lensing among the propagation of the graviton, thus it is also of at least order one.

Finally, we can write Eq.142 at first order as

$$\frac{\partial f}{\partial \eta} + \frac{\partial f}{\partial x^i} n^i + \left[\frac{d\Psi}{d\eta} - \frac{1}{2}\frac{d\chi_{jk}}{d\eta} n^j n^k - \frac{d\Phi}{dx^i} n^i\right] q \frac{\partial f}{\partial q} = 0 \,, \tag{163}$$

37 At higher order this includes time delay effects due to the deviation of the geodetic when passing through distorted regions by massive objects.

4.2 SOLUTIONS OF THE BOLTZMANN EQUATIONS

In order to find the solutions of the above equations and to mimic exactly the analogous CMB procedure, it is useful to decompose the gravitons distribution function into a background contribution plus a first order one [18, 25, 26]

$$f(\eta, q, x^i, n^i) \simeq \bar{f}(\eta, q) + \delta f(\eta, q, x^i, n^i) \,. \tag{164}$$

where: $\bar{f}(\eta, q)$ = solution of the zeroth order equation, giving $\frac{\partial \bar{f}(\eta,q)}{\partial \eta} = 0$ [38];
$\delta f(\eta, q, x^i, n^i)$ = solution of the first order equation.

In order to simplify the first order Boltzmann equation, it is standard habit to parametrize it with a function $\Gamma(\eta, q, x^i, n^i)$ in the following way (see [18, 53])

$$\delta f(\eta, q, x^i, n^i) \equiv -q \frac{\partial \bar{f}}{\partial q} \Gamma(\eta, q, x^i, n^i) \,. \tag{165}$$

In the case of a thermal distribution of temperature T, such as the CMB, $\Gamma = \delta T/T$, which indeed corresponds to what we will call Θ in Ch.5. However, the difference between the two cases, i.e. CMB and CGWB, is that in the former photons were thermal, thus the continuous scatterings produced frequency-independent perturbations; whereas in the latter, being the collision term negligible, Γ retains in general a $\mathcal{O}(1)$ dependency on the frequency.
Going back to the Boltzmann equations, at first order holds

$$\begin{aligned}
&\frac{\partial f}{\partial \eta} + \frac{\partial f}{\partial x^i} n^i + \left[\frac{d\Psi}{d\eta} - \frac{1}{2}\frac{d\chi_{jk}}{d\eta} n^j n^k - \frac{d\Phi}{dx^i} n^i\right] q \frac{\partial f}{\partial q} \simeq \\
\simeq &\frac{\partial \bar{f}}{\partial \eta} - \frac{\partial}{\partial \eta}\left(q \frac{\partial \bar{f}}{\partial q}\Gamma\right) + \frac{\partial \bar{f}}{\partial x^i} n^i - n^i \frac{\partial}{\partial x^i}\left(q \frac{\partial \bar{f}}{\partial q}\Gamma\right) + \frac{dq}{d\eta}\frac{\partial \bar{f}}{\partial q} + \\
&- \frac{dq}{d\eta}\frac{\partial}{\partial q}\left(q \frac{\partial \bar{f}}{\partial q}\Gamma\right) \simeq \\
\simeq &- q \frac{\partial \bar{f}}{\partial q}\frac{\partial \Gamma}{\partial \eta} + n^i q \frac{\partial \bar{f}}{\partial q}\frac{\partial \Gamma}{\partial x^i} + \frac{dq}{d\eta}\frac{\partial \bar{f}}{\partial q} = -q \frac{\partial \bar{f}}{\partial q}\left[\frac{\partial \Gamma}{\partial \eta} + n^i \frac{\partial \Gamma}{\partial x^i} - \frac{1}{q}\frac{dq}{d\eta}\right] \simeq \\
\simeq &- q \frac{\partial \bar{f}}{\partial q}\left[\frac{\partial \Gamma}{\partial \eta} + n^i \frac{\partial \Gamma}{\partial x^i} - \frac{d\Psi}{d\eta} + \frac{d\Phi}{dx^i} n^i + \frac{1}{2}\frac{d\chi_{jk}}{d\eta} n^j n^k\right] = 0 \,.
\end{aligned} \tag{166}$$

At this point we can define the source function

$$S(\eta, x^i, n^i) \equiv \frac{d\Psi}{d\eta} - \frac{d\Phi}{dx^i} n^i - \frac{1}{2}\frac{d\chi_{jk}}{d\eta} n^j n^k \,, \tag{167}$$

38 Also further in this Thesis, the over-line $-$ on top of a quantity will indicate that it is a background, i.e. zeroth order, one.

in order to write the first order Boltzmann equation as

$$\frac{\partial \Gamma}{\partial \eta} + n^i \frac{\partial \Gamma}{\partial x^i} = S(\eta, x^i, n^i) \, . \tag{168}$$

The source function contains the scalar and tensor perturbations, which will affect the further propagation of gravitons through the first order Boltzmann equation, providing the "anisotropies" of the distribution function. It is also interesting to notice that S do not depend on q, indicating that these propagation effects are q-independent, at least at first order in the perturbations.
It is convenient to go into Fourier space through

$$\Gamma \equiv \int \frac{d^3k}{(2\pi)^3} e^{i \vec{k} \vec{x}} \Gamma(\eta, \vec{k}, q, \hat{n}) \, , \tag{169}$$

$$S \equiv \int \frac{d^3k}{(2\pi)^3} e^{i \vec{k} \vec{x}} S(\eta, \vec{k}, \hat{n}) = \Psi' - ik\mu\Phi - \frac{1}{2} n^i n^j \chi'_{ij} \tag{170}$$

to recast Eq.168 to

$$\Gamma' + ik\mu\Gamma = S(\eta, \vec{k}, \hat{n}) \, , \tag{171}$$

where $\mu \equiv \hat{k} \cdot \hat{n}$ is the cosine of the angle between the wavevector of each Fourier mode and the GW direction of motion.
The formal solution of Eq.171 is given by [25, 26] and reads [39]

$$\begin{aligned} &\Gamma(\eta, \vec{k}, q, \hat{n}) = \\ &= \int_{\eta_{in}}^{\eta} d\eta' e^{ik\mu(\eta'-\eta)} \left[\Gamma\left(\eta', \vec{k}, q, \hat{n}\right) \delta\left(\eta' - \eta_{in}\right) + S\left(\eta', \vec{k}, \hat{n}\right) \right] = \\ &= \int_{\eta_{in}}^{\eta} d\eta' e^{ik\mu(\eta'-\eta)} \left[\Gamma\left(\eta', \vec{k}, q, \hat{n}\right) \delta\left(\eta' - \eta_{in}\right) + \Psi' - ik\mu\Phi - \frac{1}{2} n^i n^j \chi'_{ij} \right] \, . \end{aligned} \tag{173}$$

39 Obtaining this is very straightforward. Eq.171 is of the type $y'(x) = a(x)y(x) + b(x)$, thus can be solved using

$$y(x) = e^{A(x)} \left[C + \int e^{-A(x)} b(x) \, dx \right] \quad \text{with} \quad A(x) = \int a(x) \, dx \, . \tag{172}$$

The integration constant C can be easily fixed imposing that, at η_{in}, Γ is equal to some initial value $\Gamma(\eta, \vec{k}, q, \hat{n}) = \Gamma\left(\eta_{in}, \vec{k}, q, \hat{n}\right)$ set by the specific production mechanism.

Then, we can integrate by parts the term $\propto \Phi$ to obtain the final form of Γ

$$\begin{aligned}
&\Gamma(\eta, \vec{k}, q, \hat{n}) = \\
=&e^{ik\mu(\eta_{in}-\eta)}\Gamma\left(\eta_{in}, \vec{k}, q, \hat{n}\right) + \int_{\eta_{in}}^{\eta} d\eta' e^{ik\mu(\eta'-\eta)}\left[\Psi' - ik\mu\Phi - \frac{1}{2}n^i n^j \chi'_{ij}\right] = \\
=&e^{ik\mu(\eta_{in}-\eta)}\Gamma\left(\eta_{in}, \vec{k}, q, \hat{n}\right) - e^{ik\mu(\eta'-\eta)}\Phi(\eta', \vec{k})\Big|_{\eta_{in}}^{\eta} + \\
&+ \int_{\eta_{in}}^{\eta} d\eta' e^{ik\mu(\eta'-\eta)}\left[\Psi' + \Phi' - \frac{1}{2}n^i n^j \chi'_{ij}\right] = \\
=&-\Phi(\eta, \vec{k}) + e^{ik\mu(\eta_{in}-\eta)}\left[\Gamma\left(\eta_{in}, \vec{k}, q, \hat{n}\right) + \Phi(\eta_{in}, \vec{k})\right] + \\
&+ \int_{\eta_{in}}^{\eta} d\eta' e^{ik\mu(\eta'-\eta)}\left[\Psi' + \Phi' - \frac{1}{2}n^i n^j \chi'_{ij}\right] .
\end{aligned} \tag{174}$$

Disregarding the first isotropic term, representing a monopole contribution to which we are not interested[40], we can write

$$\begin{aligned}
&\Gamma(\eta, \vec{k}, q, \hat{n}) = e^{ik\mu(\eta_{in}-\eta)}\Gamma\left(\eta_{in}, \vec{k}, q, \hat{n}\right) + \\
&+ \int_{\eta_{in}}^{\eta} d\eta' e^{ik\mu(\eta'-\eta)}\left[\Phi(\eta', \vec{k})\delta(\eta'-\eta_{in}) + \frac{\partial\left(\Psi(\eta', \vec{k}) + \Phi(\eta', \vec{k})\right)}{\partial\eta'}\right] + \\
&- \int_{\eta_{in}}^{\eta} d\eta' e^{ik\mu(\eta'-\eta)}\left[\frac{1}{2}n^i n^j \frac{\partial\chi_{ij}(\eta', \vec{k})}{\partial\eta'}\right] \\
=&\Gamma_I(\eta, \vec{k}, q, \hat{n}) + \Gamma_S(\eta, \vec{k}, \hat{n}) + \Gamma_T(\eta, \vec{k}, \hat{n}) .
\end{aligned} \tag{175}$$

Here, we have distinguished three different contributions to Γ, indicated by the subscripts I, S, T:

- the first term represents the initial condition set by some cosmological process at η_{in}.

$$\Gamma_I(\eta, \vec{k}, q, \hat{n}) \equiv e^{ik\mu(\eta_{in}-\eta)}\Gamma\left(\eta_{in}, \vec{k}, q, \hat{n}\right) . \tag{176}$$

  It carries the "memory" of the initial conditions to the following evolution of the distribution function in a completely different way w.r.t. what one observes for the CMB. Indeed, CMB photons were thermally coupled before the recombination epoch, thus the continuous and very efficient scatterings erased any trace of the initial conditions, leaving

40 Notice that indeed Φ does not depend on $\hat{n}$, thus on the direction of observation in the sky. The only angle dependency on that term is inside the exponent of $e^{ik\mu(\eta_{in}-\eta)}$, however this particular combination is still isotropic on the full-sky.

behind a nearly memory-less plasma [41]. Once they decoupled, they started free-streaming causing us to see the CMB. Gravitons instead have never being thermal (at least below the Planck energy [23]).

- The second term is the scalar sourced contribution to the distribution function.

$$\Gamma_S(\eta, \vec{k}, q, \hat{n}) \equiv \int_{\eta_{in}}^{\eta} d\eta' e^{ik\mu(\eta'-\eta)} \Phi(\eta', \vec{k}) \delta(\eta' - \eta_{in}) + \\ + \int_{\eta_{in}}^{\eta} d\eta' e^{ik\mu(\eta'-\eta)} \frac{\partial\left(\Psi(\eta', \vec{k}) + \Phi(\eta', \vec{k})\right)}{\partial\eta'} . \tag{177}$$

  Inside it, the first term represents the SW effect, whereas an anisotropy set by the value of the gravitational potential Φ at η_{in}. The second one accounts for the propagation of CMB photons from η_{in} to us today, including the ISW effect, i.e. propagation during radiation domination, and the RS effect, i.e. propagation during the very late Universe in dark energy domination.

- The last term is the tensor sourced one, i.e. generated by GW perturbations having a much smaller wavelength than the background one. Intuitively, one can think of these as small ripples on top of the much larger geometry of the Universe. These two are well separated in terms of wavelength, or frequency.

$$\Gamma_T(\eta, \vec{k}, q, \hat{n}) \equiv -\int_{\eta_{in}}^{\eta} d\eta' e^{ik\mu(\eta'-\eta)} \left[\frac{1}{2} n^i n^j \frac{\partial \chi_{ij}(\eta', \vec{k})}{\partial\eta'}\right] . \tag{178}$$

4.3 SPHERICAL HARMONICS DECOMPOSITION

At this point is is convenient to decompose these fluctuations in spherical harmonics, in order to obtain the angular power spectrum at the end of the calculation, which will fully describe the CGWB in the sky.
As mentioned, the decomposition amounts of doing

$$\Gamma(\hat{n}) = \sum_{\ell} \sum_{m=-\ell}^{\ell} \Gamma_{\ell m} Y_{\ell m}(\hat{n}) \quad \text{inverted by} \quad \Gamma_{\ell m} = \int d^2 n \Gamma(\hat{n}) Y^*_{\ell m}(\hat{n}) , \tag{179}$$

where: $Y_{\ell m}(\theta, \varphi)$ = are the SHs;
$\Gamma_{\ell m}$ = coefficients of the SH decomposition. The higher the coefficient is, the more the associated SH will contribute the the total $\Gamma(\hat{n})$.

41 In other words, the mean free path of photons was very short.

For completion, we remind the reader the few definitions behind SH: firstly

$$Y_\ell^m(\theta,\varphi) \equiv \sqrt{\frac{(2\ell+1)}{4\pi}\frac{(\ell-m)!}{(\ell+m)!}}\, P_\ell^m(\cos\theta)\, e^{im\varphi} \ , \tag{180}$$

where $P_\ell^m(\cos\theta)$ are the Associate Legendre Polynomials (ALPs) defined as a function of the Legendre Polynomials (LPs) as

$$P_\ell^m(x) \equiv (-1)^m(1-x^2)^{m/2}\frac{d^m}{dx^m}\left(P_\ell(x)\right) \ , \tag{181}$$

with the Rodriguez's formula expression of the LP yielding

$$P_n(x) \equiv \frac{1}{2^n n!}\frac{d^n}{dx^n}(x^2-1)^n \ . \tag{182}$$

Going back to our Γs, we plug into Eq.179 the expression of the $\Gamma(\hat{n})$ shown by Eq.175 in order to write

$$\begin{aligned}\Gamma_{\ell m} =& \int d^2n\, Y^*_{\ell m}(\hat{n}) \int \frac{d^3k}{(2\pi)^3} e^{i\vec{k}\cdot\vec{x}}\left[\Gamma_I(\eta,\vec{k},q,\hat{n}) + \Gamma_S(\eta,\vec{k},\hat{n}) + \Gamma_T(\eta,\vec{k},\hat{n})\right] \\ =& \Gamma_{\ell m,I} + \Gamma_{\ell m,S} + \Gamma_{\ell m,T} \ ,\end{aligned} \tag{183}$$

where we have carried onto the SH coefficients the same notation used to identify the different contributions to Γ.
Let us look into every term more deeply.

4.3.1 *Initial Condition Term*

The initial condition term reads

$$\Gamma_{\ell m,I} = \int \frac{d^3k}{(2\pi)^3} e^{i\vec{k}\cdot\vec{x}_0}\Gamma_I(\eta,\vec{k},q,\hat{n}) \int d^2n\, Y^*_{\ell m}(\hat{n}) e^{-ik(\eta_0-\eta_{in})\hat{k}\cdot\hat{n}} \ . \tag{184}$$

$\vec{x}_0$ is the origin of the reference frame where the observer is, which we can set to $\vec{x}_0 = 0$ without loss of generality and that η_{in} represents the last time in which cosmological GWs have being produced, i.e. the end of inflation.
In order to make a little more explicit the initial conditions term, we can make use of a useful decomposition of the exponential as function of Spherical Bessel Functions (SBFs), LPs and SHs reading

$$\begin{aligned} e^{-i\vec{k}\cdot\vec{y}} =& \sum_\ell (-i)^\ell(2\ell+1) j_\ell(ky) P_\ell(\hat{k}\cdot\hat{y}) = \\ =& 4\pi\sum_\ell\sum_{m=-\ell}^{\ell}(-i)^\ell j_\ell(ky) Y_{\ell m}(\hat{k}) Y^*_{\ell m}(\hat{y}) \ . \end{aligned} \tag{185}$$

In our case, it yields

$$e^{-ik(\eta_0-\eta_{in})\hat{k}\cdot\hat{n}} = 4\pi \sum_{\ell'} \sum_{m'=-\ell'}^{\ell'} (-i)^{\ell'} j_{\ell'}[k(\eta_0-\eta_{in})] Y_{\ell' m'}(\hat{n}) Y^*_{\ell' m'}(\hat{k}) \, . \tag{186}$$

Plugging this expansion into Eq.184 and remembering the orthogonality condition of SHs

$$\int d\hat{k} Y^*_{\ell m}(\hat{k}) Y_{\ell' m'}(\hat{k}) = \delta_{\ell\ell'}\delta_{mm'} \, , \tag{187}$$

one obtains

$$\Gamma_{\ell m,I} = 4\pi(-i)^{\ell} \int \frac{d^3k}{(2\pi)^3} \Gamma_I(\eta, \vec{k}, q, \hat{n}) Y^*_{\ell m}(\hat{k}) j_{\ell}[k(\eta_0-\eta_{in})] \, , \tag{188}$$

where we stress the presence of a dependency on the frequency q, which indicate the role of the specific physics we are considering behind the initial conditions.

4.3.2 *Scalar Sourced Term*

As aforementioned, this term accounts for anisotropies of the distribution function produced by the propagation of GWs in a perturbed Universe, specifically due to scalar perturbations.
In this context, these perturbations are typically expressed as

$$\Phi = \zeta(\vec{k}) \times \{\text{Transfer Function}(k)\} \times \{\text{Growth Function}(\eta)\} \, , \tag{189}$$

where: $\zeta(\vec{k})$ = primordial value of the curvature perturbation set during inflation;
Transfer Function(k) = evolution of perturbations through the epochs of horizon crossing and radiation/-matter transition;
Growth Function(η) = wavelength-independent growth at late times [18].

From now on, until differently specified, we will refer with the name "transfer function" to the actual product of {Transfer Function(k) $\times$ Growth Function(η)} of Eq.189, in such a way that we can write

$$\Phi(\eta, \vec{k}) = T_\Phi(\eta, \vec{k})\zeta(\vec{k}) \quad , \quad \Psi(\eta, \vec{k}) = T_\Psi(\eta, \vec{k})\zeta(\vec{k}) \, . \tag{190}$$

Being in an isotropic situation and not considering any anisotropic stress, we consider for simplicity $T_\Phi = T_\Psi$.
This is not the only way to describe the gravitational potentials since one

could have considered the presence of more than one stochastic mode. Indeed, here ζ is the only stochastic variable, but in Ch.6, we will write it as a function of 3 stochastic ones as

$$\zeta(\vec{k}) = g_1(\vec{k})\Big(1 + h(\vec{k})\Big) + g_2(\vec{k}) \,. \tag{191}$$

We will not enter into the details of these variables just now, since, as mentioned, this will be treated in Ch.6 and will represent the very core of this Thesis.
Anyway, sticking to the parametrization of Eq.190 and exploiting the same expansion of the exponential shown in Eq.186, we can write

$$\begin{aligned}\Gamma_{\ell m,S} &= 4\pi(-i)^\ell \int \frac{d^3k}{(2\pi)^3}\zeta(\vec{k})Y^*_{\ell m}(\hat{k})\Big\{T_\Phi(\eta_{in},k)j_\ell[k(\eta_0-\eta_{in})] \\ &\qquad + \int_{\eta_{in}}^{\eta_0} d\eta' \frac{\partial\Big[\Psi(\eta',\vec{k})+\Phi(\eta',\vec{k})\Big]}{\partial\eta'} j_\ell\big[k(\eta_0-\eta')\big]\Big\} \\ &= 4\pi(-i)^\ell \int \frac{d^3k}{(2\pi)^3}\zeta(\vec{k})Y^*_{\ell m}(\hat{k})T^S_\ell(k,\eta_0,\eta_{in}) \,,\end{aligned} \tag{192}$$

where we have introduced the linear transfer function

$$\begin{aligned}T^S_\ell(k,\eta_0,\eta_{in}) \equiv & T_\Phi(\eta_{in},k)j_\ell[k(\eta_0-\eta_{in})] \\ & + \int_{\eta_{in}}^{\eta_0} d\eta' \frac{\partial\Big[\Psi(\eta',\vec{k})+\Phi(\eta',\vec{k})\Big]}{\partial\eta'} j_\ell\big[k(\eta_0-\eta')\big] \,,\end{aligned} \tag{193}$$

encoding the time evolution of the graviton fluctuations originated from the primordial scalar perturbations.

4.3.3 *Tensor Sourced Term*

Finally, the last contribution coming from tensor perturbations reads

$$\Gamma_{\ell m,T} = -\int d^2n\, Y^*_{\ell m}(\hat{n}) \int \frac{d^3k}{(2\pi)^3}\frac{n^i n^j}{2}\int_{\eta_{in}}^{\eta} d\eta' e^{ik(\eta'-\eta_0)\mu}\frac{\partial\chi_{ij}(\eta',\vec{k})}{\partial\eta'} \,. \tag{194}$$

Evaluating this term require a quite lenghty algebra and we are not interested in the details in this context; for this reason, we will just state the main passages and report the final result.

Firstly, one has to decompose χ_{ij} in right/left-handed circular polarizations as (see e.g. [29])

$$\chi_{ij} = \sum_{\lambda=\pm 2} e_{ij,\lambda}(\widehat{k})\, \chi(\eta, k)\, \xi_\lambda(k^i)\ , \tag{195}$$

where $e_{ij,\lambda}(\widehat{k})$ are the polarization operators defined from the more familiar polarization tensors relative to the $+$ and $\times$ polarizations, $\chi(\eta, k)$ is the tensor mode function and $\xi_\lambda(k^i)$ is the stochastic variable analogue of ζ for the scalar term.
Then, it will be necessary to rotate the system using a rotation matrix of the form

$$S\left(\Omega_k\right) \equiv \begin{pmatrix} \cos\theta_k \cos\phi_k & -\sin\phi_k & \sin\theta_k \cos\phi_k \\ \cos\theta_k \sin\phi_k & \cos\phi_k & \sin\theta_k \sin\phi_k \\ -\sin\theta_k & 0 & \cos\theta_k \end{pmatrix}\ , \tag{196}$$

which will be used to rotate the SHs following

$$Y^*_{\ell m}\left(\Omega_n\right) = \sum_{m'=-\ell}^{\ell} D^{\ell}_{mm'}\left(S\left(\Omega_k\right)\right) Y^*_{\ell m'}\left(\Omega_{k,n}\right)\ , \tag{197}$$

where $D^{\ell}_{mm'}\left(S\left(\Omega_k\right)\right)$ is the Wigner rotation matrix [63]

$$D^{\ell}_{ms}\left(S\left(\Omega_k\right)\right) \equiv \sqrt{\frac{4\pi}{2\ell+1}} (-1)^s {}_{-s}Y^*_{\ell m}\left(\Omega_k\right)\ . \tag{198}$$

The above expression make use of the spin-weighted SHs, which read[63]

$$\begin{aligned} {}_{-s}Y^*_{\ell m}\left(\Omega_k\right) \equiv & (-1)^m \sqrt{\frac{(\ell+m)!(\ell-m)!(2\ell+1)}{4\pi(\ell+s)!(\ell-s)!}} \sin^{2\ell}\left(\frac{\theta_k}{2}\right) \\ & \times \sum_{r=0}^{\ell-s} \begin{pmatrix} \ell-s \\ r \end{pmatrix} \begin{pmatrix} \ell+s \\ r+s-m \end{pmatrix} (-1)^{\ell-r-s} \\ & \times e^{im\phi_k} \cot^{2r+s-m}\left(\frac{\theta_k}{2}\right)\ . \end{aligned} \tag{199}$$

Then, exploiting the properties of SHs and of ALPs, one can finally arrive at the result:

$$\begin{aligned}\Gamma_{\ell m,T} &= \pi(-i)^{\ell}\sqrt{\frac{(\ell+2)!}{(\ell-2)!}}\int\frac{d^3k}{(2\pi)^3}e^{i\vec{k}\cdot\vec{x}_0}\sum_{\lambda=\pm2}{}_{-\lambda}Y^*_{\ell m}(\Omega_k)\,\xi_\lambda(\vec{k}) \\ &\qquad\times\int_{\eta_{in}}^{\eta_0}d\eta\,\chi'(\eta,k)\frac{j_\ell(k(\eta_0-\eta))}{k^2(\eta_0-\eta)^2} = \\ &= 4\pi(-i)^{l}\int\frac{d^3k}{(2\pi)^3}e^{i\vec{k}\cdot\vec{x}_0}\sum_{\lambda=\pm2}{}_{-\lambda}Y^*_{\ell m}(\Omega_k)\,\xi_\lambda(\vec{k})T^T_\ell(k,\eta_0,\eta_{in})\ ,\end{aligned} \tag{200}$$

where we introduced again a linear transfer function for the tensor modes reading

$$T^T_\ell(k,\eta_0,\eta_{in}) \equiv \frac{1}{4}\sqrt{\frac{(\ell+2)!}{(\ell-2)!}}\int_{\eta_{in}}^{\eta_0}d\eta\,\chi'(\eta,k)\frac{j_\ell(k(\eta_0-\eta))}{k^2(\eta_0-\eta)^2}\ . \tag{201}$$

4.4 CONNECTION WITH OBSERVABLES

Now, we have an explicit expression for the SH decomposition's coefficients. Thus, we can see what are the observables quantities connected to the distribution function of gravitons and to the CGWB.

4.4.1 *Energy Density*

Just like any other energy source of the Universe, GWs contribute to the overall energy density. Given that we are working with the distribution function of gravitons in a Boltzmann approach, to find the energy density of GWs it is sufficient to follow the natural route of integrating the distribution function, i.e. the average number of gravitons in a volume d^3p, multiplied by the energy contribution of the single particle:

$$\begin{aligned}\rho_{GW}(\eta_0,\vec{x}) &= \int d^3p\ pf(\eta_0,\vec{x},q,\hat{n}) \\ &= \frac{1}{a^4}\int d^3q\ qf(\eta_0,\vec{x},q,\hat{n}) \\ &= \frac{1}{a^4}\int d\ln q\,q^4\int d^2\hat{n}f(\eta_0,\vec{x},q,\hat{n}) \\ &\equiv \rho_{crit}\int d\ln q\times\frac{1}{\rho_{crit}}\frac{q^4}{a^4}\int d^2\hat{n}f(\eta_0,\vec{x},q,\hat{n}) \\ &\equiv \rho_{crit}\int d\ln q\times\Omega_{GW}(\eta_0,\vec{x},q)\ ,\end{aligned} \tag{202}$$

where: $\rho_{crit} \equiv \frac{3H_0^2}{8\pi G} = 3H_0^2 M_P^2$ is the critical density of a Universe perfectly flat;

$\Omega_{GW} =$ spectral energy density for GWs, i.e. the logarithmic contribution to the energy density.

We can write the spectral energy density as

$$\Omega_{GW} = \int d^2\hat{n}\, \omega_{GW}(\vec{x}, q, \hat{n}) \,, \tag{203}$$

where we have introduced the angular contribution of the spectral energy

$$\omega_{GW}(\vec{x}, q, \hat{n}) \equiv \bar{\omega}_{GW}(\eta_0, q)\left[1 + \frac{\delta\omega(\eta_0, \vec{x}, q, \hat{n})}{\bar{\omega}_{GW}(\eta_0, q)}\right] = \frac{1}{\rho_{crit}}\frac{q^4}{a^4} f(\eta, \vec{x}, q, \hat{n}) \,, \tag{204}$$

from which we can define the quantity [25, 26]

$$\delta_{GW}(\eta_0, \vec{x}, q, \hat{n}) \equiv \frac{\delta\omega(\eta_0, \vec{x}, q, \hat{n})}{\bar{\omega}_{GW}(\eta_0, q)} \,. \tag{205}$$

Then, the zeroth order homogeneous component of Ω_{GW} will be

$$\bar{\Omega}_{GW}(q) = \frac{4\pi}{\rho_{crit}}\left(\frac{q}{a}\right)^4 \bar{f}(q) = 4\pi\bar{\omega}_{GW}(q) \,. \tag{206}$$

These variables allow to write the energy density contribution of GWs as

$$\begin{aligned}
\rho_{GW}(\eta_0, \vec{x}) &= \rho_{crit}\int d\ln q \int d^2\hat{n}\,\omega_{GW} \\
&= \rho_{crit}\int d\ln q \int d^2\hat{n}(\bar{\omega}_{GW} + \delta\omega_{GW}) = \\
&= \rho_{crit}\int d\ln q \int d^2\hat{n}\left(\frac{q}{a}\right)^4\left(\bar{f} - q\frac{\partial\bar{f}}{\partial q}\Gamma\right) = \\
&= \rho_{crit}\int d\ln q\left(\frac{q}{a}\right)^4\bar{f}\int d^2\hat{n}\left(1 - \frac{\partial\ln\bar{f}}{\partial\ln q}\Gamma\right) = \\
&= \rho_{crit}\int d\ln q\int d^2\hat{n}\bar{\omega}_{GW} + \rho_{crit}\int d\ln q\int d^2\hat{n}\bar{\omega}_{GW}\delta_{GW} \,.
\end{aligned} \tag{207}$$

Exploiting now Eq.206, one can find

$$\begin{aligned}
\frac{\partial\ln\bar{f}}{\partial\ln q} &= \frac{q}{\bar{f}}\frac{\partial\bar{f}}{\partial q} = \frac{4\pi q^5}{\rho_{crit}a^4\bar{\Omega}_{GW}}\frac{\rho_{crit}a^4}{4\pi}\left(\frac{\partial\bar{\Omega}_{GW}}{\partial q}\frac{q}{q^5} - \frac{4}{q^5}\bar{\Omega}\right) = \\
&= \frac{q}{\bar{\Omega}}\frac{\partial\bar{\Omega}_{GW}}{\partial q} - 4 = \frac{\partial\ln\bar{\Omega}_{GW}}{\partial\ln q} - 4 \,,
\end{aligned} \tag{208}$$

which allows to write finally

$$\delta_{GW}(\eta, \vec{x}, q, \hat{n}) = \left[4 - \frac{\partial \ln \overline{\Omega}_{GW}}{\partial \ln q}\right] \Gamma(\eta, \vec{x}, q, \hat{n}) \, . \tag{209}$$

Through the presence of the Γ, all the different terms introduced before will act onto the energy density of the Universe. E.g., the memory of the production mechanisms carried by the initial condition can affect directly the GW energy density we can observe today.

4.4.2 *Correlators and Angular power Spectrum*

As previously mentioned in Sec.3.3.4, in order to compare theoretical predictions with observations, we must study the two point correlation function of the quantities involved. In fact, all the stochastic variables we have introduced ($\Gamma(\eta_{in}, \vec{k}, q)$, $\zeta(\vec{k})$, $\xi_\lambda(\vec{k})$) find their seeds in the quantum perturbations enhanced to macroscopic scales by inflation. This causes the fact that their expectation value is null, whereas their 2-point correlation functions are not.
In particular, assuming that the statistical variables have approximately a Gaussian behavior (experimentally verified for the large-scale perturbations of ζ and ξ_λ, as obtained from the CMB data [64], and assumed for the initial condition term), we can write

$$\begin{aligned}
\left\langle \Gamma(\eta_{in}, \vec{k}, q) \Gamma^*(\eta_{in}, \vec{k}', q) \right\rangle &= \frac{2\pi^2}{k^3} P_I(q, k) (2\pi)^3 \delta(\vec{k} - \vec{k}') \, , \\
\left\langle \zeta(\vec{k}) \zeta^*(\vec{k}') \right\rangle &= \frac{2\pi^2}{k^3} P_\zeta(k) (2\pi)^3 \delta(\vec{k} - \vec{k}') \, , \\
\left\langle \xi_\lambda(\vec{k}) \xi^*_{\lambda'}(\vec{k}') \right\rangle &= \frac{2\pi^2}{k^3} P_\lambda(k) \delta_{\lambda\lambda'} (2\pi)^3 \delta(\vec{k} - \vec{k}') \, .
\end{aligned} \tag{210}$$

Assuming also statistical isotropy, which will be relaxed in Ch.6, we can also write the angular correlators of the SH decomposition coefficients as[42]

$$\langle \Gamma_{\ell m} \Gamma^*_{\ell' m'} \rangle \equiv \delta_{\ell\ell'} \delta_{mm'} \widetilde{C}_\ell = \delta_{\ell\ell'} \delta_{mm'} \left[\widetilde{C}_{\ell,I}(q) + \widetilde{C}_{\ell,S} + \widetilde{C}_{\ell,T} \right] \, , \tag{211}$$

where we have used the usual notation to distinguish the various contributions.

42 Here we have assumed that the various terms are not cross-correlated. This assumption can be relaxed as in [57], where the anisotropic distribution of the GW originated in models with primordial BHs was studied.

As an example let us explicitly perform the calculi for the initial condition term; the other two will be nearly identical.

$$\begin{aligned}
\langle \Gamma_{\ell m,I}\Gamma^*_{\ell' m',I}\rangle =&(4\pi)^2(-i)^{\ell-\ell'}\int\frac{d^3k}{(2\pi)^3}\int\frac{d^3k'}{(2\pi)^3}\left\langle\Gamma(\eta_{in},\vec{k},q)\Gamma^*(\eta_{in},\vec{k}',q)\right\rangle\\
&\times Y^*_{\ell m}(\hat{k})Y_{\ell' m'}(\hat{k}')\; j_\ell[k(\eta_0-\eta_{in})]j_{\ell'}\left[k'(\eta_0-\eta_{in})\right]=\\
=&(4\pi)^2(-i)^{\ell-\ell'}\int\frac{d^3k}{(2\pi)^3}\int\frac{d^3k'}{(2\pi)^3}\frac{2\pi^2}{k^3}P_I(q,k)(2\pi)^3\delta(\vec{k}-\vec{k}')\\
&\times Y^*_{\ell m}(\hat{k})Y_{\ell' m'}(\hat{k}')\; j_\ell[k(\eta_0-\eta_{in})]j_{\ell'}\left[k'(\eta_0-\eta_{in})\right]=\\
=&4\pi(-i)^{\ell-\ell'}\int d^3k\frac{1}{k^3}P_I(q,k)\; j_\ell[k(\eta_0-\eta_{in})]j_{\ell'}[k(\eta_0-\eta_{in})]\\
&\times Y^*_{\ell m}(\hat{k})Y_{\ell' m'}(\hat{k})=\\
=&4\pi(-i)^{\ell-\ell'}\int\frac{dk}{k}P_I(q,k)\; j_\ell[k(\eta_0-\eta_{in})]j_{\ell'}[k(\eta_0-\eta_{in})]\\
&\times\int d^2\hat{k}Y^*_{\ell m}(\hat{k})Y_{\ell' m'}(\hat{k})=\\
=&\delta_{\ell\ell'}\delta_{mm'}4\pi\int\frac{dk}{k}P_I(q,k)\; j^2_\ell[k(\eta_0-\eta_{in})]\\
=&\delta_{\ell\ell'}\delta_{mm'}\widetilde{C}_{\ell,I}(q)\;.
\end{aligned}\tag{212}$$

Thus, summarizing we can define

$$\begin{aligned}
\widetilde{C}_{\ell,I}&\equiv 4\pi\int\frac{dk}{k}\; j^2_\ell[k(\eta_0-\eta_{in})]\; P_I(q,k)\;,\\
\widetilde{C}_{\ell,S}&\equiv 4\pi\int\frac{dk}{k}T^{(S)2}_\ell(k,\eta_0,\eta_{in})\; P_\zeta(k)\;,\\
\widetilde{C}_{\ell,T}&\equiv 4\pi\int\frac{dk}{k}T^{(T)2}_\ell(k,\eta_0,\eta_{in})\sum_{\lambda=\pm2}P_\lambda(k)\;,
\end{aligned}\tag{213}$$

where the transfer functions are defined in Eq.193 and Eq.201.
These functions in Eq.213 represent the contribution to the angular power spectra of the GW energy density, relative to the different source terms, and fully describe it in the full-sky.
We stress again that the fact that they are diagonal in both ℓ and m is a consequence of statistical isotropy. We will see that relaxing this assumption will give rise to non-diagonal couplings between different multipoles ℓ and ℓ'.

Part II

DEPARTURE FROM ISOTROPY

In this part, we will explore what happens if we relax the hypothesis of statistical isotropy. In particular, we will consider a modulation of the gravitational potential Φ, which will cause a local break of isotropy. We will briefly present the subject in the CMB context, where these kind of modulations find their phenomenological justification. This modulation will then be plugged in the framework of the CGWB (in the form of a modulation of the stochastic variable inside the definition of the gravitational potentials), following the same Boltzmann approach showed in Ch.4.

5

CMB POWER ASYMMETRY

We have already mentioned in Ch.2 that a crucial prediction of Big-Bang cosmology is the CMB: a relic radiation coming from the LSS of photons, which gives us the most ancient snapshot of the Universe we can observe with Electro-Magnetic (EM) radiation. Besides being characterized by (nearly) the same temperature in every direction, it presents also anisotropies caused by various effects. Also, CMB hides some hints of possible departures from the standard model of Cosmology, the so-called "CMB anomalies". In this chapter, we will briefly describe these features and we will focus on the so-called CMB "power asymmetry" and on how people in the literature have tried to characterize it as the effect of an isotropy-breaking modulation of the gravitational potentials.

5.1 COSMIC MICROWAVE BACKGROUND

The CMB represents literally the most ancient point in time we are able to explore via EM radiation, coming from the moment when the Universe was only 380 thousands years old.
Before that moment, photons and electrons scattered efficiently and, thus, were in thermal equilibrium. This fact assures that photons should have a blackbody spectrum. Indeed, this is true and has been the object on many observations throughout the years, since COsmic Background Explorer (COBE) [65, 66], to the point that the CMB is actually the most perfect blackbody we know (see Fig.10). What "triggered" the free-streaming behavior of photons was a phenomenon called "recombination" [18, 44].
As the Universe expanded, the temperature of the plasma kept dropping, thus one can expect that, once it reached energies of the order of the atomic bounds (13.6 eV for the hydrogen), electrons and protons would start to combine in the more energetic-convenient hydrogen. Indeed, this is broadly what happened at recombination, with the caveat of the energy scale: it is necessary to wait until the plasma reached $\approx$ 1 eV to have the actual recombination, since the photons in the tails of the Gaussian distribution were still energetic enough to ionize the hydrogen at higher energies [18].
However, the outcome is the same: after a transient, the Universe got filled of neutral hydrogen atoms, instead of ionized particles, which did not allow anymore photons to scatter, maintaining the thermal equilibrium. From that moment on, they traveled nearly undisturbed to us.
In spite of this, CMB is far more interesting than a completely smooth picture of the Universe, since it is characterized by small anisotropies that photons have acquired through their journey.

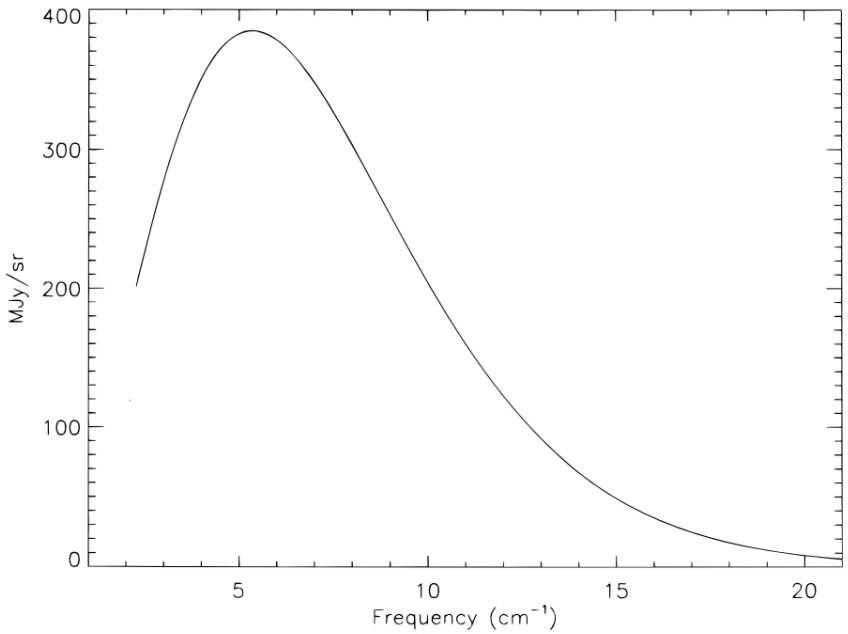

Figure 10: Monopole spectrum of CMB. The error bars of data are so small that it is impossible to distinguish them from the underlying theoretical prediction for a blackbody spectrum [67].

5.2 CMB ANISOTROPIES

In Ch.3 we have seen that quantum fluctuations of the inflaton field driving an expanding phase of the Universe are the seeds of perturbations causing the Universe to leave homogeneity and isotropy.
In addition, in Ch.4, we have mentioned that a way to describe the CMB is following the Boltzmann approach we have introduced for the CGWB. Indeed, following more or less identically the steps done for the CGWB, it is possible to find the Boltzmann equations for the CMB photons' distribution function. In fact, in a collisionless scenario and considering only scalar perturbations of the metric, one can write [18]

$$\frac{\partial f}{\partial t} + \frac{\hat{p}^i}{a}\frac{\partial f}{\partial x^i} - p\frac{\partial f}{\partial p}\left[H + \frac{\partial \Psi}{\partial t} + \frac{\hat{p}^i}{a}\frac{\partial \Phi}{\partial x^i}\right] = 0\,, \tag{214}$$

which is completely analogous to Eq.163. As we mentioned, the first two terms accounts for free-streaming of hydrodynamics, leading to the continuity and Euler equations [18]. The third one tells us that photons lose energy while the Universe keep expanding, whereas the last two ones keep track of the effects caused by the scalar perturbations of the metric.
In the case of photons, we know that the distribution function takes the

form of a Bose-Einstein distribution, perturbed by the presence of inhomogeneities [18]:

$$f(\vec{x}, p, \hat{p}, t) \equiv \left[\exp\left\{\frac{p}{T(t)(1+\Theta(\vec{x}, \hat{p}, t))}\right\} - 1\right]^{-1}, \tag{215}$$

which can be written as Eq.164 as [18]

$$\begin{aligned} f =& \bar{f} - p\frac{\partial \bar{f}}{\partial p}\Theta \\ \simeq& \frac{1}{e^{p/T}-1} + \left[\frac{\partial}{\partial T}\left(\frac{1}{e^{p/T}-1}\right)\right]T\Theta\,. \end{aligned} \tag{216}$$

Here, the factor $-p\frac{\partial \bar{f}}{\partial p}\Theta$ represents a parametrization of the first order perturbation of the distribution function f, which allows to simplify the Boltzmann equation [18]. Indeed, notice that this is the same thing we have done for the CGWB in Eq.165, where we mentioned that in the CMB it would be frequency-independent. In fact, notice that here $\Theta = \Theta(\vec{x}, \hat{p}, t)$ do not depend on p, while, in Ch.4, $\Gamma = \Gamma(\eta, q, x^i, n^i)$.

With these few equations we have just sketched the beginning of the CMB photons treatment via Boltzmann approach, however we are not interested in giving the details (which, e.g., you can find in [18]). It is sufficient to know that from here one can consider a number of different interactions between photons and other particles species, which will affect the distribution function in many different ways.
Anyway, at the end of the day one turns toward the angular power spectrum to obtain the full description of the spectrum we observe. In order to do so, it is sufficient to remember the SH decomposition introduced by Eq.179, which here we write as

$$\Theta(\vec{x}, \hat{p}, \eta) = \sum_{\ell=1}^{\infty}\sum_{m=-\ell}^{\ell} a_{\ell m}(\vec{x}, \eta) Y_{\ell m}(\hat{p})\,, \tag{217}$$

where $a_{\ell m}(\vec{x}, \eta)$ are the SH decomposition coefficients, which will encode the statistical properties of Θ.
At this point, one can define the angular power spectrum C_ℓ as[18]

$$\langle a_{\ell m} a^*_{\ell' m'}\rangle = \delta_{\ell\ell'}\delta_{mm'}C_\ell\,. \tag{218}$$

5.2.1 *Overview*

Without entering into the details, which are beyond the goals of this Thesis, let us see from a phenomenological and observational point of view what these anisotropies can look like.

- As mentioned, before decoupling, photons and electrons were able to interact efficiently through Compton/Thompson scattering. This would also generate a competing pressure, provided by photons, to the gravitational attraction of matter.
  In other words, gravitational infall compresses the fluid until resistance from photon pressure reverses the motion [68], in such a way that acoustic waves were generated. These left visible relics on the CMB spectrum, named Barionic Acoustic Oscillations (BAOs) [69, 70].

- Studying into the details the CMB, one can find that as the photons climb out of potential wells at LSS (so after decoupling), related to the presence of Φ in the equations, gravity redshifts the temperature from $\frac{\delta T}{T}$ to $\frac{\delta T}{T} + \Phi$. The effective perturbation at LSS will thus result similar to $[\frac{\delta T}{T} + \Phi](\eta_{cmb})$. The particular combination of intrinsic temperature fluctuations and gravitational redshift is called the ordinary SW effect [68, 71].
  Indeed, intuitively speaking, Φ represents a perturbation of the gravitational potential in the form of potential wells. These potential wells "attract" primarily matter, which tends to gather in them; however, the highly efficient coupling between matter and photons makes the latter to "fall" in the same way into these wells. Subsequently, when the decoupling happens, photons start to free-stream and their frequency acquire a redshift equal to Φ while climbing back the potential well towards us [68].

Effects as the SW effect are called "primary" anisotropies, since they happened at the LSS, whereas subsequent effects are called "secondary" anisotropies and affect CMB photons along their journey to us [43].
Let us now cite some examples of secondary anisotropies:

- if the gravitational potentials vary with time, the photon will experience differential redshifts due to the gradient of Φ, which no longer yield equal and opposite contributions as the photons enter and exit the potential well, and time dilation effect relate to Ψ [68]. The sum of these contributions along the line of sight is called the ISW effect. Usually, this effect is divided in a early-ISW effect, accounting for the radiation dominated epoch, and a late-ISW, accounting for the Λ-dominated epoch [68, 71]. Another similar effect is the RS one, where higher order corrections to the density evolution cause time dependence in the gravitational potentials from the Poisson equation [72];

43 The more careful reader should have noticed that the over-densities are indeed 3D inhomogeneities and not anisotropies, thus an explanation is due. The LSS is a 2D surface of radius η_{CMB}, corresponding to the length covered by light from the moment of recombination to now, where we observe the effects of the inhomogeneities. Thus, the fact that the 3D inhomogeneities are being projected on a 2D surface cause the fact that we see them as anisotropies on the CMB, meaning that changing the direction in the full-sky we observe a slightly different temperature of the radiation.

- after the reionization of the Universe, the radiation scattering onto free charges gets polarized and deviated, tending to erase small-scales peaks in the spectrum [73];
- gravitational lensing causes the geodetics of CMB photons to change based on the spacetime distortions induces by massive objects [74].

All these anisotropies, along with many others we are not mentioning, carry information on a number of cosmological parameters, allowing us to draw a nearly complete picture of the Universe.

5.3 CMB ANOMALIES

CMB anomalies have appeared in data in the form of unexpected statistical properties since WMAP measurements [2] and then reassured by Planck data [3], where many of these anomalies were found to have a significance level of $2-3\sigma$. Even tho this level is not sufficient to clearly claim the presence of new physics, there is surely some room to it, encouraging to study their possible physical cosmological origin.
Some of these anomalies are [9]:

- an excess of power in one of the two hemispheres of the sky;
- the quadrupole and the octopole appear to be aligned;
- the power spectra for $\ell < 30$ appear to have low power w.r.t. the values predicted by the best fit cosmological model;
- the presence of an excess kurtosis at angular scales of $\sim 10^\circ$, which originates from a "cold spot".

The former anomaly is named "power asymmetry" and will be the focus of the rest of this chapter.

5.4 CMB POWER ASYMMETRY

Since the first-year data of WMAP (see for example [1]), hints of a possible departure from statistical isotropy have started to show to the Cosmology community. In particular, exploiting many simulated realizations of the CMB, it was possible to show that the ratio between the power on the two ecliptic hemispheres in the sky we observe is generally higher than the one obtained in the far majority of the simulations ($\approx 99\%$) [1]. Over the subsequent years, this signature has been reassessed, for example, using the five-years data from WMAP, showing that only the $\approx 0.3\%$ of the simulated data achieved similar level of asymmetry [2], or even the most recent Planck data [3, 50], where it was also emphasized the role of the "a posteriori" statistics.
All these "evidences" of some possible new physics lurking behind this anomaly have obviously drawn a lot of attention in the scientific community, thus various proposal solutions were studied.

An example, can be to invoke non-Gaussian behaviors [9], or to consider some modulating field breaking local isotropy, as we will review in this Thesis [10].

5.4.1 *Modulation of Gravitational Potential*

People have tried to describe the CMB power asymmetry introducing in the model a super-horizon scale modulation of the gravitational potential, which will cause the temperature field to seem anisotropic on a local basis, without flawing the underlying hypothesis of a globally isotropic Universe. To see this in an intuitive way it is sufficient to imagine our Hubble volume as a circle of radius R: any small-scale fluctuating field will have a wavelength much smaller than R, thus they cannot contribute to a departure from isotropy and will determine the "standard" characteristics we see in the CMB. However, if we consider a modulating field having a wavelength larger than R, it will generate a local break of isotropy through its gradient. Considering now a lot of Hubble volumes, the modulating field would still average to 0, re-establishing the isotropy. To translate this in a more quantitative way, we can

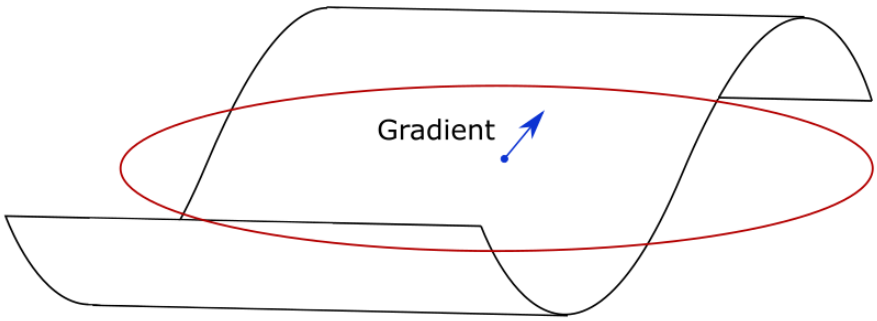

Figure 11: Intuitive idea of how a modulating field can break the local isotropy. Here the modulating field is represented as a plain wave, our Hubble volume is the red circle and the gradient of the modulating field is the blue arrow, which will naturally pick a direction in the Hubble volume, folowing the characteristics of the mode

assume that the gravitational potential $\Phi(\vec{x})$, introduced in Ch.4 as one of the scalar perturbations of the metric, actually depends on two fields $g(\vec{x})$ and $h(\vec{x})$, where the latter is only related to super-horizon scales fluctuations and the former to sub-horizon ones [10]. h will assume a deterministic value in our Hubble volume, whereas g will look like a standard stochastic fluctuation. As aforementioned, across the Hubble volume an observer will see broken statistical isotropy as an effect of the slow modulation of h, while its local gradient and curvature will pick a preferred direction, breaking statistical isotropy. Specifically we write

$$\Phi(\vec{x}) = g_1(\vec{x})[1 + h(\vec{x})] + g_2(\vec{x}) \, , \tag{219}$$

where: $g_1(\vec{x})$ = Gaussian random field accounting for fluctuations around the horizon scales;
$g_2(\vec{x})$ = Gaussian random field accounting for fluctuations on well-sub-horizon scales, which makes our considerations compatible with the observed statistical homogeneity and isotropy on small scales;
$h(\vec{x})$ = modulating field breaking isotropy.

Going into Fourier space, the product of g_1 and h in real space becomes naturally a convolution, thus Φ gets recast to

$$\Phi(\vec{k}) = g_1(\vec{k}) + \int \frac{d^3k'}{(2\pi)^3} g_1(\vec{k}')h(\vec{k}-\vec{k}') + g_2(\vec{k}) \,. \tag{220}$$

Given the Gaussian assumption we have made for the g fields, we can write their power spectra as

$$\left\langle g_i^*(\vec{k}) g_i(\vec{k}') \right\rangle = (2\pi^3)\delta(\vec{k}-\vec{k}')P_{g_i}(k) \quad \text{with} \quad i = 1,2 \,, \tag{221}$$

which obviously do not couple any mode of different $\vec{k}$ thanks to the Dirac's delta.
We must now stress that we are doing ensemble averages only on one Hubble volume, thus only the g_i fields will get averaged, while h keeps its "deterministic" value. This allows us to write the 2-point correlation function of Φ as

$$\begin{aligned}\left\langle \Phi^*(\vec{k})\Phi(\vec{k}') \right\rangle =& (2\pi)^3\delta(\vec{k}-\vec{k}')[P_{g_1}(k) + P_{g_2}(k)] \\ &+ \left[P_{g_1}(k) + P_{g_1}(k')\right] h(\vec{k}'-\vec{k}) \\ &+ \int \frac{d^3\widetilde{k}}{(2\pi)^3} P_{g_1}(\widetilde{k}) h^*(\vec{k}-\widetilde{\vec{k}}) h(\vec{k}'-\widetilde{\vec{k}}) \,.\end{aligned} \tag{222}$$

Already now, we can notice some peculiarity: in spite of what we have just told for the 2-points correlation functions of g_i, through the presence of $h(\vec{k}'-\vec{k})$ modes with different wavenumber get correlated, assuming that they are separated by less than the wavenumber of the modulating field h.
This already gives us some information to work on, however what we observe in the sky is the temperature of CMB photons, thus we must relate Φ with that, exploiting [10]

$$\frac{\Delta T}{T}(\vec{x}) = -\frac{1}{3}\Phi(\vec{x}) \,, \tag{223}$$

which can be decomposed in SHs as in Eq.179. In this case

$$\frac{\Delta T}{T}(\hat{n}) = \sum_\ell \sum_{m=-\ell}^{\ell} a_{\ell m} Y_{\ell m}(\hat{n}) \,, \tag{224}$$

inverted by (we have followed the same passages shown in Ch.4 for the CGWB case)

$$\begin{aligned} a_{\ell m} &= \int \frac{d^3k}{(2\pi)^3} \frac{\Delta T}{T}(\hat{n}) 4\pi i^\ell j_\ell\,(kD_{rec})\, Y^*_{\ell m}(\hat{k}) \\ &= -\frac{1}{3}\int \frac{d^3k}{(2\pi)^3}\Phi(\vec{x}) 4\pi i^\ell j_\ell\,(kD_{rec})\, Y^*_{\ell m}(\hat{k})\ , \end{aligned} \tag{225}$$

where: $j_\ell(x) =$ SBF;

D_{rec} = distance to the recombination surface, i.e. the LSS.

The SBFs are one of the two solutions of the Helmholtz equation

$$x^2\frac{d^2y}{dx^2} + 2x\frac{dy}{dx} + \Big(x^2 - n(n+1)\Big)\,y = 0\ . \tag{226}$$

They are defined from the "ordinary" Bessel functions as

$$j_\ell(x) \equiv \sqrt{\frac{\pi}{2x}} J_{\ell+\frac{1}{2}}(x)\ , \tag{227}$$

which can be written as

$$J_\ell(x) = \sum_{m=0}^{\infty} \frac{(-1)^m}{m!\Gamma(m+\ell+1)}\left(\frac{x}{2}\right)^{2m+\ell}\ . \tag{228}$$

As expected, in the isotropic and homogeneous case the temperature fields will obey to

$$\langle a^*_{\ell' m'} a_{\ell m}\rangle = C^{TT}_\ell \delta_{\ell\ell'}\delta_{mm'}\ , \tag{229}$$

where C^{TT}_ℓ is the angular power spectrum. Here, the very presence of the $\delta_{\ell\ell'}$ is the direct consequence of having assumed statistical isotropy. However, in the presence of a modulating field, things change, due to the modified expression of the 2-points correlation function of Φ.

For simplicity, we will consider a modulation of the following form

$$\Phi(\vec{x}) = g(\vec{x})[1 + h(\vec{x})]\ , \tag{230}$$

so that we only compute the interesting modulated component, without bothering to carry on also the standard isotropic results that $g_2(\vec{x})$ would have given (one can obtain the full result by adding the non-modulated one). Hence, in Fourier space

$$\Phi(\vec{k}) = g(\vec{k}) + \int \frac{d^3k'}{(2\pi)^3} g(\vec{k}')h(\vec{k} - \vec{k}')\ , \tag{231}$$

$$\begin{aligned}\left\langle \Phi^*(\vec{k})\Phi(\vec{k}')\right\rangle =&(2\pi)^3\delta(\vec{k}-\vec{k}')P_g(k)\\ &+\left[P_g(k)+P_g(k')\right]h(\vec{k}-\vec{k}')\\ &+\int\frac{d^3\widetilde{k}}{(2\pi)^3}P_g(\widetilde{k})h^*(\vec{k}-\widetilde{\vec{k}})h(\vec{k}'-\widetilde{\vec{k}})\,.\end{aligned} \tag{232}$$

Now, we can write the correlation function for the SH coefficients at different ℓ and m as

$$\begin{aligned}\langle a^*_{\ell m}a_{\ell' m'}\rangle =&\frac{1}{9}\int\frac{d^3k}{(2\pi)^3}\int\frac{d^3k'}{(2\pi)^3}\left\langle\Phi^*(\vec{k})\Phi\left(\vec{k}'\right)\right\rangle\\ &\times(4\pi)^2 i^{\ell'-\ell}j_\ell\left(kD_{rec}\right)j_{\ell'}\left(k'D_{rec}\right)\\ &\times Y_{\ell m}(\widehat{k})Y^*_{\ell' m'}\left(\widehat{k}'\right)\,.\end{aligned} \tag{233}$$

To proceed further we need to plug here Eq.232, which requires us to specify the expression for the modulating field.
There is no right or wrong choice for the modulation, but it all depends on what we want to obtain. In our case, we want to reproduce an excess power in one of the two hemispheres of the CMB, thus the most natural and simple choice is to go for a dipole modulation, such as [10]

$$h(\vec{x}) = w_1\sqrt{\frac{3}{4\pi}}\frac{1}{k_0 D_{rec}}\sin\vec{k}_0\cdot\vec{x}\,, \tag{234}$$

$$h(\vec{k}) = \frac{w_1}{2i}\sqrt{\frac{3}{4\pi}}\frac{(2\pi)^3}{k_0 D_{rec}}\left[\delta\left(\vec{k}-\vec{k}_0\right)-\delta\left(\vec{k}+\vec{k}_0\right)\right]\,. \tag{235}$$

where: $\vec{k}_0$ = wavenumber of the modulating field fluctuation;
w_1 = amplitude of the modulation;
1 = the subscript on the amplitude will remind us that we are considering a dipole modulation.

In first approximation, we can think this modulation as $\propto Y_{10}$ (dipole), but, again, one could have considered something different. E.g., [10] considers also a quadrupolar modulation $\propto Y_{20}$ to explain another CMB anomaly, the alignment of the quadrupole and octopole.
Without entering into the details of the subsequent calculations bringing to the final angular power spectrum, which we will profusely explore in Ch.6 for the CGWB case, we report only the final results, so that in the end we can compare them. Just be aware that in [10] the ISW effect was disregarded.

Firstly, the apex $^{(i)}$ will indicate a term at i-order in powers of h, i.e. the modulating field; thus, at zeroth order in the modulation we obtain [44]

$$\langle a^*_{\ell m} a_{\ell' m'} \rangle^{(0)} = \delta_{\ell\ell'} \delta_{mm'} C_\ell^{TT} \,, \tag{236}$$

where the angular power spectrum reads

$$C_\ell^{TT} \equiv \frac{4\pi}{9} \int \frac{dk}{k} \frac{k^3 P_g(k)}{2\pi^2} j_\ell^2(k\eta_{rec}) \,. \tag{237}$$

One can notice that this expression is basically the same obtained in Ch.4 for the CGWB.

For what regard the first order term (in the modulating field), one finds

$$\langle a^*_{\ell m} a_{\ell' m'} \rangle^{(1)} = \delta_{mm'} w_1 \left[R^{1,\ell}_{\ell' m} C_\ell^{TT} + R^{1,\ell'}_{\ell m} C_{\ell'}^{TT} \right] , \tag{238}$$

where

$$\begin{aligned} R^{\ell_1,\ell_2}_{\ell m} \equiv & (-1)^m \sqrt{\frac{(2\ell+1)\,(2\ell_1+1)\,(2\ell_2+1)}{4\pi}} \\ & \times \begin{pmatrix} \ell_1 & \ell_2 & \ell \\ 0 & 0 & 0 \end{pmatrix} \begin{pmatrix} \ell_1 & \ell_2 & \ell \\ 0 & m & -m \end{pmatrix} \end{aligned} \tag{239}$$

is a coupling matrix, which in our case (for example $\ell_1 = 1$ and $\ell_2 = \ell'$) couples modes with ℓ to $\ell \pm 1$ through the triangle rule of the $3-j$ Wigner's symbols [63].

Finally, without reporting the calculus, the second order term (in the modulating field) is given by [10] and reads

$$\langle a^*_{\ell m} a_{\ell' m'} \rangle^{(2)} = \delta_{mm'} w_1^2 \left[\sum_j R^{1,j}_{\ell m} R^{1,j}_{\ell' m} C_j^{TT} \right] , \tag{240}$$

which instead couples ℓ to $\ell \pm 2$.

The first thing we notice is that every term preserves the proportionality to $\delta_{mm'}$, meaning that only coefficients with the same m are correlated. On the other hand, the overall correlation between $a_{\ell m}$ will not be diagonal in ℓ, but there will be some non-diagonal terms correlating the first ($\ell \pm 1$) and second adjacent ($\ell \pm 2$) terms.

44 The apex $^T T$ just indicates that we are considering the self-correlation of the temperature field. In a more general context where one introduces other fields, such as the polarization ones E and B, it is possible to look also at the cross-correlations.

6

MODULATION ON THE GRAVITATIONAL WAVE BACKGROUND

We have briefly seen in Ch.5 what consequences a dipole modulation carries onto the CMB temperature field, but now we will plug the same dipole modulation in the framework introduced in Ch.4.
This time we will perform all the calculations in an explicit way, so that all the passages are clear to the reader. We will see that some similarity with the CMB case will pop up, together with some difference. Anyway, the same passages we are about to present can be used to obtain the final expressions of Ch.5 for the contributions to $\left\langle T_{\ell m} T^*_{\ell' m'} \right\rangle$.

6.1 SCALAR CONTRIBUTION OF THE ANGULAR POWER SPECTRUM OF THE CGWB

In Ch.4, we have seen that the gravitational potentials act on the CGWB through the SW and ISW effects. These two are part of the scalar contribution to the angular power spectrum of the CGWB, thus let us remind few expressions found in Ch.4 and Ch.5, which are very important to have clear. The scalar sourced term of Γ, defined in Eq.177, reads:

$$\begin{aligned}\Gamma_S\left(\eta_0, \vec{k}, \hat{n}\right) &= \int_{\eta_{in}}^{\eta_0} d\eta' e^{ik\mu(\eta'-\eta_0)} \left[T_\Phi(\eta', k)\delta(\eta'-\eta_{in}) + \frac{\partial\left[T_\Psi(\eta', k) + T_\Phi(\eta', k)\right]}{\partial\eta'}\right] \zeta(\vec{k}) \\ &\equiv \int_{\eta_{in}}^{\eta_0} d\eta' e^{-ik\mu(\eta_0-\eta')} T_S\left(\eta', k\right) \zeta(\vec{k}) \,.\end{aligned} \tag{241}$$

We can then decompose it in SH using Eq.179. The coefficients of such decomposition are equal to

$$\begin{aligned}\Gamma_{\ell m,S} &= 4\pi(-i)^l \int \frac{d^3k}{(2\pi)^3} e^{i\vec{k}\cdot\vec{x}_0} \zeta(\vec{k}) Y^*_{\ell m}(\hat{k}) \Big\{ T_\Phi\left(\eta_{in}, k\right) j_\ell\left(k\left(\eta_0 - \eta_{in}\right)\right) \\ &\qquad + \int_{\eta_{in}}^{\eta_0} d\eta' \frac{\partial\left[T_\Psi(\eta', k) + T_\Phi(\eta', k)\right]}{\partial\eta'} j_\ell\left(k\left(\eta_0 - \eta'\right)\right) \Big\} \\ &= 4\pi(-i)^l \int \frac{d^3k}{(2\pi)^3} e^{i\vec{k}\cdot\vec{x}_0} \zeta(\vec{k}) Y^*_{\ell m}(\hat{k}) T^S_\ell\left(k, \eta_0, \eta_{in}\right) \,,\end{aligned} \tag{242}$$

where we have introduced the transfer function

$$T_\ell^S(k,\eta_0,\eta_{in}) \equiv T_\Phi(\eta_{in},k)\, j_\ell(k(\eta_0-\eta_{in})) + \int_{\eta_{in}}^{\eta_0} d\eta' \frac{\partial[T_\Psi(\eta',k)+T_\Phi(\eta',k)]}{\partial\eta'} j_\ell(k(\eta_0-\eta')) \ . \tag{243}$$

As aforementioned when discussing Eq.191, instead of the stochastic variable $\zeta(k)$ used in Ch.4, we can plug the modulation of the gravitational potential of Eq.231 in Eq.242, introducing a Gaussian random field $g(k)$, having power near the horizon scale, and the modulation field $h(k)$, called "modulating field" and accounting for the symmetry breaking long-wavelength mode. This allows us also to carry on in the calculations the transfer function T_Φ, maintaining a general approach. Indeed, we will specify its explicit expression only after having obtained the general expressions of the angular power spectrum of the CGWB.
Thus, we write ζ as

$$\zeta(k) = g(k) + \int \frac{d^3k'}{(2\pi)^3} g(k')h(k-k') \ . \tag{244}$$

Hence, the correlation function becomes

$$\begin{aligned}\left\langle \zeta(\vec{k})\zeta^*\left(\vec{k}'\right)\right\rangle =& (2\pi)^3\delta\left(\vec{k}-\vec{k}'\right)P_g(k) \\ &+ \left[P_g(k)+P_g\left(k'\right)\right]h\left(\vec{k}-\vec{k}'\right) \\ &+ \int \frac{d^3\widetilde{k}}{(2\pi)^3} P_g(\widetilde{k})h(\vec{k}-\widetilde{\vec{k}})h^*\left(\vec{k}'-\widetilde{\vec{k}}\right) \ ,\end{aligned} \tag{245}$$

which can be plugged into

$$\begin{aligned}\langle \Gamma_{\ell m,S}\Gamma^*_{\ell' m',S}\rangle =& (4\pi)^2(-i)^{\ell-\ell'}\int \frac{d^3k}{(2\pi)^3} e^{i\vec{k}\cdot\vec{x}_0}\int \frac{d^3k'}{(2\pi)^3} e^{-i\vec{k}'\cdot\vec{x}_0}\left\langle \zeta(\vec{k})\zeta^*\left(\vec{k}'\right)\right\rangle \\ &\times Y^*_{\ell m}(\widehat{k})Y_{\ell' m'}\left(\widehat{k}'\right)\times T_\ell^S(k,\eta_0,\eta_{in})\, T_{\ell'}^S\left(k',\eta_0,\eta_{in}\right) \ .\end{aligned} \tag{246}$$

Identifying the terms of Eq.245 based on their order in $h(\vec{k})$, we can write the different contributions to the correlation of the Γ_S.

6.1.1 *Zeroth Order Term in the Modulating Field*

Starting from the zeroth order term (in the modulating field), it is easy to find

$$\begin{aligned}
&\langle \Gamma_{\ell m,S}\Gamma^{*}_{\ell' m',S}\rangle^{(0)} = \\
=&(4\pi)^2(-i)^{\ell-\ell'}\int\frac{d^3k}{(2\pi)^3}e^{i\vec{k}\cdot\vec{x}_0}\int\frac{d^3k'}{(2\pi)^3}e^{-i\vec{k}'\cdot\vec{x}_0}\times(2\pi)^3\delta\left(\vec{k}-\vec{k}'\right)P_g(k) \\
&\times Y^{*}_{\ell m}(\widehat{k})Y_{\ell' m'}\left(\widehat{k}'\right)\times T^{S}_{\ell}\left(k,\eta_0,\eta_{in}\right)T^{S}_{\ell'}\left(k',\eta_0,\eta_{in}\right) = \\
=&(4\pi)^2(-i)^{\ell-\ell'}\int\frac{d^3k}{(2\pi)^3}P_g(k)\times Y^{*}_{\ell m}(\widehat{k})Y_{\ell' m'}\left(\widehat{k}\right)\times T^{S}_{\ell}\left(k,\eta_0,\eta_{in}\right)T^{S}_{\ell'}\left(k,\eta_0,\eta_{in}\right) = \\
=&(4\pi)^2\int\frac{dk}{k(2\pi)^3}k^3P_g(k)\delta_{mm'}\delta_{\ell\ell'}T^{(S)2}_{\ell}\left(k,\eta_0,\eta_{in}\right) = \\
=&4\pi\int\frac{dk}{k}\Delta_g(k)\delta_{mm'}\delta_{\ell\ell'}T^{(S)2}_{\ell}\left(k,\eta_0,\eta_{in}\right) = \\
=&\delta_{\ell\ell'}\delta_{mm'}C^{(0)}_{\ell}\,,
\end{aligned} \tag{247}$$

where $\Delta_g \equiv \frac{k^3}{2\pi^2}P_g$. Here, we have used the orthogonality condition of SHs and the fact that the observer is positioned in $\vec{x}_0 = 0$. As one can expect by sending the modulating field to zero, this term gives the isotropic term found in Ch.4, where one have to substitute $\Delta_g \leftrightarrow P_\zeta$[45].

6.1.2 *First Order Term in the Modulating Field*

For what regard the first order term (in the modulating field), we must fix an explicit expression of $h(\vec{k})$. In order to mimic what we have done in Ch.5, following [10], we assume a dipole modulation, thus we can write

$$h(\vec{k}) = \frac{w_1}{2i}\sqrt{\frac{3}{4\pi}}\frac{(2\pi)^3}{k_0\left(\eta_0-\eta_{in}\right)}\left[\delta\left(\vec{k}-\vec{k}_0\right)-\delta\left(\vec{k}+\vec{k}_0\right)\right]\,. \tag{248}$$

We stress again that this choice of the modulating field is not mandatory, but instead represents the most simple example we could use to study a departure from isotropy. For now, we stick to this parametrization, but in the future it would be interesting to explore more general choices.

45 Once have defined which is the power spectrum and its adimensional counterpart, the two expression are completely equivalent as one would expect.

To go on with our calculation we need to make explicit h in $\vec{k}' - \vec{k}$, thus using the expression above in Fourier space

$$h(\vec{k}' - \vec{k}) = \frac{w_1}{2i}\sqrt{\frac{3}{4\pi}}\frac{(2\pi)^3}{k_0\,(\eta_0 - \eta_{in}\,)}\left[\delta\left(\vec{k}' - \vec{k} - \vec{k}_0\right) - \delta\left(\vec{k}' - \vec{k} + \vec{k}_0\right)\right], \tag{249}$$

which allows to find

$$\begin{aligned}
&\langle \Gamma_{\ell m,S}\Gamma^*_{\ell' m',S}\rangle^{(1)} = \\
&(4\pi)^2(-i)^{\ell-\ell'}\int\frac{d^3k}{(2\pi)^3}e^{i\,\vec{k}\cdot\vec{x}_0}\int\frac{d^3k'}{(2\pi)^3}e^{-i\,\vec{k}'\cdot\vec{x}_0}\times\left[P_g(k) + P_g\left(k'\right)\right]h\left(\vec{k}' - \vec{k}\right)\\
&\times Y^*_{\ell m}(\widehat{k})Y_{\ell' m'}\left(\widehat{k}'\right)\times T^S_\ell\left(k,\eta_0,\eta_{in}\right)T^S_{\ell'}\left(k',\eta_0,\eta_{in}\right)\\
=&(4\pi)^2(-i)^{\ell-\ell'}\int\frac{d^3k}{(2\pi)^3}e^{i\,\vec{k}\cdot\vec{x}_0}\int\frac{d^3k'}{(2\pi)^3}e^{-i\,\vec{k}'\cdot\vec{x}_0}\times\left[P_g(k) + P_g\left(k'\right)\right]\\
&\times Y^*_{\ell m}(\widehat{k})Y_{\ell' m'}\left(\widehat{k}'\right)\times T^S_\ell\left(k,\eta_0,\eta_{in}\right)T^S_{\ell'}\left(k',\eta_0,\eta_{in}\right)\\
&\times\frac{w_1}{2i}\sqrt{\frac{3}{4\pi}}\frac{(2\pi)^3}{k_0\,(\eta_0 - \eta_{in}\,)}\left[\delta\left(\vec{k}' - \vec{k} - \vec{k}_0\right) - \delta\left(\vec{k}' - \vec{k} + \vec{k}_0\right)\right].
\end{aligned} \tag{250}$$

Let us consider the first of the two Dirac deltas and solve that term. Again, assuming the origin in $x_0 = 0$ we can get rid of the exponentials and, integrating the delta, we get

$$\begin{aligned}
&\langle \Gamma_{\ell m,S}\Gamma^*_{\ell' m',S}\rangle^{(1)}_{1st} = \\
=&(4\pi)^2(-i)^{\ell-\ell'}\int\frac{d^3k}{(2\pi)^3}\int\frac{d^3k'}{(2\pi)^3}\times\left[P_g(k) + P_g\left(k'\right)\right]\\
&\times Y^*_{\ell m}(\widehat{k})Y_{\ell' m'}\left(\widehat{k}'\right)\times T^S_\ell\left(k,\eta_0,\eta_{in}\right)T^S_{\ell'}\left(k',\eta_0,\eta_{in}\right)\\
&\times\frac{w_1}{2i}\sqrt{\frac{3}{4\pi}}\frac{(2\pi)^3}{k_0\,(\eta_0 - \eta_{in}\,)}\delta\left(\vec{k}' - \vec{k} - \vec{k}_0\right)\\
=&\frac{(4\pi)^2}{(2\pi)^3}(-i)^{\ell-\ell'}\int d^3k\left[P_g(k) + P_g\left(|\vec{k} + \vec{k}_0|\right)\right]\\
&\times Y^*_{\ell m}(\widehat{k})Y_{\ell' m'}\left(\frac{\vec{k} + \vec{k}_0}{|\vec{k} + \vec{k}_0|}\right)\times T^S_\ell\left(k,\eta_0,\eta_{in}\right)T^S_{\ell'}\left(|\vec{k} + \vec{k}_0|,\eta_0,\eta_{in}\right)\\
&\times\frac{w_1}{2i}\sqrt{\frac{3}{4\pi}}\frac{1}{k_0\,(\eta_0 - \eta_{in})}.
\end{aligned} \tag{251}$$

Now, we can make explicit the product of the transfer function and the SHs evaluated in $|\vec{k}+\vec{k}_0|$, where we can identify the SW (second line) and the ISW (third line) effects for the CGWB

$$\begin{aligned}
&\frac{1}{k_0\,(\eta_0-\eta_{in})}\sqrt{\frac{3}{4\pi}}T_{\ell'}^{S}\left(|\vec{k}+\vec{k}_0|,\eta_0,\eta_{in}\right)Y_{\ell'm'}\left(\frac{\vec{k}+\vec{k}_0}{|\vec{k}+\vec{k}_0|}\right)=\\
&\frac{1}{k_0\,(\eta_0-\eta_{in})}\sqrt{\frac{3}{4\pi}}\Bigg[T_\Phi\left(\eta_{in}\,,|\vec{k}+\vec{k}_0|\right)j_{\ell'}\left[|\vec{k}+\vec{k}_0|\,(\eta_0-\eta_{in})\right]\\
&+\int_{\eta_{in}}^{\eta_0}d\eta'\frac{\partial\left[T_\Psi(\eta',|\vec{k}+\vec{k}_0|)+T_\Phi(\eta',|\vec{k}+\vec{k}_0|)\right]}{\partial\eta'}j_{\ell'}\left[|\vec{k}+\vec{k}_0|\,(\eta_0-\eta')\right]\Bigg]\\
&\times Y_{\ell'm'}\left(\frac{\vec{k}+\vec{k}_0}{|\vec{k}+\vec{k}_0|}\right)\,.
\end{aligned}\tag{252}$$

Now, we can introduce an approximation to expand the product of a SBF and a SH in the previous expression for $k_0 \ll k$. Specifically, one can show that [10]

$$\begin{aligned}
&\tfrac{1}{k_0(\eta_0-\eta_{in})}\sqrt{\tfrac{3}{4\pi}}j_\ell\left(\left|\vec{k}+\alpha\vec{k}_0\right|(\eta_0-\eta_{in})\right)Y_{\ell m}\left(\tfrac{\vec{k}+\alpha\vec{k}_0}{|\vec{k}+\alpha\vec{k}_0|}\right)\\
&\approx\tfrac{1}{k_0(\eta_0-\eta_{in})}\sqrt{\tfrac{3}{4\pi}}j_\ell(k\,(\eta_0-\eta_{in}))Y_{\ell m}(\widehat{k})\\
&\quad-\tfrac{\alpha}{2}R_{\ell m}^{1,\ell+1}j_{\ell+1}(k\,(\eta_0-\eta_{in}))Y_{\ell+1,m}(\widehat{k})\\
&\quad+\tfrac{\alpha}{2}R_{\ell m}^{1,\ell-1}j_{\ell-1}(k\,(\eta_0-\eta_{in}))Y_{\ell-1,m}(\widehat{k})\,,
\end{aligned}\tag{253}$$

where

$$\begin{aligned}
R_{\ell m}^{\ell_1,\ell_2}\equiv&(-1)^m\sqrt{\frac{(2\ell+1)\,(2\ell_1+1)\,(2\ell_2+1)}{4\pi}}\\
&\times\begin{pmatrix}\ell_1&\ell_2&\ell\\0&0&0\end{pmatrix}\begin{pmatrix}\ell_1&\ell_2&\ell\\0&m&-m\end{pmatrix}\,.
\end{aligned}\tag{254}$$

In our case we have $\alpha = 1$ and $\ell \to \ell'$, $m \to m'$, thus [46]

$$\begin{aligned}
&\frac{1}{k_0(\eta_0-\eta_{in})}\sqrt{\frac{3}{4\pi}} j_{\ell'}\left(\left|\vec{k}+\vec{k}_0\right|(\eta_0-\eta_{in})\right) Y_{\ell' m'}\left(\frac{\vec{k}+\vec{k}_0}{|\vec{k}+\vec{k}_0|}\right)\\
&\approx \frac{1}{k_0(\eta_0-\eta_{in})}\sqrt{\frac{3}{4\pi}} j_{\ell'}(k(\eta_0-\eta_{in}))Y_{\ell' m'}(\hat{k})\\
&\quad -\frac{1}{2}R^{1,\ell'+1}_{\ell' m'} j_{\ell'+1}(k(\eta_0-\eta_{in}))Y_{\ell'+1,m'}(\hat{k})\\
&\quad +\frac{1}{2}R^{1,\ell'-1}_{\ell' m'} j_{\ell'-1}(k(\eta_0-\eta_{in}))Y_{\ell'-1,m'}(\hat{k})\,.
\end{aligned} \tag{256}$$

With this approximation, we can write for the SW effect (second line of Eq.252)

$$\begin{aligned}
&\frac{1}{k_0(\eta_0-\eta_{in})}\sqrt{\frac{3}{4\pi}} T_\Phi\left(\eta_{in}, |\vec{k}+\vec{k}_0|\right) j_{\ell'}\left[|\vec{k}+\vec{k}_0|(\eta_0-\eta_{in})\right]\\
&\times Y_{\ell' m'}\left(\frac{\vec{k}+\vec{k}_0}{|\vec{k}+\vec{k}_0|}\right) =\\
&\approx \frac{1}{k_0(\eta_0-\eta_{in})}\sqrt{\frac{3}{4\pi}} T_\Phi\left(\eta_{in}, |\vec{k}+\vec{k}_0|\right) j_{\ell'}(k(\eta_0-\eta_{in}))Y_{\ell' m'}(\hat{k})\\
&-\frac{1}{2}R^{1,\ell'+1}_{\ell' m'} T_\Phi\left(\eta_{in}, |\vec{k}+\vec{k}_0|\right) j_{\ell'+1}(k(\eta_0-\eta_{in}))Y_{\ell'+1,m'}(\hat{k})\\
&+\frac{1}{2}R^{1,\ell'-1}_{\ell' m'} T_\Phi\left(\eta_{in}, |\vec{k}+\vec{k}_0|\right) j_{\ell'-1}(k(\eta_0-\eta_{in}))Y_{\ell'-1,m'}(\hat{k}) =\\
&= \frac{1}{k_0(\eta_0-\eta_{in})}\sqrt{\frac{3}{4\pi}} T^{SW}_{\ell'}\left(|\vec{k}+\vec{k}_0|\right) Y_{\ell' m'}(\hat{k})\\
&-\frac{1}{2}R^{1,\ell'+1}_{\ell' m'} T^{SW}_{\ell'+1}\left(|\vec{k}+\vec{k}_0|\right) Y_{\ell'+1,m'}(\hat{k})\\
&+\frac{1}{2}R^{1,\ell'-1}_{\ell' m'} T^{SW}_{\ell'-1}\left(|\vec{k}+\vec{k}_0|\right) Y_{\ell'-1,m'}(\hat{k})\,,
\end{aligned} \tag{257}$$

where we have defined the following quantity

$$T^{SW}_{\ell}\left(|\vec{k}+\vec{k}_0|\right) \equiv T_\Phi\left(\eta_{in}, |\vec{k}+\vec{k}_0|\right) j_\ell(k(\eta_0-\eta_{in}))\,. \tag{258}$$

46 In spite of what is reported in [10], in Eq.253 we presented an extra 1/2 factor in front of the first order terms in the expansion. This factors is due to the known relation of the derivative of Bessel functions [49]

$$\frac{dJ_\ell(z)}{dz} = \boxed{\frac{1}{2}}[J_{\ell-1}(z) - J_{\ell+1}(z)]\,. \tag{255}$$

Even if this does not seem the case at first sight, this factor is indeed crucial to reconcile our results with the ones of [10] (we will come back on this later on in this Thesis).

We stress that this transfer function is different from the SW contribution of Eq.243 because here T_Φ is evaluated in $|\vec{k}+\vec{k}_0|$ and not in $\vec{k}$.
Looking now at the ISW effect (third line of Eq.252), we can write similarly

$$
\begin{aligned}
&\frac{1}{k_0(\eta_0-\eta_{in})}\sqrt{\frac{3}{4\pi}}\int_{\eta_{in}}^{\eta_0}d\eta'\frac{\partial\left[T_\Psi(\eta',|\vec{k}+\vec{k}_0|)+T_\Phi(\eta',|\vec{k}+\vec{k}_0|)\right]}{\partial\eta'}\\
&\times j_{\ell'}\left[|\vec{k}+\vec{k}_0|\,(\eta_0-\eta')\right]Y_{\ell'm'}\left(\frac{\vec{k}+\vec{k}_0}{|\vec{k}+\vec{k}_0|}\right)=\\
&\approx\frac{1}{k_0(\eta_0-\eta_{in})}\sqrt{\frac{3}{4\pi}}\int_{\eta_{in}}^{\eta_0}d\eta'\frac{\partial\left[T_\Psi(\eta',|\vec{k}+\vec{k}_0|)+T_\Phi(\eta',|\vec{k}+\vec{k}_0|)\right]}{\partial\eta'}\\
&\times j_{\ell'}\left(k\left(\eta_0-\eta'\right)\right)Y_{\ell'm'}\left(\widehat{k}\right)+\\
&-\frac{1}{2}R^{1,\ell'+1}_{\ell'm'}\int_{\eta_{in}}^{\eta_0}d\eta'\frac{\eta_0-\eta'}{\eta_0-\eta_{in}}\frac{\partial\left[T_\Psi(\eta',|\vec{k}+\vec{k}_0|)+T_\Phi(\eta',|\vec{k}+\vec{k}_0|)\right]}{\partial\eta'}\\
&\times j_{\ell'+1}\left(k\left(\eta_0-\eta'\right)\right)Y_{\ell'+1,m'}\left(\widehat{k}\right)+\\
&+\frac{1}{2}R^{1,\ell'-1}_{\ell'm'}\int_{\eta_{in}}^{\eta_0}d\eta'\frac{\eta_0-\eta'}{\eta_0-\eta_{in}}\frac{\partial\left[T_\Psi(\eta',|\vec{k}+\vec{k}_0|)+T_\Phi(\eta',|\vec{k}+\vec{k}_0|)\right]}{\partial\eta'}\\
&\times j_{\ell'-1}\left(k\left(\eta_0-\eta'\right)\right)Y_{\ell'-1,m'}\left(\widehat{k}\right)=\\
&=\frac{1}{k_0(\eta_0-\eta_{in})}\sqrt{\frac{3}{4\pi}}T^{ISW}_{\ell'}\left(|\vec{k}+\vec{k}_0|\right)Y_{\ell'm'}(\widehat{k})\\
&-\frac{1}{2}R^{1,\ell'+1}_{\ell'm'}T^{ISW\star}_{\ell'+1}\left(|\vec{k}+\vec{k}_0|\right)Y_{\ell'+1,m'}(\widehat{k})\\
&+\frac{1}{2}R^{1,\ell'-1}_{\ell'm'}T^{ISW\star}_{\ell'-1}\left(|\vec{k}+\vec{k}_0|\right)Y_{\ell'-1,m'}(\widehat{k})\,.
\end{aligned}
\tag{259}
$$

This time the approximation of Eq.253 gives us a new extra factor inside the integral.
Indeed, when computing the first order term of the expansion, one has to evaluate

$$
\frac{dj_\ell(z(\alpha))}{d\alpha}=\frac{dj_\ell(z)}{dz}\frac{dz(\alpha)}{d\alpha}\,,
\tag{260}
$$

where: $z(\alpha)\equiv|\vec{k}+\alpha\vec{k}_0|\,(\eta_0-\eta')$;
$\alpha\ll1\rightarrow$ this allows to realize $\alpha k_0\ll k$.

Then, looking at the derivative of z w.r.t. α

$$\begin{aligned}\frac{dz(\alpha)}{d\alpha} =&(\eta_0-\eta')\frac{d}{d\alpha}\left(\sqrt{k^2+\alpha^2k_0^2+2\alpha\cos(\theta)kk_0}\right)\\ \simeq&(\eta_0-\eta')\frac{d}{d\alpha}\left(\sqrt{k^2+2\alpha\cos(\theta)kk_0}\right)\\ =&(\eta_0-\eta')\frac{1}{2}\frac{2\cos(\theta)kk_0}{\sqrt{k^2+2\alpha\cos(\theta)kk_0}}\simeq(\eta_0-\eta')\frac{\cos(\theta)kk_0}{k}\\ \simeq&(\eta_0-\eta')\cos(\theta)k_0\simeq k_0(\eta_0-\eta')\,,\end{aligned} \tag{261}$$

where we approximated the cosine to 1 as done for Eq.253. We can see that now the derivative just obtained does not cancel out the front factor present in Eq.259, giving instead an extra factor

$$\frac{\eta_0-\eta'}{\eta_0-\eta_{in}}\neq 1\,. \tag{262}$$

For this reason in Eq.259, we have defined two different transfer functions, distinguished by a $\star$

$$\begin{aligned}T_\ell^{ISW}\left(|\vec{k}+\vec{k}_0|\right)\equiv&\int_{\eta_{in}}^{\eta_0}d\eta'\frac{\partial\left[T_\Psi(\eta',|\vec{k}+\vec{k}_0|)+T_\Phi(\eta',|\vec{k}+\vec{k}_0|)\right]}{\partial\eta'}\\ &\times j_\ell\left(k\left(\eta_0-\eta'\right)\right)\,,\\ T_\ell^{ISW\star}\left(|\vec{k}+\vec{k}_0|\right)\equiv&\int_{\eta_{in}}^{\eta_0}d\eta'\frac{\partial\left[T_\Psi(\eta',|\vec{k}+\vec{k}_0|)+T_\Phi(\eta',|\vec{k}+\vec{k}_0|)\right]}{\partial\eta'}\\ &\times\frac{\eta_0-\eta'}{\eta_0-\eta_{in}}j_\ell\left(k\left(\eta_0-\eta'\right)\right)\,.\end{aligned} \tag{263}$$

We stress again that this transfer function is in general different from the ISW contribution of T_ℓ^S (see Eq.243) because here T_Φ and T_Ψ are evaluated in $|\vec{k}+\vec{k}_0|$ and not in $\vec{k}$.
Also, the presence of the extra factor, induced by the modulation, represents a signature of the departure from isotropy of the CGWB, given that it is not present in the isotropic computations (we will come back to this point in

Ch.7).
Neglecting for the moment the ISW effect, Eq.251 becomes

$$\begin{aligned}
&\langle \Gamma_{\ell m,S}\Gamma^{*}_{\ell' m',S}\rangle^{(1)}_{1st} = \\
=&\frac{(4\pi)^2}{(2\pi)^3}(-i)^{\ell-\ell'}\frac{w_1}{2i}\int dk k^2\left[P_g(k)+P_g\left(|\vec{k}+\vec{k}_0|\right)\right]T^S_\ell\left(k,\eta_0,\eta_{in}\right)\\
&\times\int d\hat{k}Y^{*}_{\ell m}(\hat{k})\Big[\frac{1}{k_0\left(\eta_0-\eta_{in}\right)}\sqrt{\frac{3}{4\pi}}T^{SW}_{\ell'}\left(|\vec{k}+\vec{k}_0|\right)Y_{\ell' m'}(\hat{k})\\
&-\frac{1}{2}R^{1,\ell'+1}_{\ell' m'}T^{SW}_{\ell'+1}\left(|\vec{k}+\vec{k}_0|\right)Y_{\ell'+1,m'}(\hat{k})+\frac{1}{2}R^{1,\ell'-1}_{\ell' m'}T^{SW}_{\ell'-1}\left(|\vec{k}+\vec{k}_0|\right)Y_{\ell'-1,m'}(\hat{k})\Big],
\end{aligned}\tag{264}$$

which, computing individually the three resulting terms, becomes

$$\begin{aligned}
&\langle \Gamma_{\ell m,S}\Gamma^{*}_{\ell' m',S}\rangle^{(1)}_{1st} = \\
=&\frac{(4\pi)^2}{(2\pi)^3}(-i)^{\ell-\ell'}\frac{w_1}{2i}\int dk k^2\left[P_g(k)+P_g\left(|\vec{k}+\vec{k}_0|\right)\right]T^S_\ell\left(k,\eta_0,\eta_{in}\right)T^{SW}_{\ell'}\left(|\vec{k}+\vec{k}_0|\right)\\
&\times\frac{1}{k_0\left(\eta_0-\eta_{in}\right)}\sqrt{\frac{3}{4\pi}}\times\int d\hat{k}Y^{*}_{\ell m}(\hat{k})Y_{\ell' m'}(\hat{k})+\\
&-\frac{(4\pi)^2}{(2\pi)^3}(-i)^{\ell-\ell'}\frac{w_1}{2i}\int dk k^2\left[P_g(k)+P_g\left(|\vec{k}+\vec{k}_0|\right)\right]T^S_\ell\left(k,\eta_0,\eta_{in}\right)T^{SW}_{\ell'+1}\left(|\vec{k}+\vec{k}_0|\right)\\
&\times\frac{1}{2}R^{1,\ell'+1}_{\ell' m'}\int d\hat{k}Y^{*}_{\ell m}(\hat{k})Y_{\ell'+1,m'}(\hat{k})+\\
&+\frac{(4\pi)^2}{(2\pi)^3}(-i)^{\ell-\ell'}\frac{w_1}{2i}\int dk k^2\left[P_g(k)+P_g\left(|\vec{k}+\vec{k}_0|\right)\right]T^S_\ell\left(k,\eta_0,\eta_{in}\right)T^{SW}_{\ell'-1}\left(|\vec{k}+\vec{k}_0|\right)\\
&\times\frac{1}{2}R^{1,\ell'-1}_{\ell' m'}\int d\hat{k}Y^{*}_{\ell m}(\hat{k})Y_{\ell'-1,m'}(\hat{k}) = \\
=&\frac{(4\pi)^2}{(2\pi)^3}\frac{w_1}{2i}\int dk k^2\left[P_g(k)+P_g\left(|\vec{k}+\vec{k}_0|\right)\right]T^S_\ell\left(k,\eta_0,\eta_{in}\right)T^{SW}_{\ell}\left(|\vec{k}+\vec{k}_0|\right)\\
&\times\frac{1}{k_0\left(\eta_0-\eta_{in}\right)}\sqrt{\frac{3}{4\pi}}\times\delta_{\ell\ell'}\delta_{mm'}+\\
&-\frac{(4\pi)^2}{(2\pi)^3}(-i)\frac{w_1}{2i}\int dk k^2\left[P_g(k)+P_g\left(|\vec{k}+\vec{k}_0|\right)\right]T^S_\ell\left(k,\eta_0,\eta_{in}\right)T^{SW}_{\ell}\left(|\vec{k}+\vec{k}_0|\right)\\
&\times\frac{1}{2}R^{1,\ell}_{\ell' m}\delta_{mm'}+\\
&+\frac{(4\pi)^2}{(2\pi)^3}(-i)^{-1}\frac{w_1}{2i}\int dk k^2\left[P_g(k)+P_g\left(|\vec{k}+\vec{k}_0|\right)\right]T^S_\ell\left(k,\eta_0,\eta_{in}\right)T^{SW}_{\ell}\left(|\vec{k}+\vec{k}_0|\right)\\
&\times\frac{1}{2}R^{1,\ell}_{\ell' m}\delta_{mm'} =
\end{aligned}$$

$$
\begin{aligned}
=&\frac{(4\pi)^2}{(2\pi)^3}\frac{w_1}{2i}\int dk k^2\left[P_g(k)+P_g\left(|\vec{k}+\vec{k}_0|\right)\right]T_\ell^S\left(k,\eta_0,\eta_{in}\right)T_\ell^{SW}\left(|\vec{k}+\vec{k}_0|\right)\\
&\times\frac{1}{k_0\left(\eta_0-\eta_{in}\right)}\sqrt{\frac{3}{4\pi}}\times\delta_{\ell\ell'}\delta_{mm'}+\\
&+\frac{(4\pi)^2}{(2\pi)^3}\frac{w_1}{2}R^{1,\ell}_{\ell' m}\delta_{mm'}\int dk k^2\left[P_g(k)+P_g\left(|\vec{k}+\vec{k}_0|\right)\right]\\
&\times T_\ell^S\left(k,\eta_0,\eta_{in}\right)T_\ell^{SW}\left(|\vec{k}+\vec{k}_0|\right).
\end{aligned}
\tag{265}
$$

In other words, we get an isotropic contribution ($\propto \delta_{\ell\ell'}$) and one that couples $\ell \pm 1$ to ℓ through the 3-j symbols in the definition of R. Indeed the triangle inequality[47] applied to the $3-j$ symbols gives the only non-null contribution when $\ell' = \ell \pm 1$.

We have just computed the first contribution to Eq.250, so we must compute the other one, coming from the other Dirac delta. However we can exploit a simple trick to fasten the procedure: if we integrate the delta in k (instead of k'), the delta sends $k \to k' + k_0$ and the procedure becomes exactly the same as in the previous case, at the cost of inverting the primes. One can show that in the end the contribution reads[48]

$$
\begin{aligned}
&\langle\Gamma_{\ell m,S}\Gamma^*_{\ell' m',S}\rangle^{(1)}_{2nd}=\\
=&-\frac{(4\pi)^2}{(2\pi)^3}\frac{w_1}{2i}\int dk k^2\left[P_g(k)+P_g\left(|\vec{k}+\vec{k}_0|\right)\right]T_\ell^S\left(k,\eta_0,\eta_{in}\right)T_\ell^{SW}\left(|\vec{k}+\vec{k}_0|\right)\\
&\times\frac{1}{k_0\left(\eta_0-\eta_{in}\right)}\sqrt{\frac{3}{4\pi}}\times\delta_{\ell\ell'}\delta_{mm'}+\\
&+\frac{(4\pi)^2}{(2\pi)^3}\frac{w_1}{2}R^{1,\ell'}_{\ell m}\delta_{mm'}\int dk' k'^2\left[P_g(k')+P_g\left(k'+k_0\right)\right]\\
&\times T_{\ell'}^S\left(k',\eta_0,\eta_{in}\right)T_{\ell'}^{SW}(k'+k_0).
\end{aligned}
\tag{267}
$$

47 For a symbol of the type

$$
\begin{pmatrix}\ell_1 & \ell_2 & \ell\\ 0 & m & -m\end{pmatrix}
\tag{266}
$$

the following has to hold: $|\ell_1-\ell_2| \leqslant \ell \leqslant \ell_1+\ell_2$. In our case this becomes $|\ell-1| \leqslant \ell' \leqslant \ell+1$, however these are all integer quantities, thus ℓ' is fixed to $\ell \pm 1$ (see [63]).

48 We included the minus sign in front of the delta in such a way that the two contributions have to be summed.

Notice that the isotropic term is the same in the two contributions, exception made for a minus sign in the latter expression, thus the final expression will be

$$\begin{aligned}
&\langle \Gamma_{\ell m,S}\Gamma^{*}_{\ell' m',S}\rangle^{(1)}_{SW} = \langle \Gamma_{\ell m,S}\Gamma^{*}_{\ell' m',S}\rangle^{(1)}_{1st} + \langle \Gamma_{\ell m,S}\Gamma^{*}_{\ell' m',S}\rangle^{(1)}_{2nd} = \\
=&\frac{(4\pi)^2}{(2\pi)^3}\frac{w_1}{2}R^{1,\ell}_{\ell' m}\delta_{mm'}\int dk k^2\left[P_g(k)+P_g\left(|\vec{k}+\vec{k}_0|\right)\right]T^S_\ell\left(k,\eta_0,\eta_{in}\right)T^{SW}_\ell\left(|\vec{k}+\vec{k}_0|\right) \\
&+\frac{(4\pi)^2}{(2\pi)^3}\frac{w_1}{2}R^{1,\ell'}_{\ell m}\delta_{mm'}\int dk' k'^2\left[P_g(k')+P_g\left(k'+k_0\right)\right]T^S_{\ell'}\left(k',\eta_0,\eta_{in}\right)T^{SW}_{\ell'}(k'+k_0) = \\
=&4\pi\frac{w_1}{2}R^{1,\ell}_{\ell' m}\delta_{mm'}\int \frac{dk}{k}\frac{k^3}{2\pi^2}\left[P_g(k)+P_g\left(|\vec{k}+\vec{k}_0|\right)\right]T^S_\ell\left(k,\eta_0,\eta_{in}\right)T^{SW}_\ell\left(|\vec{k}+\vec{k}_0|\right) \\
&+4\pi\frac{w_1}{2}R^{1,\ell'}_{\ell m}\delta_{mm'}\int \frac{dk'}{k'}\frac{k'^3}{2\pi^2}\left[P_g(k')+P_g\left(k'+k_0\right)\right]T^S_{\ell'}\left(k',\eta_0,\eta_{in}\right)T^{SW}_{\ell'}(k'+k_0) = \\
=&\frac{w_1}{2}\delta_{mm'}\left[R^{1,\ell}_{\ell' m}C^{SW}_\ell + R^{1,\ell'}_{\ell m}C^{SW}_{\ell'}\right],
\end{aligned} \tag{268}$$

where we defined the angular power spectrum (of the CGWB) relative to this contribution as

$$C^{SW}_\ell \equiv 4\pi\int \frac{dk}{k}\frac{k^3}{2\pi^2}\left[P_g(k)+P_g\left(|\vec{k}+\vec{k}_0|\right)\right]T^S_\ell\left(k,\eta_0,\eta_{in}\right)T^{SW}_\ell\left(|\vec{k}+\vec{k}_0|\right). \tag{269}$$

In order to simplify our computation, until now we had temporarily neglected the ISW effect contribution, leaving only the easier-to-treat SW one. However, in spite of the different explicit expressions of the two effects, they can be treated in the same way; one has just to pay attention to the presence of the modified transfer functions that characterize the ISW effect. In other words, without reporting the same passages done for the SW case, we can write for its integrated counterpart

$$\langle \Gamma_{\ell m,S}\Gamma^{*}_{\ell' m',S}\rangle^{(1)}_{ISW} = \frac{w_1}{2}\delta_{mm'}\left[R^{1,\ell}_{\ell' m}C^{ISW}_\ell + R^{1,\ell'}_{\ell m}C^{ISW}_{\ell'}\right], \tag{270}$$

where now

$$C^{ISW}_\ell \equiv 4\pi\int \frac{dk}{k}\frac{k^3}{2\pi^2}\left[P_g(k)+P_g\left(|\vec{k}+\vec{k}_0|\right)\right]T^S_\ell\left(k,\eta_0,\eta_{in}\right)T^{ISW\star}_\ell\left(|\vec{k}+\vec{k}_0|\right). \tag{271}$$

To obtain the full first order contribution to the correlation of the SH coefficients, we can then sum Eq.268 and Eq.270 to obtain

$$\langle \Gamma_{\ell m,S}\Gamma^{*}_{\ell' m',S}\rangle^{(1)} = \frac{w_1}{2}\delta_{mm'}\left[R^{1,\ell}_{\ell' m}C^{(1)}_\ell + R^{1,\ell'}_{\ell m}C^{(1)}_{\ell'}\right], \tag{272}$$

where

$$\begin{aligned}\mathcal{C}_\ell^{(1)} \equiv & 4\pi \int \frac{dk}{k} \frac{k^3}{2\pi^2} \left[P_g(k) + P_g\left(|\vec{k} + \vec{k}_0|\right) \right] T_\ell^S\left(k, \eta_0, \eta_{in}\right) \\ & \times \left[T_\ell^{SW}\left(|\vec{k} + \vec{k}_0|\right) + T_\ell^{ISW\star}\left(|\vec{k} + \vec{k}_0|\right) \right] \\ = & 4\pi \int \frac{dk}{k} \frac{k^3}{2\pi^2} \left[P_g(k) + P_g\left(|\vec{k} + \vec{k}_0|\right) \right] T_\ell^S\left(k, \eta_0, \eta_{in}\right) \times U_\ell^\star\left(|\vec{k} + \vec{k}_0|\right) . \end{aligned} \tag{273}$$

Here, we defined a new transfer function

$$U_\ell^\star\left(|\vec{k} + \vec{k}_0|\right) \equiv T_\ell^{SW}\left(|\vec{k} + \vec{k}_0|\right) + T_\ell^{ISW\star}\left(|\vec{k} + \vec{k}_0|\right) , \tag{274}$$

which is different from the "regular" $T_\ell^S\left(k, \eta_0, \eta_{in}\right)$ of Eq.243 since T_Φ, T_Ψ are evaluated in $|\vec{k} + \vec{k}_0|$ and the ISW term contains the extra factor $\frac{\eta_0 - \eta'}{\eta_0 - \eta_{in}}$ (see Eq.263 for the full expression of the transfer functions containing this term).

6.1.3 *Second Order Term in the Modulating Field*

We now compute the term $\left\langle \Gamma^*_{\ell m,S}(q)\Gamma_{\ell' m',S}(q)\right\rangle^{(2)}$, which however requires a longer calculation to be carried out.
Reminding the expression of $h(\vec{k}-\vec{k}')$ of Eq.249, we can write

$$
\begin{aligned}
&\langle \Gamma_{\ell m,S}\Gamma^*_{\ell' m',S}\rangle^{(2)} = \\
&(4\pi)^2(-i)^{\ell-\ell'}\int\frac{d^3k}{(2\pi)^3}\int\frac{d^3k'}{(2\pi)^3}\times\int\frac{d^3\widetilde{k}}{(2\pi)^3}P_g(\widetilde{k})h^*(\vec{k}-\widetilde{\vec{k}})h\left(\vec{k}'-\widetilde{\vec{k}}\right)\\
&\times Y^*_{\ell m}(\widehat{k})Y_{\ell' m'}\left(\widehat{k}'\right)\times T^S_\ell\left(k,\eta_0,\eta_{in}\right)T^S_{\ell'}\left(k',\eta_0,\eta_{in}\right) = \\
=&(4\pi)^2(-i)^{\ell-\ell'}\int\frac{d^3k}{(2\pi)^3}\int\frac{d^3k'}{(2\pi)^3}\int\frac{d^3\widetilde{k}}{(2\pi)^3}P_g(\widetilde{k})\\
&\times Y^*_{\ell m}(\widehat{k})Y_{\ell' m'}\left(\widehat{k}'\right)\times T^S_\ell\left(k,\eta_0,\eta_{in}\right)T^S_{\ell'}\left(k',\eta_0,\eta_{in}\right)\\
&\times\frac{w_1^2}{4}\frac{3}{4\pi}\frac{(2\pi)^6}{k_0^2(\eta_0-\eta_{in})^2}\left[\delta(\vec{k}-\widetilde{\vec{k}}-\vec{k}_0)-\delta(\vec{k}-\widetilde{\vec{k}}+\vec{k}_0)\right]\\
&\times\left[\delta(\vec{k}'-\widetilde{\vec{k}}-\vec{k}_0)-\delta(\vec{k}'-\widetilde{\vec{k}}+\vec{k}_0)\right] = \\
=&\frac{4\pi}{2\pi^2}\frac{w_1^2}{4}(-i)^{\ell-\ell'}\int d^3k\int d^3k'\int d^3\widetilde{k}\,P_g(\widetilde{k})\\
&\times Y^*_{\ell m}(\widehat{k})Y_{\ell' m'}\left(\widehat{k}'\right)\times T^S_\ell\left(k,\eta_0,\eta_{in}\right)T^S_{\ell'}\left(k',\eta_0,\eta_{in}\right)\\
&\times\frac{3}{4\pi}\frac{1}{k_0^2(\eta_0-\eta_{in})^2}\Big[\delta(\vec{k}-\widetilde{\vec{k}}-\vec{k}_0)\delta(\vec{k}'-\widetilde{\vec{k}}-\vec{k}_0)\\
&-\delta(\vec{k}-\widetilde{\vec{k}}-\vec{k}_0)\delta(\vec{k}'-\widetilde{\vec{k}}+\vec{k}_0)+\delta(\vec{k}-\widetilde{\vec{k}}+\vec{k}_0)\delta(\vec{k}'-\widetilde{\vec{k}}+\vec{k}_0)\\
&-\delta(\vec{k}-\widetilde{\vec{k}}+\vec{k}_0)\delta(\vec{k}'-\widetilde{\vec{k}}-\vec{k}_0)\Big]\,.
\end{aligned}
\tag{275}
$$

Following the same idea of the first order term (in the modulating field), we calculate one contribution at a time, however in this case every term contains a couple of deltas, instead of a single one. For all of them, the "secret" to obtain a fairly simple calculation is to integrate $\vec{k}$ and $\vec{k}'$, leaving behind

$\widetilde{\vec{k}}$.

Naturally, we start from the first one, which gives the following expression

$$\begin{aligned}
&\langle \Gamma_{\ell m,S}\Gamma^{*}_{\ell' m',S}\rangle^{(2)}_{1st} = \\
=&\frac{4\pi}{2\pi^2}\frac{w_1^2}{4}(-i)^{\ell-\ell'}\int d^3k\int d^3k'\int d^3\widetilde{k}\, P_g(\widetilde{k}) \\
&\times Y^{*}_{\ell m}(\widehat{k})Y_{\ell' m'}\left(\widehat{k}'\right)\times T^{S}_{\ell}\left(k,\eta_0,\eta_{in}\right)T^{S}_{\ell'}\left(k',\eta_0,\eta_{in}\right) \\
&\times\frac{3}{4\pi}\frac{1}{k_0^2(\eta_0-\eta_{in})^2}\delta(\vec{k}-\widetilde{\vec{k}}-\vec{k}_0)\delta(\vec{k}'-\widetilde{\vec{k}}-\vec{k}_0) = \\
=&\frac{4\pi}{2\pi^2}\frac{w_1^2}{4}(-i)^{\ell-\ell'}\int d^3\widetilde{k}\, P_g(\widetilde{k}) \\
&\times\sqrt{\frac{3}{4\pi}}\frac{1}{k_0(\eta_0-\eta_{in})}Y^{*}_{\ell m}\left(\frac{\widetilde{\vec{k}}+\vec{k}_0}{|\widetilde{\vec{k}}+\vec{k}_0|}\right)T^{S}_{\ell}\left(|\widetilde{\vec{k}}+\vec{k}_0|,\eta_0,\eta_{in}\right) \\
&\times\sqrt{\frac{3}{4\pi}}\frac{1}{k_0(\eta_0-\eta_{in})}Y_{\ell' m'}\left(\frac{\widetilde{\vec{k}}+\vec{k}_0}{|\widetilde{\vec{k}}+\vec{k}_0|}\right)T^{S}_{\ell'}\left(|\widetilde{\vec{k}}+\vec{k}_0|,\eta_0,\eta_{in}\right).
\end{aligned} \tag{276}$$

We can then apply again Eq.253 for each of the product of transfer function and SH [49]. Reminding that the transfer function can be divided in a SW and a ISW contribution, where we must keep track of the starred components, we can write

$$\begin{aligned}
&\langle \Gamma_{\ell m,S}\Gamma^{*}_{\ell' m',S}\rangle^{(2)}_{1st} = \\
=&\frac{4\pi}{2\pi^2}\frac{w_1^2}{4}(-i)^{\ell-\ell'}\int d^3\widetilde{k}\, P_g(\widetilde{k}) \\
&\times\Big[\frac{1}{k_0\,(\eta_0-\eta_{in})}\sqrt{\frac{3}{4\pi}}U_{\ell}\left(|\widetilde{\vec{k}}+\vec{k}_0|\right)Y^{*}_{\ell m}(\widehat{\widetilde{k}}) \\
&-\frac{1}{2}R^{1,\ell+1}_{\ell m}U^{\star}_{\ell+1}\left(|\widetilde{\vec{k}}+\vec{k}_0|\right)Y^{*}_{\ell+1,m}(\widehat{\widetilde{k}}) \\
&+\frac{1}{2}R^{1,\ell-1}_{\ell m}U^{\star}_{\ell-1}\left(|\widetilde{\vec{k}}+\vec{k}_0|\right)Y^{*}_{\ell-1,m}(\widehat{\widetilde{k}})\Big] \\
&\times\Big[\frac{1}{k_0\,(\eta_0-\eta_{in})}\sqrt{\frac{3}{4\pi}}U_{\ell'}\left(|\widetilde{\vec{k}}+\vec{k}_0|\right)Y_{\ell' m'}(\widehat{\widetilde{k}}) \\
&-\frac{1}{2}R^{1,\ell'+1}_{\ell' m'}U^{\star}_{\ell'+1}\left(|\widetilde{\vec{k}}+\vec{k}_0|\right)Y_{\ell'+1,m'}(\widehat{\widetilde{k}}) \\
&+\frac{1}{2}R^{1,\ell'-1}_{\ell' m'}U^{\star}_{\ell'-1}\left(|\widetilde{\vec{k}}+\vec{k}_0|\right)Y_{\ell'-1,m'}(\widehat{\widetilde{k}})\Big],
\end{aligned} \tag{277}$$

49 See also footnote 46.

where we defined

$$U_\ell\left(|\widetilde{\vec{k}}+\vec{k}_0|\right)\equiv T_\ell^{SW}\left(|\widetilde{\vec{k}}+\vec{k}_0|\right)+T_\ell^{ISW}\left(|\widetilde{\vec{k}}+\vec{k}_0|\right). \tag{278}$$

Let us now compute the product of the square brackets, multiplied by $(-i)^{\ell-\ell'}$ (all the spherical harmonics will depend on $\widehat{\widetilde{k}}$ and the transfer functions on $\left(|\widetilde{\vec{k}}+\vec{k}_0|\right)$, so we drop dependencies for the sake of notation):

$$\begin{aligned}
&(-i)^{\ell-\ell'}\Big[\frac{3}{4\pi}\frac{1}{k_0^2(\eta_0-\eta_{in})^2}U_\ell U_{\ell'}Y_{\ell'm'}Y^*_{\ell m}+\\
&-\frac{1}{2k_0\,(\eta_0-\eta_{in})}\sqrt{\frac{3}{4\pi}}R^{1,\ell'+1}_{\ell'm'}U_\ell U^\star_{\ell'+1}Y^*_{\ell m}Y_{\ell'+1,m'}+\\
&+\frac{1}{2k_0\,(\eta_0-\eta_{in})}\sqrt{\frac{3}{4\pi}}R^{1,\ell'-1}_{\ell'm'}U_\ell U^\star_{\ell'-1}Y^*_{\ell m}Y_{\ell'-1,m'}+\\
&-\frac{1}{2k_0\,(\eta_0-\eta_{in})}\sqrt{\frac{3}{4\pi}}R^{1,\ell+1}_{\ell m}U^\star_{\ell+1}U_{\ell'}Y^*_{\ell+1,m}Y_{\ell'm'}+\\
&+\frac{1}{2k_0\,(\eta_0-\eta_{in})}\sqrt{\frac{3}{4\pi}}R^{1,\ell-1}_{\ell m}U^\star_{\ell-1}U_{\ell'}Y^*_{\ell-1,m}Y_{\ell'm'}+\\
&-\frac{1}{4}R^{1,\ell+1}_{\ell m}R^{1,\ell'-1}_{\ell'm'}U^\star_{\ell+1}U^\star_{\ell'-1}Y^*_{\ell+1,m}Y_{\ell'-1,m'}+\\
&+\frac{1}{4}R^{1,\ell+1}_{\ell m}R^{1,\ell'+1}_{\ell'm'}U^\star_{\ell+1}U^\star_{\ell'+1}Y^*_{\ell+1,m}Y_{\ell'+1,m'}+\\
&-\frac{1}{4}R^{1,\ell-1}_{\ell m}R^{1,\ell'+1}_{\ell'm'}U^\star_{\ell-1}U^\star_{\ell'+1}Y^*_{\ell-1,m}Y_{\ell'+1,m'}+\\
&+\frac{1}{4}R^{1,\ell-1}_{\ell m}R^{1,\ell'-1}_{\ell'm'}U^\star_{\ell-1}U^\star_{\ell'-1}Y^*_{\ell-1,m}Y_{\ell'-1,m'}\Big].
\end{aligned} \tag{279}$$

Integrating in $\int \widehat{\widetilde{dk}}$ the products of spherical harmonics will provide several different Kronecker deltas, which will then make explicit also the power of $-i$ for each term:

$$\begin{aligned}
&\frac{3}{4\pi}\frac{1}{k_0^2(\eta_0-\eta_{in})^2}U_\ell U_\ell \delta_{\ell\ell'}\delta_{mm'}(-i)^0+\\
&-\frac{1}{2k_0\,(\eta_0-\eta_{in})}\sqrt{\frac{3}{4\pi}}R^{1,\ell}_{\ell' m}U_\ell U^\star_\ell \delta_{mm'}(-i)^1+\\
&+\frac{1}{2k_0\,(\eta_0-\eta_{in})}\sqrt{\frac{3}{4\pi}}R^{1,\ell}_{\ell' m}U_\ell U^\star_\ell \delta_{mm'}(-i)^{-1}+\\
&-\frac{1}{2k_0\,(\eta_0-\eta_{in})}\sqrt{\frac{3}{4\pi}}R^{1,\ell'}_{\ell m}U^\star_{\ell'} U_{\ell'} \delta_{mm'}(-i)^{-1}+\\
&+\frac{1}{2k_0\,(\eta_0-\eta_{in})}\sqrt{\frac{3}{4\pi}}R^{1,\ell'}_{\ell m}U^\star_{\ell'} U_{\ell'} \delta_{mm'}(-i)^{1}+\\
&-\frac{1}{4}\sum_j R^{1,j}_{\ell m}R^{1,j}_{\ell' m}U^\star_j U^\star_j \delta_{mm'}(-i)^{-2}+\\
&+\frac{1}{4}\sum_j R^{1,j}_{\ell m}R^{1,j}_{\ell' m}U^\star_j U^\star_j \delta_{mm'}(-i)^{0}+\\
&-\frac{1}{4}\sum_j R^{1,j}_{\ell m}R^{1,j}_{\ell' m}U^\star_j U^\star_j \delta_{mm'}(-i)^{2}+\\
&+\frac{1}{4}\sum_j R^{1,j}_{\ell m}R^{1,j}_{\ell' m}U^\star_j U^\star_j \delta_{mm'}(-i)^{0}\,.
\end{aligned} \tag{280}$$

Thus, summing the various terms one ends up with

$$\begin{aligned}
&\langle \Gamma_{\ell m,S}\Gamma^*_{\ell' m',S}\rangle^{(2)}_{1st}=\\
=&\frac{4\pi}{2\pi^2}\frac{w_1^2}{4}\int \widetilde{dk}\,P_g(\widetilde{k})\Big[\frac{3}{4\pi}\frac{1}{k_0^2(\eta_0-\eta_{in})^2}U_\ell U_\ell \delta_{\ell\ell'}\delta_{mm'}+\\
&+\frac{i}{k_0\,(\eta_0-\eta_{in})}\sqrt{\frac{3}{4\pi}}R^{1,\ell}_{\ell' m}U_\ell U^\star_\ell \delta_{mm'}-\frac{i}{k_0\,(\eta_0-\eta_{in})}\sqrt{\frac{3}{4\pi}}R^{1,\ell'}_{\ell m}U^\star_{\ell'} U_{\ell'} \delta_{mm'}+\\
&+\sum_j R^{1,j}_{\ell m}R^{1,j}_{\ell' m}U^\star_j U^\star_j \delta_{mm'}\Big]\,.
\end{aligned} \tag{281}$$

At this point, one would have to compute the other three terms coming from the other couples of Dirac deltas of Eq.275, however one can exploit the following shortcut to reach the final solution:

- the sign in front of the isotropic term ($\propto \delta_{\ell\ell'}$) is exclusively defined by the sign in front of the couple of Dirac deltas (see the first term of Eq.281 for example);

- the Dirac delta imposing $k = \widetilde{k} \pm k_0$ translates into a final term $\propto \mp R^{1,\ell'}_{\ell m}$ (see the third term of Eq.281 for example);
- the Dirac delta imposing $k' = \widetilde{k} \pm k_0$ translates into a final term $\propto \pm R^{1,\ell}_{\ell' m}$ (see the second term of Eq.281 for example);
- if the two deltas has agreeing signs in front of k_0, one ends up with a plus in front of the term with the sum over j, otherwise one gets a minus sign (see the fourth term of Eq.281 for example).

Applying these rules, one can show that the only surviving term is the one proportional to the sum over j [50]:

$$\begin{aligned}
&\langle \Gamma_{\ell m,S} \Gamma^*_{\ell' m',S} \rangle^{(2)} \\
=&\frac{4\pi}{2\pi^2}\frac{w_1^2}{4}\int d\widetilde{k}\, P_g(\widetilde{k}) 4 \sum_j R^{1,j}_{\ell m} R^{1,j}_{\ell' m} U_j^\star U_j^\star \delta_{mm'} \\
=&w_1^2 \delta_{mm'} 4\pi \int \frac{d^3\widetilde{k}}{\widetilde{k}} \frac{\widetilde{k}^3}{2\pi^2} P_g(\widetilde{k}) \sum_j R^{1,j}_{\ell m} R^{1,j}_{\ell' m} U_j^\star U_j^\star \\
=&w_1^2 \delta_{mm'} \sum_j R^{1,j}_{\ell m} R^{1,j}_{\ell' m} \mathcal{C}^{(2)}_j \,,
\end{aligned} \tag{282}$$

where

$$\mathcal{C}^{(2)}_\ell \equiv 4\pi \int \frac{dk}{k} \frac{k^3}{2\pi^2} P_g(k) U_\ell^\star(k) U_\ell^\star(k) \,. \tag{283}$$

6.1.4 *Full Expression of the Correlator*

Finally we are able to write the full expression for $\langle \Gamma_{\ell m,S} \Gamma^*_{\ell' m',S} \rangle$, which will contain the zeroth, first and second order contributions (in the modulating field) just derived (this subsection is intended to be a summary of the previously obtained expressions). It reads

$$\begin{aligned}
\langle \Gamma_{\ell m,S} \Gamma^*_{\ell' m',S} \rangle =& \delta_{\ell\ell'}\delta_{mm'} \mathcal{C}^{(0)}_\ell + \frac{w_1}{2}\delta_{mm'}\left[R^{1,\ell}_{\ell' m} \mathcal{C}^{(1)}_\ell + R^{1,\ell'}_{\ell m} \mathcal{C}^{(1)}_{\ell'} \right] + \\
&+ w_1^2 \delta_{mm'} \sum_j R^{1,j}_{\ell m} R^{1,j}_{\ell' m} \mathcal{C}^{(2)}_j \,,
\end{aligned} \tag{284}$$

50 We implicitly assume here that the transfer function in $\widetilde{k} \pm k_0$ is approximately equal to the one evaluated in $\widetilde{k}$. Having done differently would have not allowed to cancel the various term disappearing in this following passage.

where

$$\begin{aligned}
\mathcal{C}_\ell^{(0)} \equiv & 4\pi \int \frac{dk}{k} \frac{k^3}{2\pi^2} P_g(k) T_\ell^{(S)2}(k) \ , \\
\mathcal{C}_\ell^{(1)} \equiv & 4\pi \int \frac{dk}{k} \frac{k^3}{2\pi^2} \left[P_g(k) + P_g\left(|\vec{k}+\vec{k}_0|\right)\right] T_\ell^S(k)\, U_\ell^\star\left(|\vec{k}+\vec{k}_0|\right) \ , \\
\mathcal{C}_\ell^{(2)} \equiv & 4\pi \int \frac{dk}{k} \frac{k^3}{2\pi^2} P_g(k) U_\ell^\star(k) U_\ell^\star(k) \ .
\end{aligned} \tag{285}$$

We also remind the expression of the transfer functions

$$\begin{aligned}
T_\ell^S(k,\eta_0,\eta_{in}) \equiv & T_\Phi(\eta_{in},k)\, j_\ell(k(\eta_0-\eta_{in})) \\
& + \int_{\eta_{in}}^{\eta_0} d\eta' \frac{\partial[T_\Psi(\eta',k)+T_\Phi(\eta',k)]}{\partial\eta'} j_\ell(k(\eta_0-\eta')) \ , \\
U_\ell^\star\left(|\vec{k}+\vec{k}_0|\right) \equiv & T_\ell^{SW}\left(|\vec{k}+\vec{k}_0|\right) + T_\ell^{ISW\star}\left(|\vec{k}+\vec{k}_0|\right) , \\
U_\ell\left(|\vec{k}+\vec{k}_0|\right) \equiv & T_\ell^{SW}\left(|\vec{k}+\vec{k}_0|\right) + T_\ell^{ISW}\left(|\vec{k}+\vec{k}_0|\right) , \\
T_\ell^{SW}\left(|\vec{k}+\vec{k}_0|\right) \equiv & T_\Phi\left(\eta_{in},|\vec{k}+\vec{k}_0|\right) j_\ell(k(\eta_0-\eta_{in})) \ , \\
T_\ell^{ISW}\left(|\vec{k}+\vec{k}_0|\right) \equiv & \int_{\eta_{in}}^{\eta_0} d\eta' \frac{\partial\left[T_\Psi\left(\eta',|\vec{k}+\vec{k}_0|\right)+T_\Phi\left(\eta',|\vec{k}+\vec{k}_0|\right)\right]}{\partial\eta'} \\
& \times j_\ell(k(\eta_0-\eta')) \ , \\
T_\ell^{ISW\star}\left(|\vec{k}+\vec{k}_0|\right) \equiv & \int_{\eta_{in}}^{\eta_0} d\eta' \frac{\partial\left[T_\Psi\left(\eta',|\vec{k}+\vec{k}_0|\right)+T_\Phi\left(\eta',|\vec{k}+\vec{k}_0|\right)\right]}{\partial\eta'} \\
& \times \frac{\eta_0-\eta'}{\eta_0-\eta_{in}} j_\ell(k(\eta_0-\eta')) \ .
\end{aligned} \tag{286}$$

Firstly, we notice that approximating these results for $\vec{k}+\vec{k}_0 \approx \vec{k}$ and neglecting the ISW effect, we get $U_\ell = U_\ell^\star = T_\ell^S$, thus $\mathcal{C}_\ell^{(0)} = \mathcal{C}_\ell^{(1)} = \mathcal{C}_\ell^{(2)}$. In other words, the results obtained in [10] are reproduced by our computation, considering that they used $T_\Phi = -\frac{1}{3}$.
The more careful readers would have noticed that, in the case of the second order term in the modulating field, the presence of the factor $1/2$ in Eq.253 (see footnote 46) have indeed allowed us to obtain the same contribution of [10] reported in Eq.240 (canceling out a 4, which would have come from the sum performed to obtain Eq.282). On the other hand, the same factor seems to have made us fail in the purpose of reproducing [10] for what concerns the first order term in the modulating field (see Eq.238). This issue will be solve in Ch.7 (see the discussion on Eq.325), but we can anticipate that the solution involves the presence in $\mathcal{C}_\ell^{(1)}$ of a sum of power spectra, which

can be assumed equal under specific conditions we will present. This will provide a factor 2, canceling out the $1/2$ we have here.

7

CGWB ANGULAR POWER SPECTRUM APPROXIMATED COMPUTATION

In Ch.6 we have found the general expression of the zeroth, first and second order (in the modulating field) contributions to the angular spectrum of the CGWB, thus we can now compute their explicit expression exploiting some approximations we are about to present.
In order to do so, we define new "sub-spectra" based on their physical origin. Indeed, each order term (in the modulating field) will contain a squared factor similar to $\left[T^{SW} + T^{ISW}\right]^2$*. Thus, depending on the specific term, we can identify* 3 *or* 4 *different contributions to the overall angular power spectrum.*
Then, we will compute all these contributions from an analytical point of view, until possible, then we will pass to a numerical approach to get the final results.

7.1 SUB-SPECTRA DEFINITION

As aforementioned, we want to define here what are the various terms we need to compute to evaluate the overall $\left\langle \Gamma_{\ell m} \Gamma^*_{\ell' m'} \right\rangle$.
To do so, we need to remind ourselves the transfer functions summarized in Eq.286. Paying then attention to the physical origin of the terms, either SW or ISW, and to the eventual presence of some starred contribution, we can write the contributions to the angular power spectra of Eq.285 as [51]

$$\begin{aligned} \mathcal{C}_\ell^{(0)} =& \mathcal{C}_{\ell,SW^2} + 2 \times \mathcal{C}_{\ell,SW\times ISW} + \mathcal{C}_{\ell,ISW^2} \,, \\ \mathcal{C}_\ell^{(1)} =& \mathcal{C}_{\ell,SW^2} + \mathcal{C}_{\ell,SW\times ISW^\star} + \mathcal{C}_{\ell,SW\times ISW} + \mathcal{C}_{\ell,ISW x ISW^\star} \,, \\ \mathcal{C}_\ell^{(2)} =& \mathcal{C}_{\ell,SW^2} + 2 \times \mathcal{C}_{\ell,SW\times ISW^\star} + \mathcal{C}_{\ell,ISW^{\star 2}} \,, \end{aligned} \tag{287}$$

where the presence of 3 or 4 terms is naturally determined by the fact that, looking at Eq.285, the (0) and (2) contributions contains the square of respectively T^S_ℓ and $U^\star_\ell$, whereas the (1) one contains the product of the two transfer functions just mentioned.
Obviously, the subscripts of the sub-spectra will indicate what effects are playing a role in that specific term, so that e.g. $SW \times ISW^\star$ will correspond to the product of T^{SW}_ℓ and $T^{ISW\star}_\ell$ of Eq.286.
Also, some contribution do repeat, so that we can identify a gran-total of 6 different terms we are about to compute.
Our journey through these terms will be divided based on the different order in the modulating field h.

51 We stress that this notation is just a way to write in synthesis what is stated in the Eq.285 by identifying the underlying physical effect of each term.

7.2 ZEROTH ORDER SPECTRUM IN THE MODULATING FIELD

We start from the zeroth order angular power spectrum (in the modulating field), which couples multipoles with the same ℓ and m and reads

$$\begin{aligned}\mathcal{C}_\ell^{(0)} =& 4\pi \int \frac{dk}{k}\frac{k^3}{2\pi^2} P_g(k) T_\ell^{(S)2}(k) = \\ =& 4\pi \int \frac{dk}{k}\frac{k^3}{2\pi^2} P_g(k) \Big[T_\Phi(\eta_{in}, k) j_\ell(k(\eta_0 - \eta_{in})) \\ &+ \int_{\eta_{in}}^{\eta_0} d\eta' \frac{\partial \left[T_\Psi(\eta', k) + T_\Phi(\eta', k)\right]}{\partial \eta'} j_\ell\left(k(\eta_0 - \eta')\right) \Big]^2 .\end{aligned} \tag{288}$$

It contains contributions from three of the six different sub-spectra we have defined in Eq.287: the pure SW one, the pure ISW one and a mixed term coming from the two combined effects.

7.2.1 *Pure Sachs-Wolfe*

The pure SW contribution reads

$$\mathcal{C}_{\ell,SW^2} \equiv 4\pi \int \frac{dk}{k}\frac{k^3}{2\pi^2} P_g(k) T_\Phi^2(\eta_{in}, k) j_\ell^2(k(\eta_0 - \eta_{in})) . \tag{289}$$

In Ch.3, we have seen that the scalar power spectrum in the most general context is equal to

$$P = \frac{H^2}{2k^3}\left(\frac{k}{aH}\right)^{3-2\nu} \quad \text{with} \quad 3 - 2\nu = 2\eta_V - 6\varepsilon = n_S - 1 . \tag{290}$$

Hence, we can plug into Eq.289 the expression of the adimensional power spectrum yielding

$$\frac{k^3 P_g(k)}{2\pi^2} = \Delta_g \equiv \Delta_0 \left(\frac{k}{k_0}\right)^{n_S - 1} , \tag{291}$$

where: k_0 = pivot scale;
$\Delta_0 = \Delta_g(k_0)$ amplitude of the spectrum at the pivot scale .

At this point, we need to evaluate the explicit expression of the transfer function of Φ. In the most general scenario its expression can be fairly complicated: firstly one could write it as in Eq.189, i.e. dividing the dependencies on k and η; then depending on the specific cosmology considered and at what scales, things can change quite abruptly [18].
Here, we will use the approximation introduced in [18] and used in [26] (see

Ch.A). In particular, we consider only modes that re-enter the horizon in matter domination, for which we can write

$$T_\Phi(k,\eta) \simeq \frac{3}{5} g(\eta) \,, \tag{292}$$

where $g(\eta)$ is the so-called growth function encoding the time dependency of the transfer function.
Eq.292 allows to drop the dependency on k of the transfer functions, greatly simplifying the calculus (and justifying a posteriori the assumption[52] used to find Eq.282), and to write

$$\begin{aligned} \mathcal{C}_{\ell,SW^2} =& 4\pi \int \frac{dk}{k} \left(\frac{3}{5}\right)^2 g^2(\eta_{in}) \Delta_0 \left(\frac{k}{k_0}\right)^{n_s-1} j_\ell^2(k(\eta_0-\eta_{in})) \\ =& \frac{36}{25}\pi g^2(\eta_{in}) \frac{\Delta_0}{k_0^{n_S-1}} \int \frac{dk}{k} k^{n_s-1} j_\ell^2(k(\eta_0-\eta_{in})) \,. \end{aligned} \tag{293}$$

It is convenient now to change variable to $\widetilde{k} = k(\eta_0-\eta_{in})$ to obtain

$$\mathcal{C}_{\ell,SW^2} = \frac{36}{25}\pi g^2(\eta_{in}) \frac{\Delta_0}{k_0^{n_S-1}} \int \frac{d\widetilde{k}}{\widetilde{k}} \frac{\widetilde{k}^{n_s-1}}{(\eta_0-\eta_{in})^{n_S-1}} j_\ell^2(\widetilde{k}) \,. \tag{294}$$

In order to proceed further, we need a way to compute the integral of the SBFs. The fastest way to do it is obviously to look for tabulated results, as the ones in [75], which provides a humongous number of different integrals involving special functions, thus we will use it in all the following paragraphs. However, to exploit [75] we need to turn our SBFs into "ordinary" Bessel functions through the definition in Eq.227 to obtain

$$j_\ell^2(x) = \frac{\pi}{2x} J^2_{\ell+\frac{1}{2}}(x) \,. \tag{295}$$

This allows to recast the equation to

$$\begin{aligned} \mathcal{C}_{\ell,SW^2} =& \frac{36}{25}\pi g^2(\eta_{in}) \frac{\Delta_0}{k_0^{n_S-1}} \int \frac{d\widetilde{k}}{\widetilde{k}} \frac{\widetilde{k}^{n_s-1}}{(\eta_0-\eta_{in})^{n_S-1}} \frac{\pi}{2\widetilde{k}} J^2_{\ell+\frac{1}{2}}(\widetilde{k}) = \\ =& \frac{36}{25}\pi^2 g^2(\eta_{in}) \frac{\Delta_0}{[k_0(\eta_0-\eta_{in})]^{n_S-1}} \frac{1}{2} \int d\widetilde{k}\, \widetilde{k}^{n_s-3} J^2_{\ell+\frac{1}{2}}(\widetilde{k}) \,, \end{aligned} \tag{296}$$

which, indeed, has the form of one of the known integrals of [75]. Specifically, the integral coming to help us reads

$$\int_0^\infty J_\mu(\alpha k) J_\nu(\alpha k) k^{-\lambda} dk = \frac{a^{\lambda-1}\Gamma(\lambda)\Gamma(\frac{\nu+\mu-\lambda+1}{2})}{2^\lambda \Gamma(\frac{\mu-\nu+\lambda+1}{2})\Gamma(\frac{\mu+\nu+\lambda+1}{2})\Gamma(\frac{-\mu+\nu+\lambda+1}{2})} \,. \tag{297}$$

52 See footnote 50.

This integral is valid for specific existence conditions, which state

$$\mathrm{Re}\,(\nu+\mu+1-\lambda)>0 \quad ; \quad \mathrm{Re}\,(\lambda)>-1 \quad ; \quad \alpha>0\,. \tag{298}$$

In our case, we have $\mu=\nu=\ell+\frac{1}{2}$, $\lambda=3-n_S$ and $\alpha=1$, thus all of them result respected.
Substituting our values for μ, ν, λ and α we obtain the final result for the pure-SW term.

$$\mathcal{C}_{\ell,SW^2}=\frac{36}{25}\pi^2\frac{g^2(\eta_{in})\Delta_0}{[k_0(\eta_0-\eta_{in})]^{n_S-1}}\frac{\Gamma(3-n_S)\Gamma(\ell-\frac{1}{2}+\frac{n_S}{2})}{2^{4-n_S}\Gamma^2(2-\frac{n_S}{2})\Gamma(\ell+\frac{5}{2}-\frac{n_S}{2})}\,. \tag{299}$$

7.2.2 *Mixed Term*

The mixed contribution present in the zeroth order contribution involves the SW effect and the standard ISW effect, thus we will have to deal with an extra integration on conformal time η carried by the ISW term. Thus, the mixed term reads

$$\begin{aligned}\mathcal{C}_{\ell,SW\times ISW}\equiv&4\pi\int\frac{dk}{k}\frac{k^3P_g(k)}{2\pi^2}T_\Phi(\eta_{in},k)j_\ell(k(\eta_0-\eta_{in}))\\&\times\int_{\eta_{in}}^{\eta_0}d\eta'\frac{d[T_\Psi(k,\eta')+T_\Phi(k,\eta')]}{d\eta'}j_\ell(k(\eta_0-\eta'))\,.\end{aligned} \tag{300}$$

Again, plugging the expression of the adimensional power spectrum of Eq.291, using the approximation of the transfer function of Eq.292 and reminding that for simplicity we take $T_\Psi=T_\Phi$, we can write

$$\begin{aligned}\mathcal{C}_{\ell,SW\times ISW}=&4\pi\int\frac{dk}{k}\Delta_0\left(\frac{k}{k_0}\right)^{n_S-1}\frac{3}{5}g(\eta_{in})j_\ell(k(\eta_0-\eta_{in}))\\&\times\int_{\eta_{in}}^{\eta_0}d\eta' 2\,\frac{3}{5}\frac{dg(\eta')}{d\eta'}j_\ell(k(\eta_0-\eta'))\,.\end{aligned} \tag{301}$$

Isolating the terms depending on k, we can write

$$\begin{aligned}
\mathcal{C}_{\ell,SW\times ISW} =& \frac{36}{25}\pi g(\eta_{in})\frac{\Delta_0}{k_0^{n_S-1}} 2\int_{\eta_{in}}^{\eta_0} d\eta' \frac{dg(\eta')}{d\eta'} \\
&\times \int \frac{dk}{k} k^{n_S-1} j_\ell(k(\eta_0-\eta_{in})) j_\ell(k(\eta_0-\eta')) = \\
=& \frac{36}{25}\pi g(\eta_{in})\frac{\Delta_0}{k_0^{n_S-1}} 2\int_{\eta_{in}}^{\eta_0} d\eta' \frac{dg(\eta')}{d\eta'} \int \frac{dk}{k} \frac{k^{n_S-1}}{\sqrt{(\eta_0-\eta_{in})(\eta_0-\eta')}} \\
&\times \frac{\pi}{2k} J_{\ell+\frac{1}{2}}(k(\eta_0-\eta_{in})) J_{\ell+\frac{1}{2}}(k(\eta_0-\eta')) = \\
=& \frac{36}{25}\pi^2 g(\eta_{in})\frac{\Delta_0}{k_0^{n_S-1}} \int_{\eta_{in}}^{\eta_0} d\eta' \frac{dg(\eta')}{d\eta'} \frac{1}{\sqrt{(\eta_0-\eta_{in})(\eta_0-\eta')}} \\
&\times \int dk k^{n_S-3} J_{\ell+\frac{1}{2}}(k(\eta_0-\eta_{in})) J_{\ell+\frac{1}{2}}(k(\eta_0-\eta')) \, .
\end{aligned} \tag{302}$$

Now, we can again try to find a known integral useful to our purposes, however, in Eq.302, the argument of the two Bessel functions is different, thus we cannot exploit the same known integral we used to find Eq.299. Fortunately, an integral of the form of the one in Eq.302 indeed exists in [75] and it reads

$$\begin{aligned}
&\int_0^\infty J_\mu(\beta k) J_\nu(\alpha k) k^{-\lambda} dk = \frac{\beta^\nu \Gamma(\frac{\nu+\mu-\lambda+1}{2})}{2^\lambda \alpha^{\mu-\lambda+1}\Gamma(\nu+1)\Gamma(\frac{\nu-\mu+\lambda+1}{2})} \\
&\times F\left[\left(\frac{\nu+\mu-\lambda+1}{2}\right), \left(\frac{\mu-\nu-\lambda+1}{2}\right); \mu+1; \frac{\beta^2}{\alpha^2}\right],
\end{aligned} \tag{303}$$

where $F(a,b;c;z)$ are the hypergeometric functions defined as the solution of the Euler's hypergeometric differential equation for $|z| < 1$

$$z(1-z)\frac{d^2w}{dz^2} + [c-(a+b+1)z]\frac{dw}{dz} - abw = 0 \, , \tag{304}$$

and represents a special case of the generalized hypergeometric functions ${}_pF_q(a_1,\dots,a_p;b_1,\dots,b_q;z)$, which can be written as

$${}_pF_q(a_1,\dots,a_p;b_1,\dots,b_q;z) \equiv \sum_{n=0}^{\infty} \frac{(a_1)_n \cdots (a_p)_n}{(b_1)_n \cdots (b_q)_n} \frac{z^n}{n!} \, . \tag{305}$$

This time the existence conditions state

$$\mathrm{Re}\,(\nu+\mu+1-\lambda) > 0 \quad ; \quad \mathrm{Re}\,(\lambda) > -1 \quad ; \quad 0 < \beta < \alpha \, , \tag{306}$$

which again are respected once we substitute our specific values for the constants[53]

$$\mu = \nu = \ell + \frac{1}{2} \quad , \quad \lambda = 3 - n_S \quad , \quad \beta = \eta_0 - \eta' \quad , \quad \alpha = \eta_0 - \eta_{in} \, . \tag{307}$$

Thus, Eq.302 gets recast to

$$\begin{aligned} \mathcal{C}_{\ell,SW\times ISW} =& \frac{36}{25}\pi^2 g(\eta_{in}) \frac{\Delta_0}{k_0^{n_S-1}} \int_{\eta_{in}}^{\eta_0} d\eta' \frac{dg(\eta')}{d\eta'} \\ & \times \frac{(\eta_0-\eta')^\ell \Gamma(\ell - \frac{1}{2} + \frac{n_S}{2})}{2^{3-n_S}(\eta_0-\eta_{in})^{\ell+n_S-1}\Gamma(\ell+\frac{3}{2})\Gamma(2-\frac{n_S}{2})} \\ & \times F\left[\ell - \frac{1}{2} + \frac{n_S}{2} \, , \, \frac{n_S}{2} - 1 \, ; \, \ell + \frac{3}{2} \, ; \, \left(\frac{\eta_0-\eta'}{\eta_0-\eta_{in}}\right)^2\right] . \end{aligned} \tag{308}$$

Subsequently, it is convenient to write the latter expression as function of a adimensional conformal time, normalized w.r.t. η_0, thus $\widetilde{\eta} = \eta/\eta_0$. Furthermore, we can assume safely that $\eta_{in} \ll \eta_0$, given that η_{in} indicates the end of inflation. Hence, we can write

$$\begin{aligned} \mathcal{C}_{\ell,SW\times ISW} =& \frac{36}{25}\pi^2 g(\eta_{in}) \frac{\Delta_0}{k_0^{n_S-1}} \frac{\Gamma(\ell - \frac{1}{2} + \frac{n_S}{2})}{2^{3-n_S}\Gamma(\ell+\frac{3}{2})\Gamma(2-\frac{n_S}{2})} \\ & \times \int_{\eta_{in}/\eta_0}^{1} d\widetilde{\eta} \frac{dg(\widetilde{\eta})}{d\widetilde{\eta}} \frac{\eta_0^\ell (1-\widetilde{\eta})^\ell}{(\eta_0-\eta_{in})^{\ell+n_S-1}} \\ & \times F\left[\ell - \frac{1}{2} + \frac{n_S}{2} \, , \, \frac{n_S}{2} - 1 \, ; \, \ell + \frac{3}{2} \, ; \, \left(\frac{\eta_0(1-\widetilde{\eta})}{\eta_0-\eta_{in}}\right)^2\right] = \\ \simeq & \frac{36}{25}\pi^2 g(\eta_{in}) \frac{\Delta_0}{(k_0\eta_0)^{n_S-1}} \frac{\Gamma(\ell - \frac{1}{2} + \frac{n_S}{2})}{2^{3-n_S}\Gamma(\ell+\frac{3}{2})\Gamma(2-\frac{n_S}{2})} \\ & \times \int_0^1 d\widetilde{\eta} \frac{dg(\widetilde{\eta})}{d\widetilde{\eta}} (1-\widetilde{\eta})^\ell \\ & \times F\left[\ell - \frac{1}{2} + \frac{n_S}{2} \, , \, \frac{n_S}{2} - 1 \, ; \, \ell + \frac{3}{2} \, ; \, (1-\widetilde{\eta})^2\right] . \end{aligned} \tag{309}$$

Approximating the derivative of the growth function $g(\widetilde{\eta})$ w.r.t. the adimensional conformal time $\widetilde{\eta}$ as shown in App.A:

$$\frac{dg(\widetilde{\eta})}{d\widetilde{\eta}} \simeq -\frac{5}{4}\widetilde{\eta}^5 \, , \tag{310}$$

53 Indeed, in principle η' could be equal to η_{in} bringing to $\alpha = \beta$ and violating the existence conditions, however this is not the cause of any inconsistency on the final results we are about to present. Also, the more careful readers would have noticed that there is an ambiguity in the choice of α and β. Indeed, they have to be chosen so that $0 < \beta < \alpha$, in order to respect the prescriptions provided by [75].

and changing variable to $\eta = 1 - \widetilde{\eta}$, we can write the final expression

$$\mathcal{C}_{\ell,\mathrm{SW}\times\mathrm{ISW}} = -\frac{9}{5}\pi^2 g(\eta_{\mathrm{in}})\frac{\Delta_0}{(k_0\eta_0)^{n_S-1}}\frac{\Gamma(\ell-\frac{1}{2}+\frac{n_S}{2})}{2^{3-n_S}\Gamma(\ell+\frac{3}{2})\Gamma(2-\frac{n_S}{2})} \times\int_0^1 d\eta\,\eta^\ell(1-\eta)^5 F\left[\ell-\frac{1}{2}+\frac{n_S}{2}\,,\ \frac{n_S}{2}-1\,;\ \ell+\frac{3}{2}\,;\ \eta^2\right]. \tag{311}$$

Unfortunately, this remaining integral in conformal time cannot be tracked back to any of the integrals present in [75], thus we will deal with it via a numerical integration in Sec.7.5[54].

7.2.3 *Pure Integrated Sachs-Wolfe*

The last term we need to evaluate in the zeroth order contribution to the correlation functions is the pure ISW term, which reads

$$\begin{aligned}\mathcal{C}_{\ell,\mathrm{ISW}^2} \equiv& 4\pi\int\frac{dk}{k}\frac{k^3 P_g(k)}{2\pi^2}\int_{\eta_{\mathrm{in}}}^{\eta_0} d\eta'\,2\frac{dT_\Phi(k,\eta')}{d\eta'}j_\ell(k(\eta_0-\eta')) \\ &\times\int_{\eta_{\mathrm{in}}}^{\eta_0} d\eta''\,2\frac{dT_\Phi(k,\eta'')}{d\eta''}j_\ell(k(\eta_0-\eta''))\,.\end{aligned} \tag{312}$$

Also in this case, we apply the aforementioned approximations and assumptions on the power spectrum and transfer functions (Eq.292 and Eq.291) to obtain

$$\begin{aligned}\mathcal{C}_{\ell,\mathrm{ISW}^2} =& 4\pi\int\frac{dk}{k}\Delta_0\left(\frac{k}{k_0}\right)^{n_S-1}\int_{\eta_{\mathrm{in}}}^{\eta_0} d\eta'\,2\,\frac{3}{5}\frac{dg(\eta')}{d\eta'}j_\ell(k(\eta_0-\eta')) \\ &\times\int_{\eta_{\mathrm{in}}}^{\eta_0} d\eta''\,2\,\frac{3}{5}\frac{dg(\eta'')}{d\eta''}j_\ell(k(\eta_0-\eta'')) = \\ =&\frac{36}{25}\pi\frac{\Delta_0}{k_0^{n_S-1}}4\int_{\eta_{\mathrm{in}}}^{\eta_0} d\eta'\int_{\eta_{\mathrm{in}}}^{\eta_0} d\eta''\frac{dg(\eta')}{d\eta'}\frac{dg(\eta'')}{d\eta''} \\ &\times\int\frac{dk}{k}k^{n_S-1}j_\ell(k(\eta_0-\eta'))j_\ell(k(\eta_0-\eta'')) = \\ =&\frac{36}{25}\pi^2\frac{\Delta_0}{k_0^{n_S-1}}2\int_{\eta_{\mathrm{in}}}^{\eta_0} d\eta'\int_{\eta_{\mathrm{in}}}^{\eta_0} d\eta''\frac{dg(\eta')}{d\eta'}\frac{dg(\eta'')}{d\eta''}\frac{1}{\sqrt{(\eta_0-\eta')(\eta_0-\eta'')}} \\ &\times\int dk k^{n_S-3}J_{\ell+\frac{1}{2}}(k(\eta_0-\eta'))J_{\ell+\frac{1}{2}}(k(\eta_0-\eta''))\,.\end{aligned} \tag{313}$$

54 In Sec.7.5, we also show the final expression of this term if one perform analytically the integral in η and leaves behind the numerical integration in k.

This time, we can use again the known integral of Bessel function we need from Eq.303 to proceed in the calculus, with the only difference that both α and β are now functions of integrating variables, and not constants. In particular, we obtain

$$\begin{aligned}\mathcal{C}_{\ell,ISW^2} =& \frac{36}{25}\pi^2\frac{\Delta_0}{k_0^{n_S-1}}2\int_{\eta_{in}}^{\eta_0}d\eta'\int_{\eta_{in}}^{\eta_0}d\eta''\frac{dg(\eta')}{d\eta'}\frac{dg(\eta'')}{d\eta''}\\ &\times\frac{(\eta_0-\eta'')^\ell\Gamma(\ell-\frac{1}{2}+\frac{n_S}{2})}{2^{3-n_S}(\eta_0-\eta')^{\ell+n_S-1}\Gamma(\ell+\frac{3}{2})\Gamma(2-\frac{n_S}{2})}\\ &\times F\left[\ell-\frac{1}{2}+\frac{n_S}{2}\,,\ \frac{n_S}{2}-1\,;\ \ell+\frac{3}{2}\,;\ \left(\frac{\eta_0-\eta''}{\eta_0-\eta'}\right)^2\right].\end{aligned} \tag{314}$$

Then, introducing again the adimensional conformal time $\widetilde{\eta}$, the approximation of the derivative of the growth function $g(\widetilde{\eta})$ from Eq.310, assuming $\eta_{in}\ll\eta_0$ and performing a couple of change of variables of the form $x=1-y$, it is possible to rewrite the latter expression as

$$\begin{aligned}\mathcal{C}_{\ell,ISW^2} =& \frac{9}{2}\pi^2\frac{\Delta_0}{(k_0\eta_0)^{n_S-1}}\frac{\Gamma(\ell-\frac{1}{2}+\frac{n_S}{2})}{2^{3-n_S}\Gamma(\ell+\frac{3}{2})\Gamma(2-\frac{n_S}{2})}\\ &\times\int_0^1 d\eta'\int_0^1 d\eta''(1-\eta')^5(1-\eta'')^5\frac{(\eta'')^\ell}{(\eta')^{\ell+n_S-1}}\\ &\times F\left[\ell-\frac{1}{2}+\frac{n_S}{2}\,,\ \frac{n_S}{2}-1\,;\ \ell+\frac{3}{2}\,;\ \left(\frac{\eta''}{\eta'}\right)^2\right].\end{aligned} \tag{315}$$

Previously, we have mentioned that $F(a,b;c;z)$ is well-defined if $|z|<1$, however, having to integrate both η'' and η', this condition becomes tricky to respect, especially from a numerical point of view, where this ambiguity leads to an error in the integration we were not able to solve.
For this reason, we must approach the $\mathcal{C}_{\ell,ISW^2}$ term in a different way, which will allow us to obtain a handier-to-integrate expression at the cost of a more complex analytical form.

We already know that

$$\begin{aligned}\mathcal{C}_{\ell,ISW^2} =& \frac{36}{25}\pi\frac{\Delta_0}{k_0^{n_S-1}}4\int\frac{dk}{k}k^{n_S-1}\int_{\eta_{in}}^{\eta_0}d\eta'\frac{dg(\eta')}{d\eta'}j_\ell(k(\eta_0-\eta'))\\ &\times\int_{\eta_{in}}^{\eta_0}d\eta''\frac{dg(\eta'')}{d\eta''}j_\ell(k(\eta_0-\eta''))\,,\end{aligned} \tag{316}$$

thus we can try to circumvent the problem by promptly integrating the conformal time, leaving behind the integral in k. Specifically, we have to compute

$$I(k) \equiv \int_{\eta_{in}}^{\eta_0} d\eta' \frac{dg(\eta')}{d\eta'} j_\ell(k(\eta_0 - \eta')) \, . \tag{317}$$

Thus, introducing the adimensional conformal time, our assumptions on the growth function in Eq.310 and $\eta_{in} \ll \eta_0$, we obtain

$$\begin{aligned} I(k) &= \int_0^1 d\widetilde{\eta} \frac{dg(\widetilde{\eta})}{d\widetilde{\eta}} j_\ell(k\eta_0(1-\widetilde{\eta})) \\ &\simeq -\frac{5}{4}\int_0^1 d\widetilde{\eta}\, \widetilde{\eta}^5 j_\ell(\widetilde{k}(1-\widetilde{\eta})) = \\ &= -\frac{5}{4}\sqrt{\frac{\pi}{2\widetilde{k}}}\int_0^1 d\widetilde{\eta}\, \widetilde{\eta}^5 (1-\widetilde{\eta})^{-\frac{1}{2}} J_{\ell+\frac{1}{2}}(\widetilde{k}(1-\widetilde{\eta})) = \\ &= -\frac{5}{4}\sqrt{\frac{\pi}{2\widetilde{k}}}\int_0^1 d\eta\, \eta^{-\frac{1}{2}} (1-\eta)^5 J_{\ell+\frac{1}{2}}(\widetilde{k}\eta) \, , \end{aligned} \tag{318}$$

where $\widetilde{k} = k\eta_0$. Once again [75] come into our help, providing another known integral of the Bessel functions yielding

$$\begin{aligned} &\int_0^1 x^\lambda (1-x)^{\mu-1} J_\nu(ax)\, dx = \frac{\Gamma(\mu)\Gamma(1+\nu+\lambda)a^\nu}{2^\nu \Gamma(\nu+1)\Gamma(1+\lambda+\nu+\mu)} \\ &\times {}_2F_3\left(\frac{\lambda+\nu+1}{2}, \frac{\lambda+\nu+2}{2}; \nu+1, \frac{\lambda+\nu+1+\mu}{2}, \frac{\lambda+\nu+2+\mu}{2}; -\frac{a^2}{4}\right) . \end{aligned} \tag{319}$$

The existence conditions read

$$\mathrm{Re}\,(\mu) > 0 \quad ; \quad \mathrm{Re}\,(\lambda+\nu) > -1 \, , \tag{320}$$

which in our case are respected since

$$\mu = 6 \quad , \quad \nu = \ell + \frac{1}{2} \quad , \quad \lambda = -\frac{1}{2} \quad , \quad a = \widetilde{k} \, . \tag{321}$$

Thus, Eq.319 allows to write

$$\begin{aligned} I(\widetilde{k}) = &-\frac{5}{4}\sqrt{\pi} \times \frac{\Gamma(6)\Gamma(\ell+1)\widetilde{k}^\ell}{2^{\ell+1}\Gamma(\ell+\frac{3}{2})\Gamma(\ell+7)} \\ &\times {}_2F_3\left(\frac{\ell+1}{2}, \frac{\ell+2}{2}; \ell+\frac{3}{2}, \frac{\ell+7}{2}, \frac{\ell+8}{2}; -\frac{\widetilde{k}^2}{4}\right) . \end{aligned} \tag{322}$$

Hence, we can write

$$\begin{aligned}\mathcal{C}_{\ell,\mathrm{ISW}^2} =& \frac{36}{25}\pi\frac{\Delta_0}{(k_0\eta_0)^{n_S-1}}4\int\frac{d\widetilde{k}}{\widetilde{k}}\widetilde{k}^{n_S-1}\times I^2(\widetilde{k}) = \\ =& 9\pi^2\frac{\Delta_0}{(k_0\eta_0)^{n_S-1}}\frac{\Gamma^2(6)\Gamma^2(\ell+1)}{2^{2\ell+2}\Gamma^2(\ell+\frac{3}{2})\Gamma^2(\ell+7)} \\ &\times\int d\widetilde{k}\,\widetilde{k}^{n_S-2+2\ell}\,{}_2F_3^2\left(\frac{\ell+1}{2},\,\frac{\ell+2}{2};\,\ell+\frac{3}{2},\,\frac{\ell+7}{2},\,\frac{\ell+8}{2};\,-\frac{\widetilde{k}^2}{4}\right),\end{aligned} \tag{323}$$

where the $\frac{1}{\eta_0^{n_S-1}}$ comes from having changed variables in the integral from k to $\widetilde{k}$.
This is the final expression of the pure-ISW term, which concludes our treatment of the zeroth order contribution to the correlation function. We pass now to the first order one.

7.3 FIRST ORDER SPECTRUM IN THE MODULATING FIELD

As aforementioned, the first order (in the modulating field) angular power spectrum consists of four terms, of which only two need to be evaluated, since the others are the same as the ones of the zeroth order spectrum (the pure-SW and the mixed term)[55]. Indeed, the first order contribution involves the SW effect and the ISW, together with the newly introduced ISW*, which contains an extra factor $\propto \eta'$.
We remind its full expression here

$$\begin{aligned}\mathcal{C}_\ell^{(1)} =& 4\pi\int\frac{dk}{k}\frac{k^3}{2\pi^2}\left[P_g(k)+P_g\left(|\vec{k}+\vec{k}_0|\right)\right]T_\ell^S(k)\,U_\ell^\star\left(|\vec{k}+\vec{k}_0|\right) = \\ =& 4\pi\int\frac{dk}{k}\frac{k^3}{2\pi^2}\left[P_g(k)+P_g\left(|\vec{k}+\vec{k}_0|\right)\right]\Big[T_\Phi(\eta_{in},k)j_\ell(k(\eta_0-\eta_{in})) \\ &+\int_{\eta_{in}}^{\eta_0}d\eta'\frac{\partial\left[T_\Psi(\eta',k)+T_\Phi(\eta',k)\right]}{\partial\eta'}j_\ell\left(k(\eta_0-\eta')\right)\Big] \\ &\times\Big[T_\Phi(\eta_{in},|\vec{k}+\vec{k}_0|)j_\ell(k(\eta_0-\eta_{in})) \\ &+\int_{\eta_{in}}^{\eta_0}d\eta'\frac{\eta_0-\eta'}{\eta_0-\eta_{in}}\frac{\partial\left[T_\Psi(\eta',|\vec{k}+\vec{k}_0|)+T_\Phi(\eta',|\vec{k}+\vec{k}_0|)\right]}{\partial\eta'}j_\ell\left(k(\eta_0-\eta')\right)\Big].\end{aligned} \tag{324}$$

55 This is true but with a caveat. See discussion of Eq.331.

First of all, let us make a comment on the power spectrum factor, as mentioned at the end of Ch.6; as the previous expression shows, we have a term

$$\left[P_g(k) + P_g\left(|\vec{k} + \vec{k}_0|\right)\right], \tag{325}$$

which we can try to simplify in some way. Indeed, we have seen that the power spectrum can be written as in Eq.291, however the second term of Eq.325 requires something more. We write it as

$$\frac{k^3}{2\pi^2} P_g\left(|\vec{k} + \vec{k}_0|\right) = \Delta_0 \left(\frac{|\vec{k} + \vec{k}_0|}{k_0}\right)^{n_s - 1}. \tag{326}$$

Clearly, in the case of a scale-invariant spectrum ($n_s = 1$), this becomes exactly equal to $P_g(k)$, but here in this Thesis we will consider a slightly tilted one with $n_s \neq 1$. Thus, we can write

$$\Delta_0 \left(\frac{|\vec{k} + \vec{k}_0|}{k_0}\right)^{n_s - 1} = \Delta_0 \left(\frac{\sqrt{k^2 + k_0^2 + 2k \cdot k_0 \cos(\theta)}}{k_0}\right)^{n_s - 1}, \tag{327}$$

where θ is the angle between $\vec{k}$ and $\vec{k}_0$. Then, reminding that we are considering the case in which $k_0 \ll k$, we can write it as

$$\begin{aligned} &\Delta_0 \left[\sqrt{\left(\frac{k}{k_0}\right)^2 + 1 + 2\frac{k}{k_0}\cos(\theta)}\right]^{n_s - 1} \\ \simeq &\Delta_0 \left(\frac{k}{k_0}\right)^{n_s - 1}, \end{aligned} \tag{328}$$

which is exactly equal to $P_g(k)$, since we kept only the first dominant term. This allows to write Eq.325 as $2P_g(k)$, carrying an extra factor of 2 in this contribution. However, in order to avoid confusing the reader and most importantly to reconcile our computation with [10] (see Eq.238 and Eq.240), we will bring out of $\mathcal{C}_\ell^{(1)}$ this factor and we will instead multiply by two the final results of the correlation function of SH coefficients, thus writing

$$\begin{aligned} \langle \Gamma_{\ell m, S} \Gamma^*_{\ell' m', S} \rangle = &\delta_{\ell\ell'}\delta_{mm'}\mathcal{C}_\ell^{(0)} + w_1 \delta_{mm'}\left[R^{1,\ell}_{\ell' m}\mathcal{C}_\ell^{(1)} + R^{1,\ell'}_{\ell m}\mathcal{C}_{\ell'}^{(1)}\right] + \\ &+ w_1^2 \delta_{mm'} \sum_j R^{1,j}_{\ell m} R^{1,j}_{\ell' m} \mathcal{C}_j^{(2)}, \end{aligned} \tag{329}$$

which "substitute" what is shown by Eq.284. In this way we can still make use of Eq.287 and all the sub-spectra we have already computed and we are

about to compute. Just for the sake of clearness, we write here the "new" definition of $\mathcal{C}_\ell^{(1)}$

$$\mathcal{C}_\ell^{(1)} \equiv 4\pi \int \frac{dk}{k} \frac{k^3}{2\pi^2} P_g(k) T_\ell^S(k)\, U_\ell^\star\left(|\vec{k}+\vec{k}_0|\right) , \tag{330}$$

which is valid if used inside Eq.329 and for which Eq.287 holds[56].

Furthermore, looking closely to Eq.324, one can notice that indeed we should introduce a couple of other "sub-spectra" together with the already presented ones in Eq.287. Indeed, from Eq.330, a term of the type

$$T_\ell^S(k)\, T_\ell^{SW}\left(|\vec{k}+\vec{k}_0|\right) \tag{331}$$

will appear, which in principle will give a different pure-SW contribution w.r.t. the one in Eq.299. This is due to the fact that T_ℓ^{SW} contains a Φ-transfer function evaluated in $|\vec{k}+\vec{k}_0|$, whereas both the transfer functions giving birth to Eq.299 are evaluated in k.
However, given that the approximation we use here for the Φ-transfer function drops its dependency on k (see Eq.292), we do not need to introduce these new terms, because they become identical to the ones we are about to compute. In spite of this, be aware that if one tries to generalize this treatment to a more general transfer function, this dependency has to be accounted for.

7.3.1 *Mixed Starred Term*

The first term we need to make explicit for what regard the first order contribution to the correlation function reads

$$\begin{aligned}\mathcal{C}_{\ell,SW\times ISW^\star} \equiv & 4\pi \int \frac{dk}{k} \frac{k^3 P_g(k)}{2\pi^2} T_\Phi(\eta_{in}, k) j_\ell(k(\eta_0-\eta_{in})) \\ & \times \int_{\eta_{in}}^{\eta_0} d\eta' \frac{\eta_0-\eta'}{\eta_0-\eta_{in}} \frac{d\left[T_\Psi(|\vec{k}+\vec{k}_0|,\eta') + T_\Phi(|\vec{k}+\vec{k}_0|,\eta')\right]}{d\eta'} \\ & \times j_\ell(k(\eta_0-\eta')) .\end{aligned} \tag{332}$$

Also in this case, we use the aforementioned assumptions on the transfer functions of Eq.292 and on the adimensional power spectrum Eq.291 to write

56 Once more, we stress the fact that this "change" of the definition of this contribution was not an attempt to confuse the reader, even if this may be the result, but a crucial passage to fully reproduce the equations showed by [10]. Indeed, in that paper, a scale-invariant spectrum was considered, thus such an explanation was not necessary.

(we avoid repeating again the intermediate steps, given that they are nearly identical)

$$\begin{aligned}\mathcal{C}_{\ell,SW\times ISW^\star} =& \frac{36}{25}\pi^2 g(\eta_{in})\frac{\Delta_0}{k_0^{n_S-1}}\int_{\eta_{in}}^{\eta_0} d\eta' \frac{dg(\eta')}{d\eta'}\frac{\eta_0-\eta'}{\eta_0-\eta_{in}} \\ &\times \int dk \frac{k^{n_S-3} J_{\ell+\frac{1}{2}}(k(\eta_0-\eta_{in}))J_{\ell+\frac{1}{2}}(k(\eta_0-\eta'))}{\sqrt{(\eta_0-\eta_{in})(\eta_0-\eta')}} .\end{aligned} \tag{333}$$

This integral is the same as Eq.302, exception made for the extra ratio $\frac{\eta_0-\eta'}{\eta_0-\eta_{in}}$ brought by the presence of the *. For this reason, the final result will be very similar to Eq.311, although not identical:

$$\begin{aligned}\mathcal{C}_{\ell,SW\times ISW^\star} =& \frac{36}{25}\pi^2 g(\eta_{in})\frac{\Delta_0}{k_0^{n_S-1}}\int_{\eta_{in}}^{\eta_0} d\eta' \frac{dg(\eta')}{d\eta'} \\ &\times \frac{(\eta_0-\eta')^{\ell+1}\Gamma(\ell-\frac{1}{2}+\frac{n_S}{2})}{2^{3-n_S}(\eta_0-\eta_{in})^{\ell+n_S}\Gamma(\ell+\frac{3}{2})\Gamma(2-\frac{n_S}{2})} \\ &\times F\left[\ell-\frac{1}{2}+\frac{n_S}{2}\,,\ \frac{n_S}{2}-1\,;\ \ell+\frac{3}{2}\,;\ \left(\frac{\eta_0-\eta'}{\eta_0-\eta_{in}}\right)^2\right] .\end{aligned} \tag{334}$$

Exploiting the very same passages of the "ordinary" mixed term, where we introduced the adimensional conformal time, Eq.310 for the derivative of the growth function, we assumed $\eta_{in} \ll \eta_0$ and we used a couple of change of variables, it is possible to obtain the final expression

$$\begin{aligned}\mathcal{C}_{\ell,SW\times ISW^\star} =& -\frac{9}{5}\pi^2 g(\eta_{in})\frac{\Delta_0}{(k_0\eta_0)^{n_S-1}}\frac{\Gamma(\ell-\frac{1}{2}+\frac{n_S}{2})}{2^{3-n_S}\Gamma(\ell+\frac{3}{2})\Gamma(2-\frac{n_S}{2})} \\ &\times \int_0^1 d\eta\, \eta^{\ell+1}(1-\eta)^5 F\left[\ell-\frac{1}{2}+\frac{n_S}{2}\,,\ \frac{n_S}{2}-1\,;\ \ell+\frac{3}{2}\,;\ \eta^2\right] ,\end{aligned} \tag{335}$$

which is identical to Eq.311, but with an exponent $\ell+1$ inside the integral, instead of a ℓ.

7.3.2 *Hybrid Integrated Sachs-Wolfe*

The second term we need to evaluate will be called from now one the "hybrid" term, because it involves both the ordinary ISW effect and its starred counterpart. It reads

$$\begin{aligned}\mathcal{C}_{\ell,ISW\times ISW^\star} =& 4\pi\int\frac{dk}{k}\frac{k^3 P_g(k)}{2\pi^2}\int_{\eta_{in}}^{\eta_0} d\eta'\, 2\frac{dT_\Phi(k,\eta')}{d\eta'} j_\ell(k(\eta_0-\eta')) \\ &\times \int_{\eta_{in}}^{\eta_0} d\eta''\frac{\eta_0-\eta''}{\eta_0-\eta_{in}}\, 2\frac{dT_\Phi(|\vec{k}+\vec{k}_0|,\eta'')}{d\eta''} j_\ell(k(\eta_0-\eta'')) .\end{aligned}$$

(336)

Wise of the calculations done for its non-starred counterpart, here we only perform the procedure leaving behind the numerical integration of k, since we know that the other procedure would have brought us to a dead end.
Thus, while following the same steps leading to Eq.323, one finds himself solving a slightly different integral of conformal time w.r.t. Eq.318, due to the extra factor present here, which changes λ of Eq.319 from $-\frac{1}{2}$ to $\frac{1}{2}$. This time we obtain

$$\begin{aligned} I'(k) \equiv & -\frac{5}{4}\sqrt{\frac{\pi}{2\widetilde{k}}}\int_0^1 d\eta \eta^{\frac{1}{2}}(1-\eta)^5 J_{\ell+\frac{1}{2}}(\widetilde{k}\eta) = \\ = & -\frac{5}{4}\sqrt{\pi}\times\frac{\Gamma(6)\Gamma(\ell+2)\widetilde{k}^{\ell}}{2^{\ell+1}\Gamma(\ell+\frac{3}{2})\Gamma(\ell+8)} \\ & \times {}_2F_3\left(\frac{\ell+2}{2}, \frac{\ell+3}{2}; \ell+\frac{3}{2}, \frac{\ell+8}{2}, \frac{\ell+9}{2}; -\frac{\widetilde{k}^2}{4}\right), \end{aligned} \tag{337}$$

which is indeed very similar to Eq.322, exception made for some Γ and the arguments of ${}_2F_3$.
Having solved this integral, it is possible to write the final expression of the hybrid contribution as

$$\begin{aligned} \mathcal{C}_{\ell,ISWxISW^\star} = & \frac{36}{25}\pi\frac{\Delta_0}{(k_0\eta_0)^{n_S-1}} 4\int\frac{d\widetilde{k}}{\widetilde{k}}\widetilde{k}^{n_S-1}\times I(\widetilde{k})I'(\widetilde{k}) = \\ = & 9\pi^2\frac{\Delta_0}{(k_0\eta_0)^{n_S-1}}\frac{\Gamma^2(6)\Gamma(\ell+1)\Gamma(\ell+2)}{2^{2\ell+2}\Gamma^2(\ell+\frac{3}{2})\Gamma(\ell+7)\Gamma(\ell+8)} \\ & \times\int d\widetilde{k}\,\widetilde{k}^{n_S-2+2\ell}\,{}_2F_3\left(\frac{\ell+1}{2}, \frac{\ell+2}{2}; \ell+\frac{3}{2}, \frac{\ell+7}{2}, \frac{\ell+8}{2}; -\frac{\widetilde{k}^2}{4}\right) \\ & \times {}_2F_3\left(\frac{\ell+2}{2}, \frac{\ell+3}{2}; \ell+\frac{3}{2}, \frac{\ell+8}{2}, \frac{\ell+9}{2}; -\frac{\widetilde{k}^2}{4}\right). \end{aligned} \tag{338}$$

This concludes our treatment of the first order contribution to the correlation function of the SH coefficients, thus we pass to the second order one.

7.4 SECOND ORDER SPECTRUM IN THE MODULATING FIELD

The second order contribution introduces only one new term. The full expression of this contribution reads

$$\begin{aligned}\mathcal{C}_\ell^{(2)} =& 4\pi \int \frac{dk}{k}\frac{k^3}{2\pi^2} P_g(k) U_\ell^\star(k) U_\ell^\star(k) = \\ =& 4\pi \int \frac{dk}{k}\frac{k^3}{2\pi^2} P_g(k) \Big[T_\Phi(\eta_{in}, k) j_\ell(k(\eta_0 - \eta_{in})) \\ &+ \int_{\eta_{in}}^{\eta_0} d\eta' \frac{\eta_0 - \eta'}{\eta_0 - \eta_{in}} \frac{\partial \left[T_\Psi(\eta', k) + T_\Phi(\eta', k)\right]}{\partial \eta'} j_\ell\left(k(\eta_0 - \eta')\right) \Big]^2 ,\end{aligned} \tag{339}$$

thus the only effects involved here are the SW and the ISW*.

7.4.1 *Pure Starred Integrated Sachs-Wolfe*

The new term we need to compute reads

$$\begin{aligned}\mathcal{C}_{\ell,ISW^{\star 2}} \equiv& 4\pi \int \frac{dk}{k}\frac{k^3 P_g(k)}{2\pi^2} \int_{\eta_{in}}^{\eta_0} d\eta' \frac{\eta_0 - \eta'}{\eta_0 - \eta_{in}} 2\frac{dT_\Phi(k, \eta')}{d\eta'} j_\ell(k(\eta_0 - \eta')) \\ &\times \int_{\eta_{in}}^{\eta_0} d\eta'' \frac{\eta_0 - \eta''}{\eta_0 - \eta_{in}} 2\frac{dT_\Phi(k, \eta'')}{d\eta''} j_\ell(k(\eta_0 - \eta'')) .\end{aligned} \tag{340}$$

Fortunately, we already have all the tools to fully compute this term, assuming again all the usual approximations (Eq.292, Eq.310, Eq.291) and using the already computed integral of Eq.337. Without repeating ourselves, the final expression reads

$$\begin{aligned}\mathcal{C}_{\ell,ISW^{\star 2}} =& \frac{36}{25}\pi \frac{\Delta_0}{(k_0\eta_0)^{n_S - 1}} 4 \int \frac{d\widetilde{k}}{\widetilde{k}} \widetilde{k}^{n_S - 1} \times \left[I'(\widetilde{k})\right]^2 = \\ =& 9\pi^2 \frac{\Delta_0}{(k_0\eta_0)^{n_S - 1}} \frac{\Gamma^2(6)\Gamma^2(\ell + 2)}{2^{2\ell+2}\Gamma^2(\ell + \frac{3}{2})\Gamma^2(\ell + 8)} \\ &\times \int d\widetilde{k}\, \widetilde{k}^{n_S - 2 + 2\ell}\, {}_2F_3^2\left(\frac{\ell+2}{2}, \frac{\ell+3}{2}; \ell + \frac{3}{2}, \frac{\ell+8}{2}, \frac{\ell+9}{2}; -\frac{\widetilde{k}^2}{4}\right) .\end{aligned} \tag{341}$$

With this last element, we have an analytic representation of all the contributions to the overall angular power spectrum of the CGWB, which however has to be integrated over conformal time, or k, in a numerical way.
We stress that we obtained these results using an approximation of the Φ-transfer function, which do not depend on k, simplifying greatly the integrals over that variable. Indeed, we remind that transfer functions as

$T_\ell^{SW}(|\vec{k}+\vec{k}_0|)$ contains $T_\Phi(|\vec{k}+\vec{k}_0|,\eta)$, which would complicate the computation if the dependency on k is not dropped.

7.5 NUMERICAL COMPUTATION OF THE ANGULAR POWER SPECTRA OF THE CGWB

To evaluate the various contributions to the angular power spectrum of the CGWB, we have just found that is necessary to perform some numerical integrations. These are done through a Python code, exploiting the functions we are about to present.
In Tab.1, we define the constants and variables useful for the computation [48].

QUANTITY	CODE NAME	INPUT VALUE
Δ_0	D0	$(2.101^{+0.031}_{-0.034})\cdot 10^{-9}$ at 68% CL
k_0	k0	$0.05\,\mathrm{Mpc}^{-1}$
n_S	ns	0.9665 ± 0.0038 at 68% CL
η_{in}	nin	$\approx 0\,\mathrm{Mpc}$
η_0	n0	$1.4\cdot 10^4\,\mathrm{Mpc}$
$g(\eta_{in})$	/	1 (see App.A)
ℓ	x	Indep. variable

Table 1: Quantities used in the numerical computation. We assumed η_{in} very small, because in principle we want to take it as near as possible to the end of inflation. However, also considering slightly higher values does not change the final results of the integrations, nor the fact that $\eta_{in} \ll \eta_0$.

7.5.1 *Pure Sachs-Wolfe*

The code we used to compute the pure SW contribution do not need any integration, but only makes use of the already defined Gamma functions. It reads

Listing 1: Sachs-Wolfe code.

```
import numpy as np
import math

def Cl_SW(x,D0,k0,n0,ns):
    return 36/25*np.pi**2*D0/(k0*n0)**(ns-1)
    *math.gamma(3-ns)*math.gamma(x-0.5+ns/2)
    /math.gamma(x+2.5-ns/2)/(math.gamma(2-ns/2))**2/2**(4-ns)
```

In order to mimic what is typically done for the CMB, we plot this function multiplied by $\ell(\ell+1)$ for the first 10 multipoles; one obtains what is shown in Fig.12.

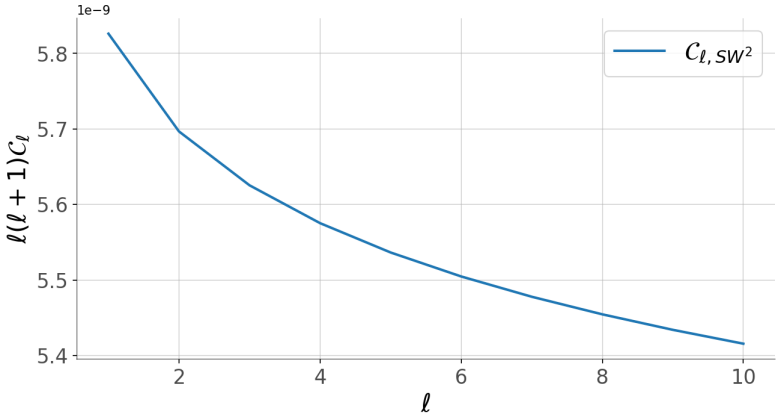

Figure 12: Pure Sachs-Wolfe contribution to the angular power spectrum of the CGWB.

7.5.2 *Mixed Terms*

For the mixed terms, either starred and non-starred, we have presented the calculation leaving behind an integral of conformal time η leading to Eq.311 and Eq.335. However, it is possible to follow the same route of the ISW terms, integrating analytically the η integral and leaving an integral on k. Since these two procedures can be carried out without encountering dead ends, this allows us to compare the results coming from the two methods, in order to check that they yield the same results in terms of the final spectrum.
To distinguish them, we will temporarily indicate with an apex ^{k}, or $^\eta$, the variable that has been numerically integrated through Python.
Eq.311 and Eq.335 already give the analytical expression, thus we only report here their code translation

Listing 2: Mixed terms code for the η integration.

```
import numpy as np
import math
import scipy.special as special
import scipy.integrate as integrate

def Cl^\eta_SWxISW(x,D0,k0,n0,ns):
    return -9/5*np.pi**2*D0/k0**(ns-1)/n0**(ns-1)
    *math.gamma(x-0.5+ns/2)/math.gamma(2-ns/2)/math.gamma(x+1.5)
    /2**(3-ns)*integrate.quad(lambda y: y**(x)*(1-y)**5
    *special.hyp2f1(x-0.5+ns/2,ns/2-1,x+1.5,y**2), 0, 1)[0]

def Cl^\eta_SWxISWstar(x,D0,k0,n0,ns):
    return -9/5*np.pi**2*D0/k0**(ns-1)/n0**(ns-1)
    *math.gamma(x-0.5+ns/2)/math.gamma(2-ns/2)/math.gamma(x+1.5)
    /2**(3-ns)*integrate.quad(lambda y :y**(x+1)*(1-y)**5
    *special.hyp2f1(x-0.5+ns/2,ns/2-1,x+1.5,y**2), 0, 1)[0]
```

For what regard the second procedure, we provide here both the final analytical expressions and their code translation[57].
The analytical expression of the mixed term is

$$\mathcal{C}^{k}_{\ell,SW\times ISW} \equiv -\frac{18}{5}\pi^{\frac{3}{2}} g(\eta_{in}) \frac{\Delta_0}{(k_0\eta_0)^{n_S-1}} \frac{\Gamma(6)\Gamma\ell+1}{2^{\ell+1}\Gamma(\ell+\frac{3}{2})\Gamma(\ell+7)} \int d\widetilde{k}\, \widetilde{k}^{\ell+n_S-2} \times j_\ell\left(\widetilde{k}\right) {}_2F_3\left(\frac{\ell+1}{2}, \frac{\ell+2}{2}; \ell+\frac{3}{2}, \frac{\ell+7}{2}, \frac{\ell+8}{2}; -\frac{\widetilde{k}^2}{4}\right), \tag{342}$$

whereas the one of its starred counterpart is

$$\mathcal{C}^{k}_{\ell,SW\times ISW^\star} \equiv -\frac{18}{5}\pi^{\frac{3}{2}} g(\eta_{in}) \frac{\Delta_0}{(k_0\eta_0)^{n_S-1}} \frac{\Gamma(6)\Gamma\ell+2}{2^{\ell+1}\Gamma(\ell+\frac{3}{2})\Gamma(\ell+8)} \int d\widetilde{k}\, \widetilde{k}^{\ell+n_S-2} \times j_\ell\left(\widetilde{k}\right) {}_2F_3\left(\frac{\ell+2}{2}, \frac{\ell+3}{2}; \ell+\frac{3}{2}, \frac{\ell+8}{2}, \frac{\ell+9}{2}; -\frac{\widetilde{k}^2}{4}\right). \tag{343}$$

Their code translation is

Listing 3: Mixed terms code for the k integration.

```
import numpy as np
import math
import scipy.special as special
from sympy.functions import hyper
import scipy.integrate as integrate

def Cl^k_SWxISW(x,D0,k0,n0,ns):
    return -18/5*np.pi**1.5*D0/k0**(ns-1)*n0**(1-ns)
    *math.gamma(x+1)*math.gamma(6)/math.gamma(x+7)
    /math.gamma(x+1.5)/2**(x+1)*integrate.quad(lambda y:
    special.jv(x,y/n0*(n0-nin))*y**(ns+x-2)*hyper([(x+1)/2,
    x/2+1],[x+3/2,x/2+7/2,x/2+4],-y**2/4), 0, 500)[0]

def Cl^k_SWxISWstar(x,D0,k0,n0,ns):
    return -18/5*np.pi**1.5*D0/k0**(ns-1)*n0**(1-ns)
    *math.gamma(x+2)*math.gamma(6)/math.gamma(x+8)
    /math.gamma(x+1.5)/2**(x+1)*integrate.quad(lambda y:
    special.jv(x,y/n0*(n0-nin))*y**(ns+x-2)*hyper([(x+2)/2,
    (x+3)/2],[x+3/2,(x+8)/2,(x+9)/2],-y**2/4), 0, 500)[0]
```

Let us make a comment on the integration bounds used.
Being solely interested in large scale phenomena, a range for k from 0 to e.g. $10\,\mathrm{Mpc}^{-1}$ should be sufficient, since it corresponds to having imposed an high pass filter with a cut-off scale of $\frac{2\pi}{10} \simeq 0.6\mathrm{Mpc}$. However, comparing

57 Here we avoided writing the intermediate steps to obtain these expressions, because they are identical to the ones leading to Eq.323, Eq.338 and Eq.341.

the two procedures with such a cut-off leads to some macroscopic difference, especially when looking at multipoles higher than 10. In order to avoid this problem, we found out that increasing sensibly the cut-off allows to the second procedure to reproduce much more faithfully the behavior of the first. Thus, we imposed the cut-off to $500\,\mathrm{Mpc}^{-1}$.
On the other hand, integrating from $0\,\mathrm{Mpc}^{-1}$ corresponds to having considered infinitely large scale, which indeed should be limited to the size of the observable Universe, at least. However, this brings no visible consequences on the results, thus we will continue to use 0 as the lower bound of the integrals.
Fig.13 shows the final results, plotted against ℓ. As we can see, the two proce-

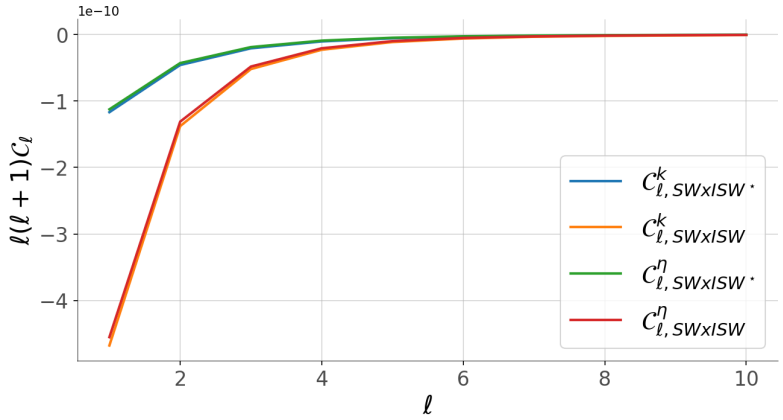

Figure 13: Mixed terms contributions to the angular power spectrum of the CGWB.

dures produce very similar results, proving their robustness. For this reason and in order to be consistent with the ISW terms, for which only the k integration can be successfully done, we will only consider these latter terms from now on, also dropping the apex ^{k}.

7.5.3 *Integrated Sachs-Wolfe*

As aforementioned, the ISW terms are only computed following the second procedure, thus numerically integrating k. Their code yields

Listing 4: Integrated Sachs-Wolfe code.

```
import numpy as np
import math
import scipy.special as special
from sympy.functions import hyper
import scipy.integrate as integrate

def Cl_ISW(x,D0,k0,n0,ns):
    return 9*np.pi**2*D0/(k0**(ns-1))*n0**(1-ns)*(math.gamma(x+1)
    *math.gamma(6)/math.gamma(x+7)/math.gamma(x+1.5)/2**(x+1))**2
    *integrate.quad(lambda y:y**(ns+2*x-2)*(hyper([(x+1)/2,
    x/2+1],[x+3/2,x/2+7/2,x/2+4],-y**2/4))**2, 0, 10)[0]
```

```
12
13 def Cl_ISWxISWstar(x,D0,k0,n0,nin,ns):
14     return 9*np.pi**2*D0/(k0*n0)**(ns-1)*math.gamma(x+1)
15     *math.gamma(x+2)*(math.gamma(6))**2/math.gamma(x+7)
16     /math.gamma(x+8)/(math.gamma(x+1.5))**2/2**(2*x+2)
17     *integrate.quad(lambda y: y**(ns+2*x-2)*hyper([(x+1)/2,x/2+1],
18     [x+3/2,x/2+7/2,x/2+4],-y**2/4)*hyper([(x+2)/2,x/2+3/2],
19     [x+3/2,x/2+8/2,x/2+9/2],-y**2/4), 0, 10)[0]
20
21 def Cl_ISWstar(x,D0,k0,n0,ns):
22     return 9*np.pi**2*D0/(k0**(ns-1))*n0**(1-ns)*(math.gamma(x+2)
23     *math.gamma(6)/math.gamma(x+8)/math.gamma(x+1.5)/2**(x+1))**2
24     *integrate.quad(lambda y: y**(ns+2*x-2)*(hyper([(x+2)/2,
25     x/2+3/2],[x+3/2,x/2+8/2,x/2+9/2],-y**2/4))**2, 0, 10)[0]
```

Finally, the ISW contributions are shown in Fig.14.

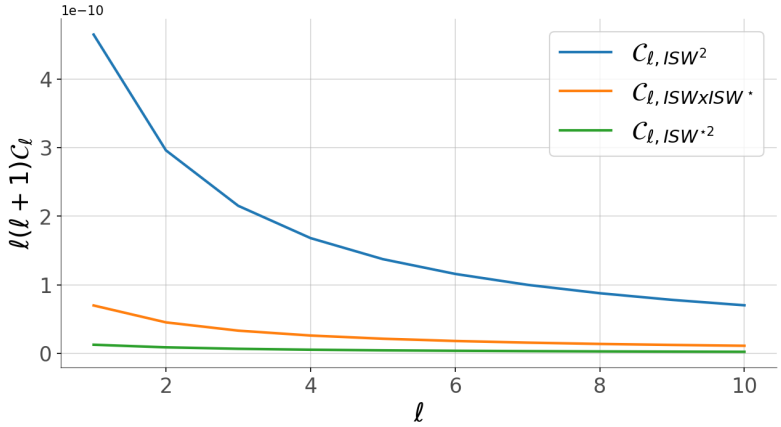

Figure 14: Pure ISW contributions to the angular power spectrum of the CGWB.

7.5.4 *Comparing the Contributions*

Firstly, Fig.15 shows the various contributions plotted together. Just for now, we dropped the factor $\ell(\ell+1)$, which would have produced the typical nearly-scale-invariant behavior, spoiling the efficacy to compare the contributions. As expected, the pure SW contribution is by far the dominant one, justifying the fact that often the ISW effects are neglected (e.g. [10]). Their subdominant behavior can be clearly shown by summing all together the subdominant contributions

$$\mathcal{C}_{\ell,\mathrm{sub}} = \mathcal{C}_{\ell,SW\times ISW} + \mathcal{C}_{\ell,SW\times ISW^\star} + \mathcal{C}_{\ell,ISW^2} + \mathcal{C}_{\ell,ISW^{\star 2}} \tag{344}$$

and dividing by the SW one to obtain what is shown in Fig.16. Furthermore, we can notice that the presence of the extra factor $\frac{\eta_0-\eta'}{\eta_0-\eta_{\mathrm{in}}}$ in the starred contributions contributes to suppress those terms. This is particularly clear looking at Fig.14, where we have a "standard" term, one with the extra factor and one with the extra factor squared. The higher the power, the more sup-

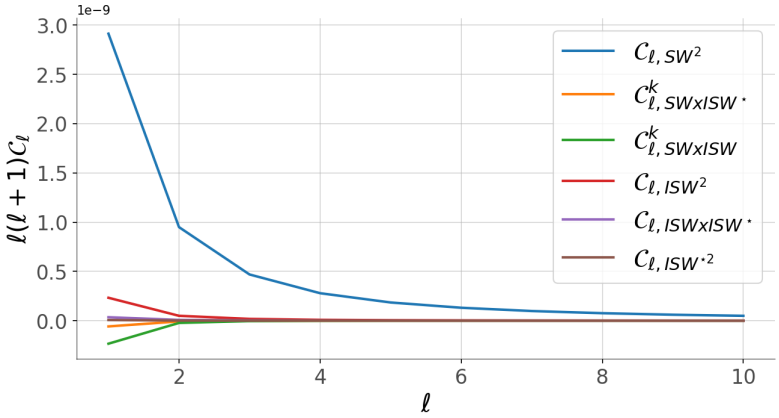

Figure 15: All contributions to the angular power spectrum of the CGWB.

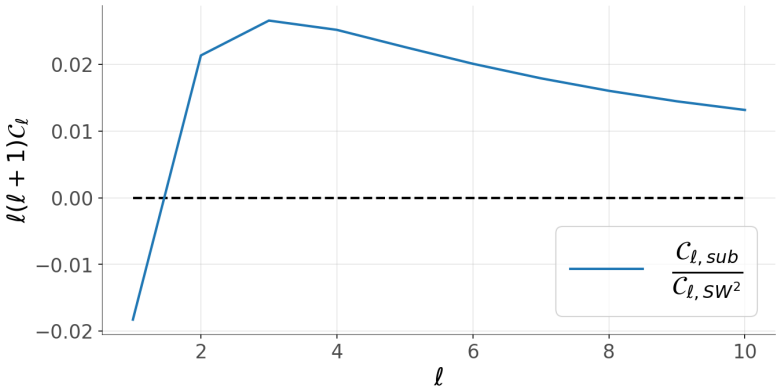

Figure 16: Comparison between subdominant contributions and the SW one.

pressed the power gets.

To be more quantitative in the comparison of all the contributions, we can also consider Tab.2, where the dipole, quadrupole and octopole of the various contributions are reported [58].

7.6 OVERALL ANGULAR POWER SPECTRUM OF THE CGWB

We can now sum back the various elements we have just computed exploiting Eq.287 to obtain the angular power spectrum contributions of each order term in h.
In particular, Fig.17 shows the results and highlights that the second order term (in the modulating field) seems to be the higher one in terms of power

58 We can compare our results with the one obtained in [76]. Firstly, a slightly different Φ-transfer function was used there, thus here we need to multiply our "data" by a factor $\frac{100}{81}$ in order to obtain a meaningful comparison (see Eq.289 and Eq.13 of [76]). Indeed looking at the SW effect, we obtain similar, but not identical, values, even if in [76] they used the complete transfer functions instead of our Eq.292 (see Fig.1 of [76]).
Also our ISW values are similar to what is shown in Fig.2 of [76]. However, in this case the difference carried by the usage of the complete transfer functions becomes more evident.

	DIPOLE ($\ell = 1$)	QUADRUPOLE ($\ell = 2$)	OCTOPOLE ($\ell = 3$)
$\mathcal{C}_{\ell,SW^2}$	$2.91 \cdot 10^{-9}$	$9.49 \cdot 10^{-10}$	$4.68 \cdot 10^{-10}$
$\mathcal{C}_{\ell,SW\text{x}ISW}$	$-2.33 \cdot 10^{-10}$	$-2.29 \cdot 10^{-11}$	$-4.33 \cdot 10^{-12}$
$\mathcal{C}_{\ell,SW\text{x}ISW^\star}$	$-5.84 \cdot 10^{-11}$	$-7.65 \cdot 10^{-12}$	$-1.73 \cdot 10^{-12}$
$\mathcal{C}_{\ell,ISW^2}$	$2.32 \cdot 10^{-10}$	$4.93 \cdot 10^{-11}$	$1.79 \cdot 10^{-11}$
$\mathcal{C}_{\ell,ISW\text{x}ISW^\star}$	$3.49 \cdot 10^{-11}$	$7.54 \cdot 10^{-12}$	$2.76 \cdot 10^{-12}$
$\mathcal{C}_{\ell,ISW^{\star 2}}$	$6.33 \cdot 10^{-12}$	$1.47 \cdot 10^{-12}$	$5.62 \cdot 10^{-13}$

Table 2: Power on the dipole, quadrupole and octopole of all the contributions.

in the dipole. This is rather interesting, since Eq.329 shows that the first order

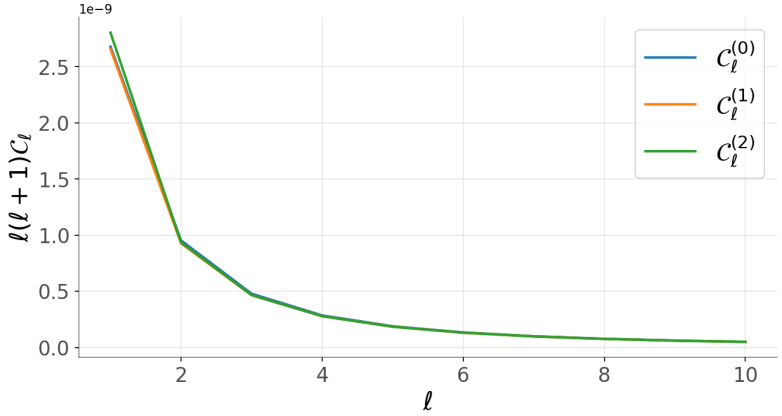

Figure 17: Comparison between the angular power spectra of the CGWB relative to each order of h.

term (in the modulating field) couples multipoles with ℓ and $\ell \pm 1$, whereas the second order one ℓ to $\ell \pm 2$. However, one must remember that these terms must be multiplied respectively by the amplitude of the modulation and its square value.

Again, in Fig.17 we dropped the factor $\ell(\ell+1)$, however re-introducing it, one obtains another interesting plot, shown in Fig.18. Indeed, Fig.18 allows to enhance greatly the features of the previous one, enabling to appreciate them form a new perspective. In particular, it is very clear now that the (2)-contribution is the dominant term for what concerns the dipole, but the (0) one promptly takes the lead from the quadrupole on. Also, we can see that also the (1)-contribution passes the (2) one after the octopole. In spite of this, the three contributions remain pretty similar throughout the first multipoles, even if the zeroth order remains overall the dominant one.

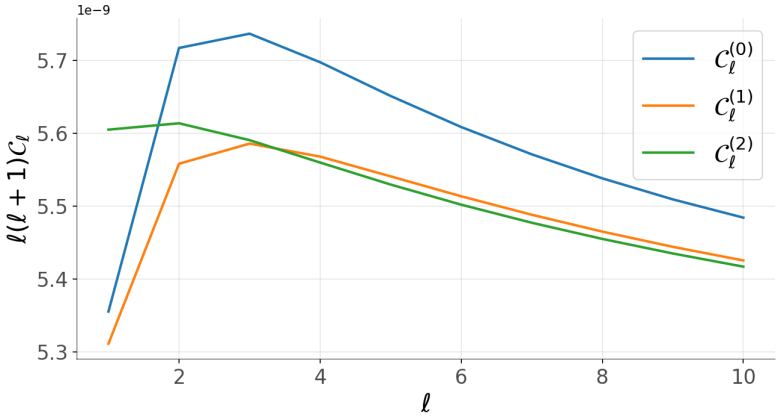

Figure 18: Comparison between the angular power spectra of the CGWB relative to each order of h, this time with the factor $\ell(\ell+1)$.

7.7 SUMMARY

In this chapter, we have computed the contributions to $\langle \Gamma_{\ell m} \Gamma^*_{\ell' m'} \rangle$ consisting of three different terms classified by their order in the modulating field (see Eq.287 and the discussion on Eq.330).
These have been further divided in 6 different sub-spectra, distinguished by the physical effects giving them birth, thus the SW and the ISW effects, together with its starred counterpart ISW*, which is an original term stemming from the presence of the modulation (see Ch.6).

After having used several approximations on the transfer functions of the gravitational potentials (see Eq.292 and Ch.A), on the growth function (see Eq.310 and Ch.A) and moving to handier variables, e.g. the adimensional conformal time, we were able to obtain an analytic expression for all the sub-spectra, which then we integrated numerically in two ways. The first one we presented was an integration in the adimensional conformal time, which however forced us to introduce the second way where we integrated the wavenumber k, since the first one was not a viable choice for the ISW terms.
Then, we presented the Python codes we used to integrate and plot the contributions, whose results are well-summarized by Fig.15, Fig.17 and Fig.18. These figures show peculiar features of the $\mathcal{C}_\ell^{(i)}$ contributions, which couples multipoles in the full expression of $\langle \Gamma_{\ell m} \Gamma^*_{\ell' m'} \rangle$ and represent signatures of a departure from statistical isotropy in our local Universe.

8 CONCLUSIONS

Throughout this Thesis we have seen how the CGWB can be described with a Boltzmann approach, typical of CMB studies, and how the presence of a modulating field in the gravitational potentials can leave relic signatures on the angular power spectrum of the CGWB.
Thus, before presenting the final results, we will summarize the main steps which allowed us to achieve them. Also, we will propose some possible development arising from this framework.

8.1 SUMMARY

The first part of this Thesis is dedicated to some background information, necessary for the rest of the work, thus in Ch.1 we briefly review the basic concepts underlying Cosmology, e.g. the Einstein's equations or the Friedmann ones, which were used in Ch.2 to justify why an accelerated stage of the Early Universe is necessary to achieve a good agreement with the observations. Indeed, the hot Big-Bang model is flawed by the so-called shortcomings, which are naturally solved by inflation.
In Ch.3 we describe the latter phenomenon, specifically in the case of a real scalar field, which drives the accelerated expansion. Most importantly, we show how quantum fluctuations of this field cause the presence of perturbations on the energy content of the Universe. Furthermore, quantum fluctuations of the tensor field of the metric produced ripples of the space-time itself, which, once enhanced by inflation, generate a CGWB.
This "smoking gun" of inflationary models is then described following a Boltzmann approach in Ch.4, where we present the main equations affecting the GW energy density at first order in perturbations, sourced by initial conditions, scalar and tensor perturbations. The observables associated to these quantities are the contributions to the angular power spectrum of GW energy density.
Given the amount of attention that a possible departure from statistical isotropy is drawing on the Cosmology community, spurred by the presence of the CMB anomalies in WMAP and Planck data, we dedicated the second core-part of this Thesis to the exploration of what such a local departure would cause on cosmological GW background signals.
Firstly, in Ch.5, we briefly describe the case of CMB, where the main prediction is a non-trivial coupling of adjacent multipoles in the correlation functions. Finally, in Ch.6, we apply the same concepts to the CGWB, keeping this time the ISW effect and concentrating on the scalar sourced terms of the Boltzmann equations.
After having found an analytical expression of the angular power spectra, in

Ch.7, we evaluate them numerically, obtaining plots of the zeroth, first and second order (in the modulating field) angular power spectrum of the CGWB.

8.2 RESULTS

8.2.1 *Integrated Sachs-Wolfe Effect*

As aforementioned in [10] the ISW effect was completely disregarded because of its sub-dominance w.r.t. the SW one. In this Thesis we include it in the equations, while keeping also track of the presence of the modulating field in the gravitational potentials.
For this reason, this Thesis can be thought as an extension of both [26] and [10]:

1. in [26], the CGWB was treated in an isotropy environment, i.e. without a modulation, which instead here is treated;

2. in [10], the CMB case was studied, but having kept the ISW effect in our calculations allow us to find the complete equations for the angular power spectrum of CGWB. These equations (see the end of Ch.6) can be promptly used for the CMB, which only differs from the CGWB case when making explicit the Φ-transfer function. As an example of this connection between the two cases, we show that plugging $T_\Phi^{CMB} = -\frac{1}{3}$, instead of $T_\Phi^{CGWB} = \frac{3}{5}g(\eta)$, allows to reproduce the results of [10].

8.2.2 *Starred Integrated Sachs-Wolfe Contributions*

In Ch.6, having kept the ISW allows us to find an original modification to the standard terms (see, e.g., Eq.263). These modifications arise exclusively in the presence of the modulating field through the approximation of the SBF in Eq.253.
Their effect on the final plots of the angular power spectrum contributions are then evaluated at the end of Ch.7, where we show that they cause a "suppression" in power of the terms they appear in (see, e.g., Fig.14). This could represent an important signature of a departure from statistical isotropy in the CGWB.

8.2.3 *Multipoles Coupling*

As expected from the CMB case in Ch.5, we show in Ch.6 that also the CGWB is affected by a non-trivial coupling of adjacent multipoles. In particular, looking at Eq.284 (or to Eq.329), one can see that $\langle \Gamma_{\ell m} \Gamma^*_{\ell' m'} \rangle$ is no more only proportional to a term diagonal in ℓ (i.e. $\propto \delta_{\ell\ell'}$), but also presents couplings between ℓ and $\ell \pm 1$, through the first order term in the modulating field, and between ℓ and $\ell \pm 2$, through the second order one. Indeed, thanks to the triangular rule of the $3-j$ Wigner's symbols contained in $R^{1,\ell'}_{\ell m}$, only

those terms survive among the relative angular power spectrum contribution.
Together with the original modification of the ISW terms, this specific feature represents another important signature of a departure from statistical isotropy in the CGWB.

8.3 FUTURE WORK

As aforementioned, this Thesis finds its motivations in the great attention that precise tests of isotropy [3] of our Universe is drawing in the Cosmology community, thus many different extending path rise from this framework.

Remaining in the domain of the scalar sourced terms we have evaluated here, one could relax some of the assumptions we made throughout the Thesis; an example are the transfer functions of the gravitational potentials (see Eq.292), or the approximation used for the power spectrum (see the discussion on Eq.325), which in general assumed $k_0 \ll k$.
Another important extension could come by considering more general, and more complex, expressions of the modulating field used for the stochastic variable in the gravitational potentials [77]. In this Thesis we use Eq.234, thus a simple sine modulation, which can basically be thought as a dipole modulation (i.e. $\propto Y_{10}$); however, one could for example consider a quadrupole modulation $\propto Y_{20}$, as was done in [10] to explain the alignment of the CMB quadrupole and octopole, or even more complex ones. This could bring to the construction of a whole set of templates, where different modulations get related to different signatures on the CGWB, useful for a comparison with an observation in the foreseeable future.
Then, the possibility to generate sky-maps of the CGWB would be very interesting. We already have given an expression of the angular power spectrum, thus exploiting e.g. HEALPix [37], one can obtain such sky-maps, once the software is properly modified to suit our needs (departure from a statistical diagonal description ect.). Also, the Boltzmann code CLASS [36] can be used to obtain the angular power spectrum of the CGWB, assuming more general transfer functions and underlying cosmologies, again once properly modified.

This would conclude the treatment of the scalar sourced terms, however one can consider similar modulations on their tensorial counterpart, for which one could follow the same main steps we performed in this Thesis and we just proposed (e.g. start with a simple modulation, lay out the whole treatment, generalize it to more complex modulations, produce sky-maps for each one).

Once accomplished this, we would have a complete framework to treat modulating fields on the CGWB, thus it would be interesting to link these modulations to their possible physical origins, which would then be translated in

some signature relics through the treatment itself.
Talking about possible cosmological origins, one cannot avoid mentioning the eventuality of living in a universe which initially had a Bianchi-like metric tensor [78, 79], which has been isotropized by inflation[80, 81]. Indeed, this process would leave traces of departure from isotropy on large-scales, which exit the horizon before inflation squeezed the metric into the standard FLRW one. Again, this would mine the standard cosmological model in favor of a new one, forcing a revision of our way of thinking about our Universe.

From a more statistical and observational point of view, one of the most important future works this Thesis needs is the "preparation" for measuring, or constraining, such on the CGWB data, aimed for a future comparison with CMB data, for example through the definition of estimators of the amplitude of the modulating field (as [10] has done for CMB), or the direction of the modulation. This is of crucial importance as it would provide an independent observable, i.e. the CGWB, with which we could explore the Early Universe physics. Indeed, detecting the same effect onto two independent observable would be a clear hint to its physical origin, mining one of the very pillars of cosmology, i.e its isotropy.
Furthermore, the same treatment could be performed on the AGWB, which can be affected by a departure from isotropy in the same way and would represent a third observable with which one can try to corroborate any statistical claim achieved with CMB+CGWB.

Last but not least, the feasibility of a detection of such signatures on the CGWB could be explored, studying such a possibility for future GW detectors, such as LISA, DECIGO, ET and CE.

Part III

APPENDIX

A

TRANSFER AND GROWTH FUNCTIONS

The gravitational potential Φ can be written as in Eq.190 as the product of a stochastic variable, a transfer function carrying the dependency on k and a growth function holding the one on η.
Then, in Eq.292 we report an approximation of the transfer function, while in Eq.310 one of the derivative of the growth function w.r.t. the adimensional conformal time $\widetilde{\eta}$.
The goal of this appendix is to justify these approximations.

A.1 CONFORMAL TIME VS COSMIC TIME

The first thing we need to do toward the final goal is to obtain an expression of the scale factor as a function of time, either physical and conformal.
From Ch.1, we know that one of the Friedmann equations (Eq.11) gives us an expression of the Hubble parameter $H = \frac{\dot{a}}{a}$, which once solved can provide us an expression of $a(t)$. Thus, if we consider a Einstein-de Sitter Universe, whereas containing only barionic matter and Λ, Eq.11 is recast to

$$H^2 = \frac{1}{3M_p^2}\left(\rho_\Lambda + \frac{\rho_{m,0}}{a^3}\right) . \tag{345}$$

Then, remembering the definition of the density parameter $\Omega_i = \frac{\rho_i}{\rho_{crit}}$ for the i species and assuming a flat Universe[59], we can write the latter equation as

$$H^2 = \frac{\rho_\Lambda}{3M_p^2}\left(1 + \frac{\Omega_{m,0}}{1-\Omega_{m,0}}\frac{1}{a^3}\right) . \tag{346}$$

For the sake of notation, we can define two useful constants

$$C \equiv \frac{\rho_\Lambda}{3M_p^2} \quad \text{and} \quad r \equiv \frac{\Omega_{m,0}}{1-\Omega_{m,0}} , \tag{347}$$

59 In a flat Universe the density parameters have to add to 1, so that the curvature of the Universe is exactly $\kappa = 0$. In our case, this implies $\Omega_\Lambda + \Omega_m = 1$.

which are useful to integrate the following expression.

$$\begin{aligned}\left(\frac{\dot{a}}{a}\right)^2 =& C + \frac{rC}{a^3} \\ \dot{a}^2 =& \frac{a^3 C + B}{a} \\ dt =& da \sqrt{\frac{a}{a^3 C + B}} \,.\end{aligned} \tag{348}$$

Now, changing variable to $\tilde{a} = \frac{a}{r^{1/3}}$

$$dt = d\tilde{a}\; C^{-\frac{1}{2}} \sqrt{\frac{\tilde{a}}{1+\tilde{a}^3}} \tag{349}$$

and performing the integration, one can obtain

$$t = \frac{2}{\sqrt{C}} \sinh^{-1} \tilde{a}^{3/2} \,, \tag{350}$$

which is inverted by

$$a = r^{\frac{1}{3}} \sinh^{\frac{2}{3}} \frac{\sqrt{C}t}{2} = \left(\frac{\Omega_{m,0}}{1-\Omega_{m,0}}\right)^{\frac{1}{3}} \sinh^{\frac{2}{3}} \frac{\sqrt{3\rho_\Lambda}}{2M_P} t \,. \tag{351}$$

This expression allows to fix the present time at

$$t_0 = \frac{2M_P}{\sqrt{3\rho_\Lambda}} \sinh^{-1} \sqrt{\frac{1-\Omega_{m,0}}{\Omega_{m,0}}} \,, \tag{352}$$

so that $a_0 = 1$ is recovered. Eq.351 gives us the explicit expression of the scale factor as a function of physical time, however at the end of the day we need the expression w.r.t. conformal time, since in Ch.7 we work with that.

Hence, to obtain that relation we firstly need some "preliminary" equations, which will be useful to achieve the final goal.
The metric in conformal time gets recast to

$$ds^2 = a^2(\eta)\left[-(1+2\Phi)d\eta^2 + (1-2\Psi)\delta_{ij} dx^i dx^j\right] \,, \tag{353}$$

The background Friedmann equations become

$$\begin{aligned}\frac{a'^2}{a^4} = \frac{\mathcal{H}^2}{a^2} =& \frac{1}{3M_P^2}[\rho_\Lambda + \rho_m] \\ \rho' + \frac{3a'}{a}(\rho + P) =& 0 \,.\end{aligned} \tag{354}$$

where: M_P = Planck's mass;
ρ = sum of the energy densities of the different species;
P = sum of the isotropic pressures of the different species[60].

We already know the expression of $a(t)$ from Eq.351, so to obtain the derivative of a w.r.t. conformal time we can exploit

$$\frac{da}{d\widetilde{\eta}} = \eta_0 \frac{da}{d\eta} = \eta_0 a \frac{da}{dt} = \eta_0 \sqrt{\frac{\rho_\Lambda}{3M_P^2}} r^{2/3} \cosh\left(\frac{\sqrt{2\rho_\Lambda}}{2M_P} t\right) \sinh^2\left(\frac{\sqrt{2\rho_\Lambda}}{2M_P} t\right). \tag{356}$$

Thus, in order to be able to integrate this to obtain $a(\eta)$, we need the expression of η w.r.t. t, which can be found solving

$$\begin{aligned}\eta &= \int_0^t \frac{dt'}{a(t')} = \frac{1}{r^{1/3}} \int_0^t \frac{dt'}{\sinh^{2/3}\left(\frac{\sqrt{2\rho_\Lambda}}{2M_P} t'\right)} = \frac{1}{r^{1/3}} \frac{2M_P}{\sqrt{3\rho_\Lambda}} \int_0^{\frac{\sqrt{3\rho_\Lambda}}{2M_P} t} \frac{dx}{\sinh^{2/3} x} \\ &= \frac{2M_P}{\sqrt{3\rho_\Lambda}} \frac{1}{r^{1/3}} e^{\frac{5i\pi}{6}} \left\{ \cosh\left(\frac{\sqrt{2\rho_\Lambda}}{2M_P} t\right) {}_2F_1\left[\frac{1}{2}, \frac{5}{6}; \frac{3}{2}; \cosh^2\left(\frac{\sqrt{2\rho_\Lambda}}{2M_P} t\right)\right] - \frac{\pi^{3/2}}{\Gamma\left(\frac{2}{3}\right)\Gamma\left(\frac{5}{6}\right)} \right\},\end{aligned} \tag{357}$$

which gives for the today conformal time η_0

$$\eta_0 = \frac{2M_P}{\sqrt{3\rho_\Lambda}} \frac{1}{r^{1/3}} e^{\frac{5i\pi}{6}} \left\{ \sqrt{1+\frac{1}{r}} {}_2F_1\left[\frac{1}{2}, \frac{5}{6}; \frac{3}{2}; 1+\frac{1}{r}\right] - \frac{\pi^{3/2}}{\Gamma\left(\frac{2}{3}\right)\Gamma\left(\frac{5}{6}\right)} \right\}. \tag{358}$$

Changing variable to

$$x \equiv \sinh\left(\frac{\sqrt{3\rho_\Lambda}}{2M_P} t\right) \quad \text{with} \quad 0 \leqslant x \leqslant \frac{1}{\sqrt{r}}, \tag{359}$$

the scale factor can be written as $a(t) = r^{1/3} x^{2/3}$ and the adimensional conformal time $\widetilde{\eta} \equiv \frac{\eta}{\eta_0}$ becomes ($0 \leqslant \widetilde{\eta} \leqslant 1$)

$$\widetilde{\eta} = \frac{\sqrt{1+x^2}\, {}_2F_1\left[\frac{1}{2}, \frac{5}{6}; \frac{3}{2}; 1+x^2\right] - \frac{\pi^{3/2}}{\Gamma\left(\frac{2}{3}\right)\Gamma\left(\frac{5}{6}\right)}}{\sqrt{1+\frac{1}{r}}\, {}_2F_1\left[\frac{1}{2}, \frac{5}{6}; \frac{3}{2}; 1+\frac{1}{r}\right] - \frac{\pi^{3/2}}{\Gamma\left(\frac{2}{3}\right)\Gamma\left(\frac{5}{6}\right)}}, \tag{360}$$

60 In this case baryons have no pressure, whereas $P_\Lambda = -\rho_\Lambda$ = constant, so the second equation can also be written as

$$\rho_m' + \frac{3a'}{a}\rho_m = 0. \tag{355}$$

while

$$\frac{da}{d\widetilde{\eta}} = \frac{2}{3} r^{1/3} e^{\frac{5i\pi}{6}} \left\{ \sqrt{1+\frac{1}{r}}\, {}_2F_1\left[\frac{1}{2}, \frac{5}{6}; \frac{3}{2}; 1+\frac{1}{r}\right] - \frac{\pi^{3/2}}{\Gamma\left(\frac{2}{3}\right)\Gamma\left(\frac{5}{6}\right)} \right\} x^{1/3} \sqrt{1+x^2}\,. \tag{361}$$

As the reader can imagine, inverting these kind of expressions is surely not a cake walk, in this case not even feasible analytically.
What one can do, however, is to tabulate $\{\widetilde{\eta},\ a\}$, fit the resulting "data" and work with a fitting function.
Indeed, we can exploit the fact that we have written both $\widetilde{\eta}$ and a as functions of x to obtain how they evolve throughout time. Then, performing a simple polynomial fit we can find a numerical expression for $a(\widetilde{\eta})$. Fig.19 shows the comparison between the exact solution and the fitting function. The explicit expression for the fitting function is

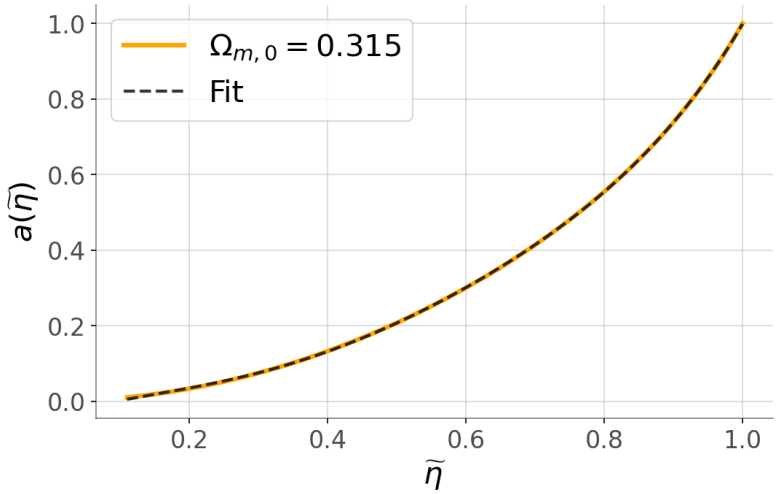

Figure 19: Comparison between the exact solution for $a(\widetilde{\eta})$, solid orange line, and a fitting function, dashed line.

$$\begin{aligned} a(\widetilde{\eta}) =& 3.65144476\,\widetilde{\eta}^5 - 8.47910726\,\widetilde{\eta}^4 + 7.71145948\,\widetilde{\eta}^3 \\ & - 2.49889549\,\widetilde{\eta}^2 + 0.66028597\,\widetilde{\eta} - 0.04662989\,, \end{aligned} \tag{362}$$

where we chose a fifth-grade polynomial, because lower ones did not correctly reproduced the behavior of the scale factor at very early times.
For completeness, we give also the numerical expression for $\frac{da}{d\widetilde{\eta}}$

$$\begin{aligned} \frac{da}{d\widetilde{\eta}} =& -7.71491905\,\widetilde{\eta}^6 + 22.39341103\,\widetilde{\eta}^5 - 26.69124986\,\widetilde{\eta}^4 \\ & + 16.17121212\,\widetilde{\eta}^3 - 5.15009289\,\widetilde{\eta}^2 + 0.55253272\,\widetilde{\eta} - 0.04631546\,, \end{aligned} \tag{363}$$

where we chose a sixth-grade polynomial, because lower ones did not correctly reproduced the behavior of the scale factor at very early times.
The comparison between the exact solution and the fitting function are shown in Fig.20.

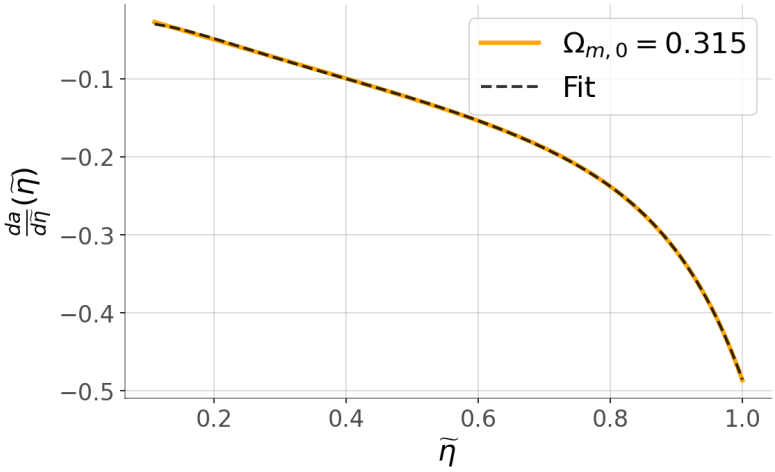

Figure 20: Comparison between the exact solution of $\frac{da}{d\widetilde{\eta}}$, solid orange line, and the fitting function, dashed line.

A.2 TRANSFER FUNCTION

In order to find how we can approximate the transfer function of Φ we need a few relations. Indeed, the transfer function relates Φ to its production mechanisms and its evolution, so we need to obtain an expression of the gravitational potential accounting for that.
We start from the stress-energy tensor

$$T_{\mu\nu} = (\rho + P)u_\mu u_\nu + P g_{\mu\nu} \ , \tag{364}$$

where: $\rho = \rho_m + \rho_\Lambda$ being in an Einstein-de-Sitter Universe;
ρ_m = energy density of baryons;
ρ_Λ = energy density of the cosmological constant Λ;
$P_m = 0$ given that baryons are pressureless;
$P_\Lambda = -\rho_\Lambda$;
$u_\mu = (1, v_{,i})$ [61];
v = scalar perturbation to the velocity of the fluid element.

61 The spatial part of the 4-velocity u_i can be expressed as done in Ch.3 with the Helmholtz theorem as

$$u_i = \partial_i v + v_i^\perp \ . \tag{365}$$

However, we are only considering scalar perturbations, thus only the first term survives.

Looking at the components of the stress-energy tensor while reminding that we are only interested in first order contributions, it is easy to find

$$\begin{aligned} T^0_0 &= -\rho_m(1+\delta) - \rho_\Lambda \,, \\ T^0_i &= \rho_m v_{,i} \,, \\ T^i_j &= -\rho_\Lambda \delta^i_j \,, \end{aligned} \tag{366}$$

where $\delta = \frac{\delta\rho_m}{\rho_m}$ is the first order scalar perturbation of the energy density of baryons and here ρ_m is intended as the unperturbed quantity at zeroth order.
With the components of the stress-energy tensor, we can then look at the Bianchi identities $\nabla_\mu T^\mu_\nu = 0$ for some other useful relation. We must first find the expression for the Christoffel symbols, which are defined as in Eq.1. Without going further into the details of the calculation and remembering the background equations from Eq.354, one can find

$$\begin{aligned} \delta' - 3\Psi' + \partial_i \partial^i v &= 0 \,, \\ v' + \frac{a'}{a} v + \Phi &= 0 \,. \end{aligned} \tag{367}$$

Furthermore, to obtain the evolution of the perturbations it is necessary to use the perturbed Einstein's equations.
Again without going into the details, we just remind that the main actors in the equations (shown in Eq.10) are the Ricci tensor (see Eq.1), the Christoffel symbols just mentioned (see Eq.1) and the stress-energy tensor.
From their spatial part, it is possible to find a term similar to [42]

$$\ldots \delta_{ij} + (\Phi - \Psi)_{,ij} = 0 \,, \tag{368}$$

which provides $\Phi = \Psi$ [62], which is what we have mentioned to justify the equality of the transfer functions of the gravitational potentials at Eq.301[63].
Looking at the other part of the spatial Einstein's equation and combining with few of the aforementioned relation (including the time-part of the equations) gives instead an EOM of Φ reading

$$\Phi'' + \frac{3a'}{a}\Phi' + \frac{a^2\rho_\Lambda}{M_P^2}\Phi = 0 \,, \tag{370}$$

62 Usually, one divides this equation in a diagonal part and an out-of-diagonal one. Clearly both have to be equal to 0 from Eq.368, so looking at the latter

$$\partial_i \partial_j (\Phi - \Psi) = 0 \quad \Rightarrow \quad \Phi = \Psi \,. \tag{369}$$

63 Introducing in the recipe of the Universe some source of anisotropic stress will generate a difference between the gravitational potential different from 0, however we will not include any.

which is solved formally by [82]

$$\Phi = C_1 g(a) + C_2 d(a) \,, \tag{371}$$

where: $C_1,\ C_2$ = integration constants;
$g(a)$ = growing mode;
$d(a)$ = decaying mode.

These two modes are proportional to [82]

$$g(a) \propto \frac{\mathcal{H}}{a} \int_0^a \frac{d\tilde{a}}{\tilde{a}^3 \tilde{H}^3} \quad \text{and} \quad d(a) \propto \frac{H}{a} \,, \tag{372}$$

with $\mathcal{H} = \frac{a'}{a}$ and $\tilde{H} = \frac{\tilde{a}'}{\tilde{a}}$.
Plugging Eq.346 into the growing mode and removing the constant factors, we can write [82]

$$g(a) \propto \sqrt{\frac{a^3 + r}{a^3}} \int_0^a dx \left(\frac{x}{x^3 + r} \right)^{\frac{3}{2}} \,, \tag{373}$$

which at early times is approximately equal to $\frac{2}{5r}$. Then, disregarding the decaying mode and choosing the proportionality constant so that at early times it goes to 1, we can write the gravitational potential as

$$\Phi = C(k) \frac{5r}{2} \sqrt{\frac{a^3 + r}{a^3}} \int_0^a dx \left(\frac{x}{x^3 + r} \right)^{\frac{3}{2}} . \tag{374}$$

In order to find the coefficient in front the the latter expression we can exploit the uniform energy density perturbation ζ, defined as

$$\zeta \equiv \Phi + H \frac{\delta\rho}{\rho'} \,. \tag{375}$$

This expression, together with Eq.354, allows to write [42]

$$\zeta = \Phi - \frac{\delta\rho}{3(1+\omega)\rho} = \left(1 + \frac{2}{3(1+\omega)} \right) \Phi = \frac{5 + 3\omega}{3(1+\omega)} \,. \tag{376}$$

This finally tells us that, if we consider only modes re-entering in matter domination where $\omega = 0$, we know that the coefficient will be

$$\Phi \simeq \boxed{\frac{3}{5}} \zeta \,, \tag{377}$$

with which we can write

$$\Phi = \frac{3}{5} \zeta_{in} \times g(a) \,. \tag{378}$$

A.3 GROWTH FUNCTION

Looking at Eq.374, we can easily write the expression of the growth function

$$g(\eta) = \frac{5r}{2}\sqrt{\frac{a^3+r}{a^3}}\int_0^a dx\left(\frac{x}{x^3+r}\right)^{\frac{3}{2}} . \tag{379}$$

This can be analytically integrated in terms of elliptic functions (see [82] for the complete solution). Here, we compare the numerical result to a fitting function provided by [83], yielding

$$g_{fit} = \frac{5}{2}\frac{\Omega_m}{\Omega_m^{4/7} - \Omega_\Lambda + \left(1+\frac{\Omega_\Lambda}{70}\right)\left(1+\frac{\Omega_m}{2}\right)} , \tag{380}$$

where: $\Omega_m \equiv \frac{\Omega_{m,0}(1+z)^3}{\Omega_{m,0}(1+z)^3+(1-\Omega_{m,0})}$;
$\Omega_\Lambda \equiv \frac{1-\Omega_{m,0}}{\Omega_{m,0}(1+z)^3+(1-\Omega_{m,0})}$;
$z = \text{redshift}$[64].

Fig.21 shows the comparison of the analytic solution and the fitting one, for different cosmologies; clearly the fit is really good. However, reminding

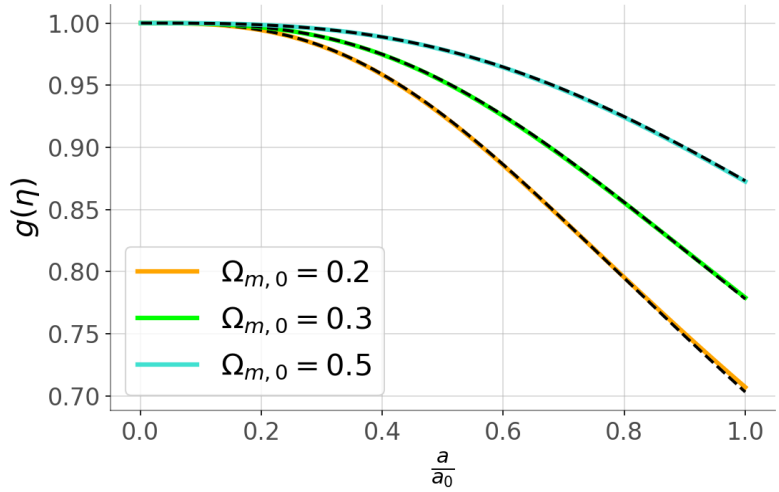

Figure 21: Comparison between the analytic solution, solid colored lines, of the growth function and a fitting one, dashed lines.

Eq.309 for example, we actually need an expression for the derivative of the growth function w.r.t. the adimensional conformal time $\widetilde{\eta}$. We know also that we can write the derivative of the scale factor w.r.t. $\widetilde{\eta}$ (see Eq.361), thus we can write

$$\frac{dg}{d\widetilde{\eta}} = \frac{dg}{da}\frac{da}{d\widetilde{\eta}} . \tag{381}$$

64 We remember that $(1+z) = a^{-1}(t)$.

Let us start from $\frac{dg}{da}$; [84] provides an approximation for the logarithmic derivative of $D(a) = g(a) \times a$, which can be written as

$$\begin{aligned} f(a) =& \frac{dD}{da}\frac{a}{D(a)} = \frac{d(g \times a)}{da}\frac{1}{g} = \frac{dg}{da}\frac{a}{g} + 1 \\ \simeq& \Omega_m^{4/7} + \left(1 + \frac{\Omega_m}{2}\right)\frac{\Omega_\Lambda}{70} \,. \end{aligned} \tag{382}$$

With this we can then write

$$\frac{dg}{da} \simeq \frac{g}{a}\left[\Omega_m^{4/7} + \left(1 + \frac{\Omega_m}{2}\right)\frac{\Omega_\Lambda}{70} - 1\right] , \tag{383}$$

which is a function of x. In order to check the "goodness" of this approximation we compare it to the analytic derivative of Eq.380. Firstly, the derivatives of Ω_m and Ω_Λ read

$$\begin{aligned} \frac{d\Omega_m}{da} =& \frac{\left(-3\Omega_{m,0}a^{-4}\right)\left(\Omega_{m,0}a^{-3} + 1 - \Omega_{m,0}\right) - \left(\Omega_{m,0}a^{-3}\right)\left(-3\Omega_{m,0}a^{-4}\right)}{\left(\Omega_{m,0}a^{-3} + 1 - \Omega_{m,0}\right)^2} \\ =& \frac{-3\Omega_{m,0}a^{-4}(1 - \Omega_{m,0})}{\left(\Omega_{m,0}a^{-3} + 1 - \Omega_{m,0}\right)^2} \,, \\ \\ \frac{d\Omega_\Lambda}{da} =& \frac{3\Omega_{m,0}a^{-4}(1 - \Omega_{m,0})}{\left(\Omega_{m,0}a^{-3} + 1 - \Omega_{m,0}\right)^2} = -\frac{d\Omega_m}{da} \,. \end{aligned} \tag{384}$$

This relation between the two derivatives is not a surprise given that we are considering an Einstein-de-Sitter Universe in which $\Omega_m + \Omega_\Lambda = 1$.
Then, we can write the expression for the derivative of g_{fit} as (we skip the passage when we exploit the relation of the derivatives of the density parameters of Eq.384)

$$\begin{aligned} \frac{dg_{fit}}{da} =& \frac{5}{2}\frac{d\Omega_m}{da}\left\{\Omega_m^{4/7} - \Omega_\Lambda + \left(1 + \frac{\Omega_m}{2}\right)\left(1 + \frac{\Omega_\Lambda}{70}\right)\right. \\ & \left. - \Omega_m\left[\frac{4}{7}\Omega_m^{-3/7} + 1 - \frac{1}{70}\left(1 + \frac{\Omega_m}{2}\right) + \frac{1}{2}\left(1 + \frac{\Omega_\Lambda}{70}\right)\right]\right\} \\ & \times \left[\Omega_m^{4/7} - \Omega_\Lambda + \left(1 + \frac{\Omega_m}{2}\right)\left(1 + \frac{\Omega_\Lambda}{70}\right)\right]^{-2} . \end{aligned} \tag{385}$$

Both Eq.383 and Eq.385 are functions of x, thus we can exploit again the trick of tabulating $\left\{\widetilde{\eta}, \frac{dg}{da}\right\}$ and $\left\{\widetilde{\eta}, \frac{dg_{fit}}{da}\right\}$ to obtain what is shown in Fig.22. As we can see, the approximation is indeed good, exception made for very late times. In spite of this we will use the approximation of Eq.383, which is easier to handle.

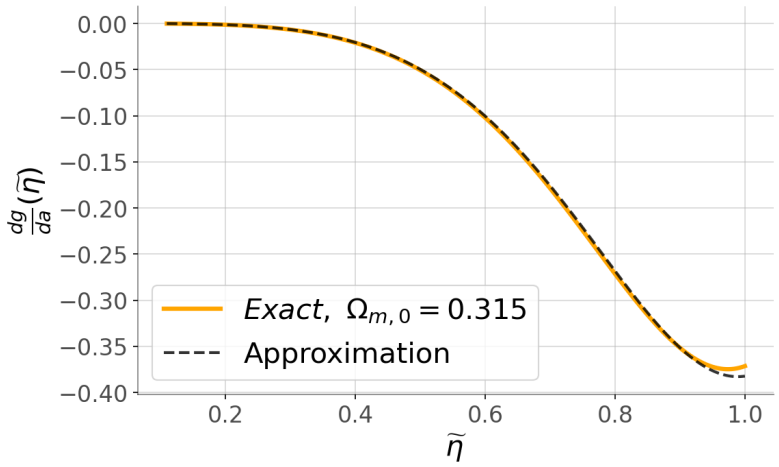

Figure 22: Comparison between the analytic expression of $\frac{dg_{fit}}{da}$, orange solid line, and the approximation introduced by Eq.383, dashed line.

At this point we just have to remind $\frac{da}{d\widetilde{\eta}}$ as a function of x from Eq.361. Thus, multiplying it by Eq.383, we obtain an expression of $\frac{dg}{d\widetilde{\eta}}$ as a function of x. Again, we can tabulate $\left\{\widetilde{\eta}, \frac{dg}{d\widetilde{\eta}}\right\}$ to obtain an approximate solution with a fit. Here, we propose the following fitting function, yielding

$$\left.\frac{dg}{d\widetilde{\eta}}\right|_{fit} = -\frac{5}{4}\widetilde{\eta}^5 \quad \text{with} \quad \Omega_{m,0} = 0.315\,. \tag{386}$$

The comparison between the exact numerical solution and the fitting one is shown in Fig.23. As we can see, the fit is good and we will be using this

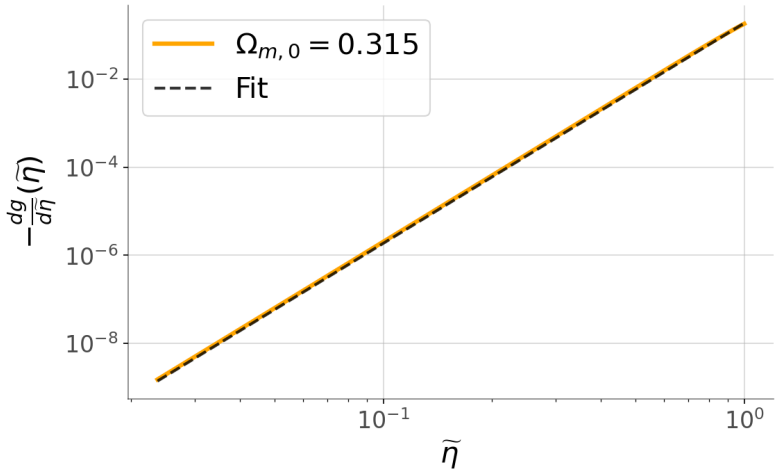

Figure 23: Comparison between the analytic expression of the derivative of the growth function, solid orange line, and the fitting one, dashed line.

approximation throughout this Thesis.

BIBLIOGRAPHY

[1] H. K. Eriksen et al. "Asymmetries in the Cosmic Microwave Background Anisotropy Field." In: *The Astrophysical Journal* 605.1 (Apr. 2004), pp. 14–20. ISSN: 1538-4357. DOI: 10.1086/382267. URL: http://dx.doi.org/10.1086/382267.

[2] F. K. Hansen et al. "Power Asymmetry In Cosmic Microwave Background Fluctuations from Full Sky to Sub-degree Scales: Is the Universe Isotropic?" In: *The Astrophysical Journal* 704.2 (Oct. 2009), pp. 1448–1458. ISSN: 1538-4357. DOI: 10.1088/0004-637x/704/2/1448. URL: http://dx.doi.org/10.1088/0004-637X/704/2/1448.

[3] Y. Akrami et al. *Planck 2018 results. VII. Isotropy and Statistics of the CMB*. 2019. arXiv: 1906.02552 [astro-ph.CO].

[4] Fabian Schmidt and Lam Hui. "Cosmic Microwave Background Power Asymmetry from Non-Gaussian Modulation." In: *Phys. Rev. Lett.* 110 (1 Jan. 2013), p. 011301. DOI: 10.1103/PhysRevLett.110.011301. URL: https://link.aps.org/doi/10.1103/PhysRevLett.110.011301.

[5] Christian T. Byrnes and Ewan R.M. Tarrant. "Scale-dependent non-Gaussianity and the CMB power asymmetry." In: *Journal of Cosmology and Astroparticle Physics* 2015.07 (July 2015), pp. 007–007. ISSN: 1475-7516. DOI: 10.1088/1475-7516/2015/07/007. URL: http://dx.doi.org/10.1088/1475-7516/2015/07/007.

[6] Christian T. Byrnes et al. "The hemispherical asymmetry from a scale-dependent inflationary bispectrum." In: *Journal of Cosmology and Astroparticle Physics* 2016.06 (June 2016), pp. 025–025. ISSN: 1475-7516. DOI: 10.1088/1475-7516/2016/06/025. URL: http://dx.doi.org/10.1088/1475-7516/2016/06/025.

[7] Amjad Ashoorioon and Tomi Koivisto. "Hemispherical anomaly from asymmetric initial states." In: *Phys. Rev. D* 94 (4 Aug. 2016), p. 043009. DOI: 10.1103/PhysRevD.94.043009. URL: https://link.aps.org/doi/10.1103/PhysRevD.94.043009.

[8] Saroj Adhikari, Sarah Shandera, and Adrienne L. Erickcek. "Large-scale anomalies in the cosmic microwave background as signatures of non-Gaussianity." In: *Phys. Rev. D* 93 (2 Jan. 2016), p. 023524. DOI: 10.1103/PhysRevD.93.023524. URL: https://link.aps.org/doi/10.1103/PhysRevD.93.023524.

[9] F. K. Hansen et al. "Isotropic non-Gaussian g_{NL}-like toy models that reproduce cosmic microwave background anomalies." In: *Astronomy & Astrophysics* 626 (June 2019), A13. ISSN: 1432-0746. DOI: 10.1051/0004-6361/201833698. URL: http://dx.doi.org/10.1051/0004-6361/201833698.

[10] C. Dvorkin, H. V. Peiris, and W. Hu. "Testable polarization predictions for models of CMB isotropy anomalies." In: *Physical Review D* 77.6 (Mar. 2008). ISSN: 1550-2368. DOI: 10.1103/physrevd.77.063008. URL: http://dx.doi.org/10.1103/PhysRevD.77.063008.

[11] B. P. Abbott et al. "Search for the isotropic stochastic background using data from Advanced LIGO's second observing run." In: *Physical Review D* 100.6 (Sept. 2019). ISSN: 2470-0029. DOI: 10.1103/physrevd.100.061101. URL: http://dx.doi.org/10.1103/PhysRevD.100.061101.

[12] Daniele Bertacca et al. "Projection effects on the observed angular spectrum of the astrophysical stochastic gravitational wave background." In: *Physical Review D* 101.10 (May 2020). ISSN: 2470-0029. DOI: 10.1103/physrevd.101.103513. URL: http://dx.doi.org/10.1103/PhysRevD.101.103513.

[13] Michele Maggiore. "Gravitational wave experiments and early universe cosmology." In: *Physics Reports* 331.6 (2000), pp. 283–367. ISSN: 0370-1573. DOI: https://doi.org/10.1016/S0370-1573(99)00102-7. URL: http://www.sciencedirect.com/science/article/pii/S0370157399001027.

[14] M. Guzzetti et al. "Gravitational waves from inflation." In: 39 (May 2016). DOI: 10.1393/ncr/i2016-10127-1.

[15] Nicola Bartolo et al. "Science with the space-based interferometer LISA. IV: probing inflation with gravitational waves." In: *Journal of Cosmology and Astroparticle Physics* 2016.12 (Dec. 2016), pp. 026–026. ISSN: 1475-7516. DOI: 10.1088/1475-7516/2016/12/026. URL: http://dx.doi.org/10.1088/1475-7516/2016/12/026.

[16] Chiara Caprini. "Stochastic background of gravitational waves from cosmological sources." In: *Journal of Physics: Conference Series* 610 (May 2015), p. 012004. ISSN: 1742-6596. DOI: 10.1088/1742-6596/610/1/012004. URL: http://dx.doi.org/10.1088/1742-6596/610/1/012004.

[17] Chiara Caprini and Daniel G Figueroa. "Cosmological backgrounds of gravitational waves." In: *Classical and Quantum Gravity* 35.16 (July 2018), p. 163001. ISSN: 1361-6382. DOI: 10.1088/1361-6382/aac608. URL: http://dx.doi.org/10.1088/1361-6382/aac608.

[18] S. Dodelson. *Modern Cosmology*. Amsterdam: Academic Press, 2003. ISBN: 978-0-12-219141-1.

[19] Vasyl Alba and Juan Maldacena. "Primordial gravity wave background anisotropies." In: *Journal of High Energy Physics* 2016.3 (Mar. 2016). ISSN: 1029-8479. DOI: 10.1007/jhep03(2016)115. URL: http://dx.doi.org/10.1007/JHEP03(2016)115.

[20] Ruth Durrer. *The Cosmic Microwave Background*. Cambridge University Press, 2008. DOI: 10.1017/CBO9780511817205.

[21] P. J. E. Peebles and J. T. Yu. "Primeval Adiabatic Perturbation in an Expanding Universe." In: *The Astrophysical Journal* 162 (Dec. 1970), p. 815. DOI: 10.1086/150713.

[22] J. R. Bond and A. S. Szalay. "The collisionless damping of density fluctuations in an expanding universe." In: *The Astrophysical Journal* 274 (Nov. 1983), pp. 443–468. DOI: 10.1086/161460.

[23] C. W. Misner, K. S. Thorne, and J. A. Wheeler. *Gravitation*. Ed. by Misner, C. W., Thorne, K. S., & Wheeler, J. A. 1973.

[24] Alice Garoffolo et al. *Gravitational waves and geometrical optics in scalar-tensor theories*. 2020. arXiv: 1912.08093 [gr-qc].

[25] N. Bartolo et al. "Anisotropies and non-Gaussianity of the cosmological gravitational wave background." In: *Physical Review D* 100.12 (Dec. 2019). ISSN: 2470-0029. DOI: 10.1103/physrevd.100.121501. URL: http://dx.doi.org/10.1103/PhysRevD.100.121501.

[26] N. Bartolo et al. "Characterizing the cosmological gravitational wave background: Anisotropies and non-Gaussianity." In: *Physical Review D* 102.2 (July 2020). ISSN: 2470-0029. DOI: 10.1103/physrevd.102.023527. URL: http://dx.doi.org/10.1103/PhysRevD.102.023527.

[27] Pau Amaro-Seoane et al. *Laser Interferometer Space Antenna*. 2017. arXiv: 1702.00786 [astro-ph.IM].

[28] Enrico Barausse et al. "Prospects for fundamental physics with LISA." In: *General Relativity and Gravitation* 52.8 (Aug. 2020). ISSN: 1572-9532. DOI: 10.1007/s10714-020-02691-1. URL: http://dx.doi.org/10.1007/s10714-020-02691-1.

[29] Nicola Bartolo et al. "Probing non-Gaussian stochastic gravitational wave backgrounds with LISA." In: *Journal of Cosmology and Astroparticle Physics* 2018.11 (Nov. 2018), pp. 034–034. ISSN: 1475-7516. DOI: 10.1088/1475-7516/2018/11/034. URL: http://dx.doi.org/10.1088/1475-7516/2018/11/034.

[30] Chiara Caprini et al. "Reconstructing the spectral shape of a stochastic gravitational wave background with LISA." In: *Journal of Cosmology and Astroparticle Physics* 2019.11 (Nov. 2019), pp. 017–017. ISSN: 1475-7516. DOI: 10.1088/1475-7516/2019/11/017. URL: http://dx.doi.org/10.1088/1475-7516/2019/11/017.

[31] Mauro Pieroni and Enrico Barausse. "Foreground cleaning and template-free stochastic background extraction for LISA." In: *Journal of Cosmology and Astroparticle Physics* 2020.07 (July 2020), pp. 021–021. ISSN: 1475-7516. DOI: 10.1088/1475-7516/2020/07/021. URL: http://dx.doi.org/10.1088/1475-7516/2020/07/021.

[32] Seiji Kawamura et al. "The Japanese space gravitational wave antenna - DECIGO." In: *Classical and Quantum Gravity* 23.8 (Mar. 2006), S125–S131. DOI: 10.1088/0264-9381/23/8/s17. URL: https://doi.org/10.1088%2F0264-9381%2F23%2F8%2Fs17.

[33] B. Sathyaprakash et al. *Scientific Potential of Einstein Telescope*. 2012. arXiv: 1108.1423 [gr-qc].

[34] Michele Maggiore et al. "Science case for the Einstein telescope." In: *Journal of Cosmology and Astroparticle Physics* 2020.03 (Mar. 2020), pp. 050–050. ISSN: 1475-7516. DOI: 10.1088/1475-7516/2020/03/050. URL: http://dx.doi.org/10.1088/1475-7516/2020/03/050.

[35] B P Abbott et al. "Exploring the sensitivity of next generation gravitational wave detectors." In: *Classical and Quantum Gravity* 34.4 (Jan. 2017), p. 044001. ISSN: 1361-6382. DOI: 10.1088/1361-6382/aa51f4. URL: http://dx.doi.org/10.1088/1361-6382/aa51f4.

[36] Julien Lesgourgues. *The Cosmic Linear Anisotropy Solving System (CLASS) I: Overview*. 2011. arXiv: 1104.2932 [astro-ph.IM].

[37] K. M. Górski et al. "HEALPix: A Framework for High-Resolution Discretization and Fast Analysis of Data Distributed on the Sphere." In: *Astrophysical Journal* 622.2 (Apr. 2005), pp. 759–771. DOI: 10.1086/427976. arXiv: astro-ph/0409513 [astro-ph].

[38] Atsushi Taruya and Hideaki Kudoh. "Probing anisotropies of gravitational-wave backgrounds with a space-based interferometer. II. Perturbative reconstruction of a low-frequency skymap." In: *Physical Review D* 72.10 (Nov. 2005). ISSN: 1550-2368. DOI: 10.1103/physrevd.72.104015. URL: http://dx.doi.org/10.1103/PhysRevD.72.104015.

[39] Atsushi Taruya. "Probing anisotropies of gravitational-wave backgrounds with a space-based interferometer. III. Reconstruction of a high-frequency sky map." In: *Physical Review D* 74.10 (Nov. 2006). ISSN: 1550-2368. DOI: 10.1103/physrevd.74.104022. URL: http://dx.doi.org/10.1103/PhysRevD.74.104022.

[40] John Baker et al. *High angular resolution gravitational wave astronomy*. 2019. arXiv: 1908.11410 [astro-ph.HE].

[41] Carlo R. Contaldi et al. "Maximum likelihood map making with the Laser Interferometer Space Antenna." In: *Physical Review D* 102.4 (Aug. 2020). ISSN: 2470-0029. DOI: 10.1103/physrevd.102.043502. URL: http://dx.doi.org/10.1103/PhysRevD.102.043502.

[42] A. Riotto. "Inflation and the Theory of Cosmological Perturbations." In: (2002). arXiv: hep-ph/0210162 [hep-ph].

[43] N. Bartolo et al. "Non-Gaussianity from inflation: theory and observations." In: *Physics Reports* 402.3-4 (Nov. 2004), pp. 103–266. ISSN: 0370-1573. DOI: 10.1016/j.physrep.2004.08.022. URL: http://dx.doi.org/10.1016/j.physrep.2004.08.022.

[44] E. W. Kolb and M. S. Turner. "The Early Universe." In: *Front. Phys.* 69 (1990), pp. 1–547.

[45] M.P. Hobson, G.P. Efstathiou, and A.N. Lasenby. *General relativity: An introduction for physicists*. Oct. 2006.

[46] Sean Carroll. *Spacetime and geometry: an introduction to general relativity; International ed.* Essex: Pearson Education, Aug. 2013. DOI: 1292026634. URL: https://cds.cern.ch/record/1602292.

[47] D. Baumann. "Inflation." In: *Theoretical Advanced Study Institute in Elementary Particle Physics: Physics of the Large and the Small*. 2011, pp. 523–686. DOI: 10.1142/9789814327183_0010. arXiv: 0907.5424 [hep-th].

[48] N. Aghanim et al. "Planck 2018 results. VI. Cosmological parameters." In: *Astron. Astrophys.* 641 (2020), A6. DOI: 10.1051/0004-6361/201833910. arXiv: 1807.06209 [astro-ph.CO].

[49] Milton Abramowitz, I. Stegun, and A. G. Greenhill. *Handbook of Mathematical Functions with Formulas, Graphs and Mathematical Tables*. 1971.

[50] Y. Akrami et al. "Planck 2018 results. X. Constraints on inflation." In: (2018). arXiv: 1807.06211 [astro-ph.CO]. URL: https://arxiv.org/abs/1807.06211v2.

[51] Nicola Bartolo, Sabino Matarrese, and Antonio Riotto. "Cosmic microwave background anisotropies at second order: I." In: *Journal of Cosmology and Astroparticle Physics* 2006.06 (June 2006), pp. 024–024. ISSN: 1475-7516. DOI: 10.1088/1475-7516/2006/06/024. URL: http://dx.doi.org/10.1088/1475-7516/2006/06/024.

[52] Nicola Bartolo, Sabino Matarrese, and Antonio Riotto. "CMB anisotropies at second-order II: analytical approach." In: *Journal of Cosmology and Astroparticle Physics* 2007.01 (Jan. 2007), pp. 019–019. ISSN: 1475-7516. DOI: 10.1088/1475-7516/2007/01/019. URL: http://dx.doi.org/10.1088/1475-7516/2007/01/019.

[53] Carlo R. Contaldi. "Anisotropies of gravitational wave backgrounds: A line of sight approach." In: *Physics Letters B* 771 (Aug. 2017), pp. 9–12. ISSN: 0370-2693. DOI: 10.1016/j.physletb.2017.05.020. URL: http://dx.doi.org/10.1016/j.physletb.2017.05.020.

[54] Sascha Husa. "Michele Maggiore: Gravitational waves. Volume 1: Theory and experiments." In: *Gen. Rel. Grav.* 41 (2009), pp. 1667–1669. DOI: 10.1007/s10714-009-0762-5.

[55] B. P. Abbott et al. "GW170817: Implications for the Stochastic Gravitational-Wave Background from Compact Binary Coalescences." In: *Physical Review Letters* 120.9 (Feb. 2018). ISSN: 1079-7114. DOI: 10.1103/physrevlett.120.091101. URL: http://dx.doi.org/10.1103/PhysRevLett.120.091101.

[56] Michael Geller et al. "Primordial Anisotropies in the Gravitational Wave Background from Cosmological Phase Transitions." In: *Physical Review Letters* 121.20 (Nov. 2018). ISSN: 1079-7114. DOI: 10.1103/physrevlett.121.201303. URL: http://dx.doi.org/10.1103/PhysRevLett.121.201303.

[57] N. Bartolo et al. "Gravitational wave anisotropies from primordial black holes." In: *Journal of Cosmology and Astroparticle Physics* 2020.02 (Feb. 2020), pp. 028–028. ISSN: 1475-7516. DOI: 10.1088/1475-7516/2020/02/028. URL: http://dx.doi.org/10.1088/1475-7516/2020/02/028.

[58] N. Bartolo et al. "Primordial Black Hole Dark Matter: LISA Serendipity." In: *Physical Review Letters* 122.21 (May 2019). ISSN: 1079-7114. DOI: 10.1103/physrevlett.122.211301. URL: http://dx.doi.org/10.1103/PhysRevLett.122.211301.

[59] N. Bartolo et al. "Testing primordial black holes as dark matter with LISA." In: *Physical Review D* 99.10 (May 2019). ISSN: 2470-0029. DOI: 10.1103/physrevd.99.103521. URL: http://dx.doi.org/10.1103/PhysRevD.99.103521.

[60] Neil Barnaby and Marco Peloso. "Large Non-Gaussianity in Axion Inflation." In: *Physical Review Letters* 106.18 (May 2011). ISSN: 1079-7114. DOI: 10.1103/physrevlett.106.181301. URL: http://dx.doi.org/10.1103/PhysRevLett.106.181301.

[61] Jessica L. Cook and Lorenzo Sorbo. "Particle production during inflation and gravitational waves detectable by ground-based interferometers." In: *Physical Review D* 85.2 (Jan. 2012). ISSN: 1550-2368. DOI: 10.1103/physrevd.85.023534. URL: http://dx.doi.org/10.1103/PhysRevD.85.023534.

[62] Nicola Bartolo et al. "Photon-graviton scattering: A new way to detect anisotropic gravitational waves?" In: *Physical Review D* 98.2 (July 2018). ISSN: 2470-0029. DOI: 10.1103/physrevd.98.023518. URL: http://dx.doi.org/10.1103/PhysRevD.98.023518.

[63] Eiichiro Komatsu. "The Pursuit of Non-Gaussian Fluctuations in the Cosmic Microwave Background." In: (July 2002).

[64] Planck Collaboration et al. *Planck 2018 results. IX. Constraints on primordial non-Gaussianity*. 2019. arXiv: 1905.05697 [astro-ph.CO].

[65] N.W. Boggess et al. "The COBE mission - Its design and performance two years after launch." In: *Astrophys. J.* 397 (1992), pp. 420–429. DOI: 10.1086/171797.

[66] George F. Smoot. "COBE observations and results." In: *Conference on 3K cosmology* (1999). DOI: 10.1063/1.59326. URL: http://dx.doi.org/10.1063/1.59326.

[67] D. J. Fixsen et al. "The Cosmic Microwave Background Spectrum from the FullCOBEFIRAS Data Set." In: *The Astrophysical Journal* 473.2 (Dec. 1996), pp. 576–587. ISSN: 1538-4357. DOI: 10.1086/178173. URL: http://dx.doi.org/10.1086/178173.

[68] Wayne T. Hu. "Wandering in the Background: A CMB Explorer." Other thesis. Aug. 1995. arXiv: astro-ph/9508126.

[69] D.J. Eisenstein. "Dark energy and cosmic sound." In: *New Astronomy Reviews* 49.7 (2005). Wide-Field Imaging from Space, pp. 360–365. ISSN: 1387-6473. DOI: https://doi.org/10.1016/j.newar.2005.08.005. URL: http://www.sciencedirect.com/science/article/pii/S1387647305000850.

[70] Daniel J. Eisenstein et al. "Detection of the Baryon Acoustic Peak in the Large-Scale Correlation Function of SDSS Luminous Red Galaxies." In: *The Astrophysical Journal* 633.2 (Nov. 2005), pp. 560–574. ISSN: 1538-4357. DOI: 10.1086/466512. URL: http://dx.doi.org/10.1086/466512.

[71] R.K. Sachs and A.M. Wolfe. "Perturbations of a cosmological model and angular variations of the microwave background." In: *Astrophys. J.* 147 (1967), pp. 73–90. DOI: 10.1007/s10714-007-0448-9.

[72] M.J. Rees and D.W. Sciama. "Large scale Density Inhomogeneities in the Universe." In: *Nature* 217 (1968), pp. 511–516. DOI: 10.1038/217511a0.

[73] Ethan T. Vishniac. "Reionization and Small-Scale Fluctuations in the Microwave Background." In: *The Astrophysics Journal* 322 (Nov. 1987), p. 597. DOI: 10.1086/165755.

[74] A. Blanchard and J. Schneider. "Gravitational lensing effect on the fluctuations of the cosmic background radiation." In: *Astronomy & Astrophysics* 184.1-2 (Oct. 1987), pp. 1–6.

[75] D. Zwillinger et al., eds. *Table of Integrals, Series, and Products (Eighth Edition)*. Eighth Edition. Boston: Academic Press, 2014. ISBN: 978-0-12-384933-5. DOI: https://doi.org/10.1016/B978-0-12-384933-5.00006-0. URL: http://www.sciencedirect.com/science/article/pii/B9780123849335000060.

[76] Lorenzo Valbusa Dall'Armi et al. *The Imprint of Relativistic Particles on the Anisotropies of the Stochastic Gravitational-Wave Background*. 2020. arXiv: 2007.01215 [astro-ph.CO].

[77] Christian T. Byrnes et al. "Implications of the cosmic microwave background power asymmetry for the early universe." In: *Physical Review D* 93.12 (June 2016). ISSN: 2470-0029. DOI: 10.1103/physrevd.93.123003. URL: http://dx.doi.org/10.1103/PhysRevD.93.123003.

[78] George F.R. Ellis and Henk van Elst. "Cosmological models: Cargese lectures 1998." In: *NATO Sci. Ser. C* 541 (1999), pp. 1–116. DOI: 10.1007/978-94-011-4455-1_1. arXiv: gr-qc/9812046.

[79] Christian G. Böhmer and Nyein Chan. "Dynamical Systems in Cosmology." In: *Dynamical and Complex Systems* (Dec. 2016), pp. 121–156. DOI: 10.1142/9781786341044_0004. URL: http://dx.doi.org/10.1142/9781786341044_0004.

[80] A Emir Gümrükçüo, Carlo R Contaldi, and Marco Peloso. "Inflationary perturbations in anisotropic backgrounds and their imprint on the cosmic microwave background." In: *Journal of Cosmology and Astroparticle Physics* 2007.11 (Nov. 2007), pp. 005–005. ISSN: 1475-7516. DOI: 10.1088/1475-7516/2007/11/005. URL: http://dx.doi.org/10.1088/1475-7516/2007/11/005.

[81] Thiago S Pereira, Cyril Pitrou, and Jean-Philippe Uzan. "Theory of cosmological perturbations in an anisotropic universe." In: *Journal of Cosmology and Astroparticle Physics* 2007.09 (Sept. 2007), pp. 006–006. ISSN: 1475-7516. DOI: 10.1088/1475-7516/2007/09/006. URL: http://dx.doi.org/10.1088/1475-7516/2007/09/006.

[82] D. J. Eisenstein. *An Analytic Expression for the Growth Function in a Flat Universe with a Cosmological Constant*. 1997. arXiv: astro-ph/9709054 [astro-ph].

[83] S. M. Carroll, W. H. Press, and E. L. Turner. "The Cosmological Constant." In: *Annual Review of Astronomy and Astrophysics* 30.1 (1992), pp. 499–542. DOI: 10.1146/annurev.aa.30.090192.002435. eprint: https://doi.org/10.1146/annurev.aa.30.090192.002435. URL: https://doi.org/10.1146/annurev.aa.30.090192.002435.

[84] O. Lahav et al. "Dynamical effects of the cosmological constant." In: *Monthly Notices of the Royal Astronomical Society* 251.1 (July 1991), pp. 128–136. ISSN: 0035-8711. DOI: 10.1093/mnras/251.1.128. eprint: https://academic.oup.com/mnras/article-pdf/251/1/128/18523334/mnras251-0128.pdf. URL: https://doi.org/10.1093/mnras/251.1.128.